University of Oklahoma

Graduate College

Site-Directed Mutagenesis As A Probe To Study The Mechanism of Sheep Liver 6-Phosphogluconate Dehydrogenase

A Dissertation

SUBMITTED TO THE GRADUATE FACULTY

in partial fulfillment of the requirements of the

Degree of

Doctor of Philosophy

By

LEI LI

Norman, Oklahoma

2006

ProQuest Information and Learning Company
300 North Zeeb Road
P.O. Box 1346
Ann Arbor, MI 48106-1346

Site-Directed Mutagenesis As A Probe To Study The Mechanism of Sheep Liver 6-Phosphogluconate Dehydrogenase

A Dissertation APPROVED FOR
THE DEPARTMENT OF CHEMISTRY AND BIOCHEMISTRY

By

Paul F. Cook, Ph.D., CHAIR

Ann H. West, Ph.D.

George B. Richter-Addo, Ph.D.

Helen Zgurskaya, Ph.D.

Penny M. Hopkins, Ph.D.

ACKNOWLEDGEMENTS

First of all I would like to express my sincere gratitude and appreciation to Dr. Paul F. Cook. Dr. Cook not only serves as my major advisor but also as a helpful friend and a considerate family member. Without him, this dissertation could not have been written within three and a half years. He is always there to very patiently listen and give advice concerning problems encountered throughout my PhD study. He led me into the enzyme world and taught me how to become an outstanding scientist. He encouraged me to ask, to think and to explore. Without his astute reasoning, most of the ideas in this dissertation would still be confusing and unclear. He also made the Cook lab a wonderful workplace and home for the past few years. I felt very lucky to be able to work with Dr. Cook, an extremely intelligent person with a great sense of humor. His kindness and enthusiasm is engraved in my memory.

I also thank all of my graduate committee members: Dr. Penny M. Hopkins, Dr. George B. Richter-Addo, Dr. Ann H. West and Dr. Helen I. Zgurskaya and my former committee member Dr. Jia Li. They guided me from the beginning of my research, through defending my proposal to the last moment of my dissertation defense. They have had a large impact on my work by giving advice and supporting me when I encountered difficulties all these years.

In addition to my advisors, I would like to thank Dr. William E. Karsten and Dr.

Lillian Chooback. They together taught me most of the techniques in molecular biology and enzyme kinetics. I thank them for their helpful comments and encouragement and having great patience in listening and discussing with me about almost any topic. They have been friends, mentors and have helped me tremendously both in science and in my personal life. I am also greatly indebted to many colleagues. Dr. Dali Liu first introduced me to Dr. Cook's lab and helped me start my research. Without him, I would not have joined this wonderful lab. I am also thankful to Daniel Copeland for his technical assistance with the PyMol program. I greatly appreciate Jean Keil and Arlene C. Crawford for helping me with administrative issues and all of the paperwork.

Special thanks also go to Zhe Jiang, a family friend. He has always been there for us whenever we need help, taking care of our kitties, collecting mail, etc. Without him, our lives would not have been as easy.

I can not forget all my lab members and friends in the University of Oklahoma: Ying Lin, Babak Andi, Florian Dworkowski, Jinghua Qian, Hengyu Xu, Mamar Baizid, Deniz Aktas, Devi Ekanayake, Rong Guan, Ashwani Vashishtha, Qiong Xue, Hui Tan, Jing Yi and her husband Xiaoping Gou. They provided the social setting without which I would not be able to enjoy my research and my life.

One of the most wonderful things that have ever happened in my life is that I

met my dear husband Lieyu Hu at OU. He is a sweet, intelligent, hardworking person. Without his unfailing support and encouragement to pursue my interests, I could never have completed this work. I am also very grateful to my family. First, my parents, Xiaolan Wu and Yinyuan Li, for bringing me into this world in the first place, for educating me with aspects from both sciences and arts, for helping me make the right decisions, and for having faith in me all the time. My brother, Lei Li, for his unconditional support in taking care of our parents, for his careful consideration about my health and study, and for believing in me. I would like to thank them for their life-love and support.

TABLE OF CONTENTS

LIST OF TABLES

LIST OF FIGURES

LIST OF ABBREVIATIONS

ADP agarose, 2', 5'-adenosine diphosphate agarose

Bis-Tris, bis(2-hydroxyethyl)iminotris(hydroxymethyl)methane

bp, base pair

CD, circular dichroism

Ches, 2-(N-cyclohexylamino)ethanesulfonic acid

3-*d*-6PG, 3-*deutero*-6-phosphogluconate

E, enzyme

Hepes, 4-(2-hydroxyethyl)-1-piperazineethanesulfonic acid

IPTG, isopropyl-β-*D*-thiogalactopyranoside

3Kd6PG, 2-deoxy-3-keto-6-phosphogluconate

kb, kilo-base

LB, Luria-Bertani

Ni-NTA agarose, nickel-nitrilotriacetic acid agarose

NAD, nicotinamide adenine dinucleotide

NADH, reduced nicotinamide adenine dinucleotide

NADP, nicotinamide adenine dinucleotide 2'-phosphate (the + sign is omitted for convenience)

NADPH, reduced nicotinamide adenine dinucleotide 2'-phosphate

Nbr^{8}ADP, nicotinamide-8-bromo-adenine dinucleotide 2'-phosphate

6PG, 6-phosphogluconate

6PGDH, 6-phosphogluconate dehydrogenase

3-*h*-6PG, 3-*protio*-6-phosphogluconate

PCR, polymerase chain reaction

Ru5P, ribulose-5-phosphate

ssDNA, single-stranded deoxyribonucleic acid

dsDNA, double-stranded deoxyribonucleic acid

TEA, triethanolamine

wt, wild type

ABSTRACT

Sheep liver 6-phosphogluconate dehydrogenase (6PGDH) shows a high specificity for NADP. Discrimination between NADP and NAD suggests that the interactions between the 2'-phosphate and 6PGDH contribute most of the binding energy for NADP. The 6-phosphate of 6-phosphogluconate (6PG) is proposed to anchor the sugar phosphate in the active site and aid in orientating the substrate for catalysis. Crystal structure of the E:Nbr^{8}ADP complex shows that Asn32, Arg33 and Thr34 are within hydrogen-bonding distance to the 2'-phosphate of NADP. And residues Y191, K260, T262, R287 and R446 are in the vicinity of the 6-phosphate of 6PG in the E:6PG binary complex. Residues S128 and N187 are within hydrogen-bonding distance to both 6PG in the E:6PG binary complex and NADPH in the E:NADPH binary complex, suggesting that these two residues may play a dual role during the catalytic reaction. In addition, residue H186 also hydrogen bonds to NADPH in the E:NADPH binary complex, while in the E:6PG binary complex it is within hydrogen-bonding distance to S128 and N187. In this study, alanine mutagenesis was used to probe the contribution of each of the eleven residues to binding the cofactor/substrate and to catalysis.

All mutant enzymes in the 2'-phosphate site exhibit an increase in K_{NADP} that ranges from 6-fold to 80-fold. A 7-fold increase in the primary kinetic ^{13}C-isotope

effect minus 1 in all mutant enzymes indicates that the decarboxylation step has become more rate-limiting. All mutant enzymes in the 6-phosphate site, with the exception of T262A exhibit an increase in K_{6PG} that ranges from 5-fold to 800-fold. The R287A and R446A mutant enzymes exhibit a dramatic decrease in V/E_t (600-fold and 300-fold, respectively) as well as in $V/K_{6PG}E_t$ (10^5-fold and 10^4-fold). All mutant enzymes also exhibit at least an order of magnitude increase in ^{13}C-isotope effect minus 1, indicating that the decarboxylation step has become more rate-liming. The S128A, H186A and N187A mutant enzymes exhibit a decrease in V/E_t, ranging from 7-fold to 67-fold. An increase in K_{6PG} was observed for S128A and H187A mutant enzymes. An increased $K_{i\ NADPH}$ was measured for all of the mutant enzymes, and all mutant enzymes also exhibit an increase in the primary kinetic ^{13}C-isotope effect minus 1, indicating that the decarboxylation step has become more rate-limiting.

Data are consistent with significant roles for N32, R33 and T34 in providing binding energy for NADP, and Y191, K260, T262, R287 and R446 in providing the binding energy for 6PG. In addition, these residues also likely ensure proper orientation of NADP/6PG for catalysis and aid in inducing the conformation change that precedes catalysis. Data also suggest that residues S128, H186 and N187 help to guide the isomerization of the cofactor and provide binding energy for NADPH.

CHAPTER 1

INTRODUCTION

1.1 Pentose Phosphate Pathway.

6-Phosphogluconate dehydrogenase (EC 1.1.1.44, 6PGDH) is the third enzyme in the pentose phosphate pathway. The pentose phosphate pathway [also called the phosphogluconate pathway or the hexose monophosphate (HMP) shunt] is the alternate way of glucose oxidation and is the major source of NADPH, the reducing power which is involved in utilizing the free energy of metabolite oxidation for reductive biosynthesis (*1*). Many endergonic reactions, such as the reductive biosynthesis of fatty acids and cholesterol, as well as photosynthesis, require NADPH in addition to ATP. Tissues, such as liver, mammary gland, adipose tissue, and adrenal cortex rich in pentose phosphate pathway enzymes are involved in fatty acid and cholesterol biosynthesis. Although NADPH and NADH chemically resemble each other (these coenzymes differ only by a phosphate group at the 2'-OH group of the adenosine ribose of NADPH), they are not metabolically interchangeable. This is made possible because the dehydrogenases involved in oxidative and reductive metabolism exhibit a high specificity towards their coenzymes. In normal cells, the [NAD]/[NADH] ratio is maintained near 1000, which favors metabolite oxidation,

while the [NADP]/[NADPH] ratio is near 0.01, which favors metabolite reduction. NADPH is also an important factor for maintaining the erythrocyte membrane integrity by generating reduced glutathione (GSH), catalyzed by glutathione reductase. Another function of the pentose phosphate pathway is to provide ribose phosphate for the biosynthesis of nucleic acids as well as nucleotide cofactors (Voet and Voet, 1995).

The overall reaction of the pentose phosphate pathway is:

$$3G6P + 6NADP + 3H_2O \rightleftharpoons 6NADPH + 6H^+ + 3CO_2 + 2F6P + GAP$$

The pathway can be divided into three stages: oxidative (also called oxidative branch; Figure 1-1), isomerization and epimerization, and a series of C-C bond cleavage and formations (Stage 2 and 3 are called non-oxidative branch). Only the first three oxidative reactions in the first stage are involved in NADPH production. In the oxidative reactions stage, glucose-6-phosphate (G6P) is oxidized to 6-phosphoglucono-δ-lactone by glucose-6-phosphate dehydrogenase (G6PDH) with the concomitant reduction of NADP to NADPH. Then, 6-phosphoglucono-δ-lactone is hydrolyzed to 6-phosphogluconate (6PG) by the 6-phosphogluconolactonase. Finally, 6-phosphogluconate dehydrogenase catalyzes the oxidative decarboxylation of 6-phosphogluconate to ribulose-5-phosphate (Ru5P) and CO_2 with a second NADPH produced. The NADPH produced is used for reductive biosynthesis, while

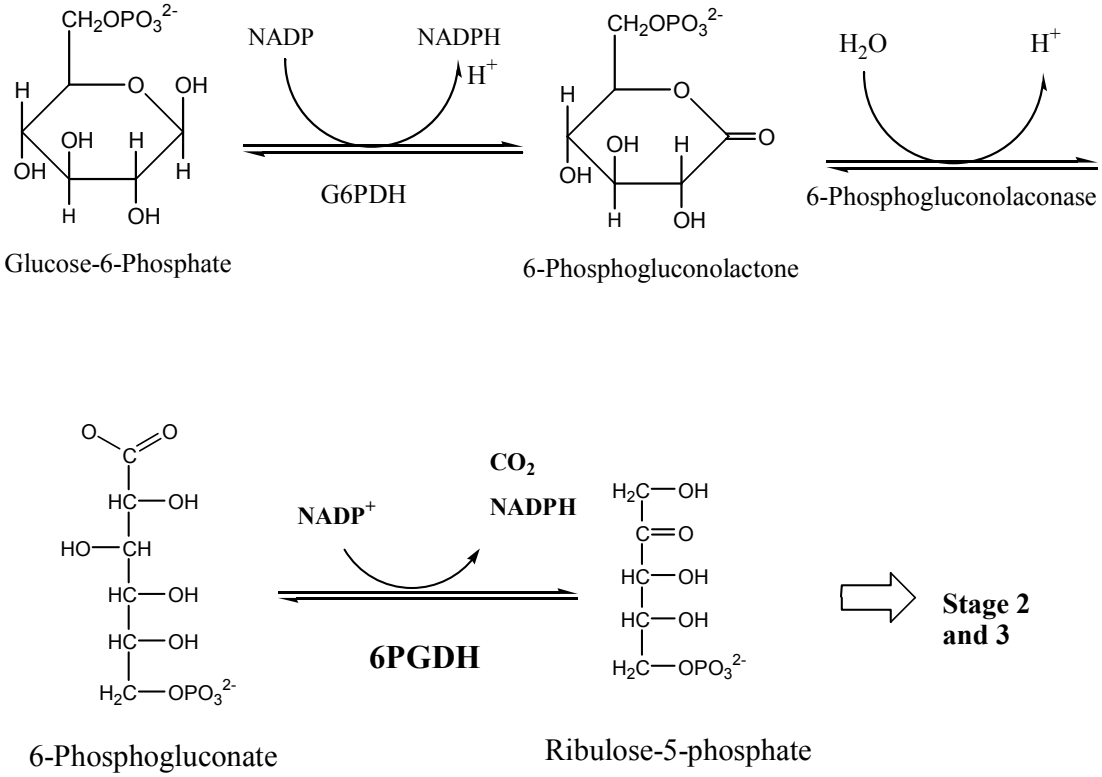

Figure 1-1. Stage 1 of the Pentose Phosphate Pathway. 6-Phosphogluconate Dehydrogenase catalyzes the reversible oxidative decarboxylation of 6-phosphgluconate to ribulose-5-phosphate and CO_2 with the reduction of NADP to NADPH.

the other product, Ru5P, enters the second stage of the pathway, which is either transformed to ribose-5-phosphate (R5P) or shunted back to the glycolytic pathway. Flux through the pentose phosphate pathway and the rate of NADPH production is controlled by G6PDH, which catalyzes the first step of the pathway. The activity of G6PDH is regulated by the NADP concentration. When the cell consumes NADPH, NADP concentration rises, and given sufficient glucose, the G6PDH activity increases, which stimulates NADPH regeneration (*1*). We will concentrate on the 6-phosphogluconate dehydrogenase (6PGDH), which catalyzes the final and irreversible step in the oxidative branch of the pathway.

6PGDH has not been reported to be related to hemolytic syndrome (*2*), as G6PDH does, however, carbamylation of 6PDGH may cause cataract in populations with high blood urea (*3*). 6PGDH from *Trypanosoma brucei* is suggested to be involved in parasitic infections (*4*).

1.2 6-Phosphogluconate Dehydrogenase.

6-Phosphogluconate dehydrogenase is the third enzyme in the pentose phosphate pathway. It catalyzes the reversible oxidative decarboxylation of 6-phosphogluconate, a β–hydroxyacid, to ribulose-5-phosphate and CO_2, reducing NADP to NADPH as shown in Figure 1-1. However, under physiological condition, the reaction is

irreversible. 6PGDH is a member of the β-hydroxyacid oxidative decarboxylases, which is a class of pyridine nucleotide-linked dehydrogenases that catalyze the oxidative decarboxylation of β-hydroxyacids. Unlike other oxidative decarboxylases, such as malic enzyme and isocitrate dehydrogenase (ICDH), 6PGDH from most sources is metal ion independent, i.e. it does not require the presence of metal ions for activity, and indeed, if the concentrations of mono- and divalent cations e.g. Na^+, K^+, Mg^{2+},exceed 0.1M, they inhibit enzyme activity. No systematic effect of anions has been observed on enzyme activity (*5, 6* and *7*).

1.2.1 Kinetic Mechanism.

Although extensive kinetic studies have been carried out for 6-phosphoglucnoate dehydrogenase from different species, including *Candida utilis*, *Cryptococcus neoformans*, *Haemophilus influenzae*, *Lactococcus*, human erythrocyte, *Schizosaccharomyces pombe*, sheep liver and *Trypanosoma brucei*, the most thoroughly studied ones are from *C. utilis* and sheep liver (*4*, *8-15*). A complete kinetic characterization of sheep liver 6PGDH including initial velocity studies, product and dead-end inhibition patterns in both reaction directions, and primary deuterium isotope effects has been performed (*12*). The initial velocity patterns in the forward reaction direction intersect to the left of the ordinate, suggesting a sequential mechanism. The V/E_t value of sheep liver 6PGDH is 9.4 s^{-1}, while the K_m values for

6PG and NADP are 25 μM and 3 μM, respectively. Product inhibition studies indicated the presence of E:NADP:Ru5P and E:NADPH:6PG dead-end complexes, suggesting a random mechanism. Equal deuterium isotope effects were measured on V, V/K_{6PG} and V/K_{NADP}, for sheep liver enzyme, indicating that hydride transfer contributes to rate-limitation (*12*, *16* and *17*). Combining all the information, Price and Cook proposed that the kinetic mechanism of the sheep liver 6PGDH is rapid equilibrium random (Figure 1-2) (*12*), consistent with the kinetic mechanism proposed for the 6PGDH from *C. utilis* (*10*).

The theory and methodology for the application of multiple isotope effects to enzyme catalyzed reactions allowed a distinction to be made between a concerted and stepwise mechanism and provides estimates of the intrinsic isotope effects on the bond-breaking steps (*18*). Hwang et al. measured primary kinetic deuterium, ^{13}C and multiple deuterium/^{13}C isotope effects for the *C. utilis* and sheep liver enzymes, using NADP and APADP as the dinucleotide substrates (*19*). A decrease in $^{13}(V/K_{6PG})$ with 3-*d*-6PG compared to 3-*h*-6PG was observed in all cases, indicating that the hydride transfer step is more rate limiting with the deuteriation at C3, and the decarboxylation step, i.e. the ^{13}C sensitive step, becomes partially masked, signaling a stepwise mechanism with oxidation preceding decarboxylation.

Based upon the collected isotope effect data, intrinsic isotope effects have been

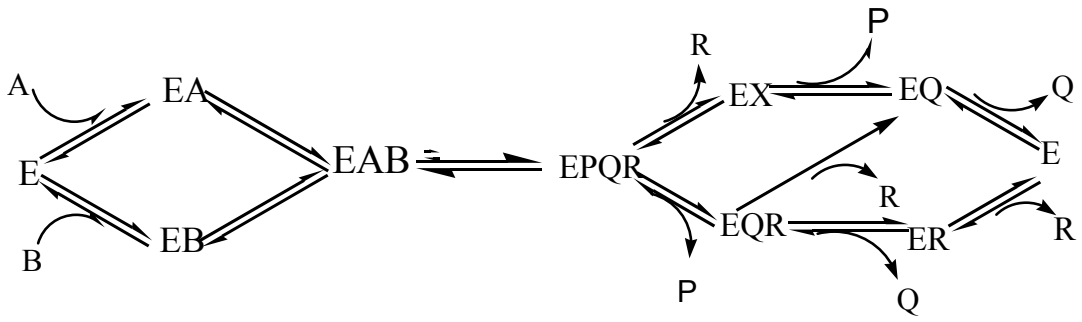

E=6PGDH A=NADP+ B=6PG
P=CO2 Q=Ru-5-P R=NADPH
X=3-keto-6-phophogluconate

Figure 1-2. The Proposed Rapid Equilibrium Random Kinetic Mechanism for Sheep Liver 6PGDH.

estimated for *Candida* 6PGDH, which provides information on transition state structure (*19*). The following range of values was obtained: ^{D}k, 2.9-3.3; C_f, 0.15-1.52; C_r, 0.23-0.79; and ^{13}k, 1.027-1.062, where C_f and C_r are the forward and the reverse commitments to catalysis, respectively, ^{D}k is the intrinsic primary deuterium isotope effect, and ^{13}k is the primary ^{13}C-isotope effect. Although ^{D}k is the best defined parameter, which represents the hydride transfer from C3 of 6PG to C4 of the nicotinamide ring of NADP, it does not distinguish an early or late transition state for hydride transfer according to Westheimer's theory (*20*, *21*). The range of 1.027-1.062 for ^{13}k suggests a later transition state for C1-C2 bond cleavage because the ^{13}C-isotope effect is expected to increase from a value very close to 1 for a very early transition state to a value of 1.05-1.07 for a late transition state. The partition ratio for the 3-keto-6PG intermediate, which is the ratio of the rates of reduction to 6PG to the rate of decarboxylation, represented by C_r is relatively small, suggesting that either an increase in the energy barrier for the reduction of 3-keto-6PG intermediate, a decrease in the energy barrier for its decarboxylation, or both can exist.

In 1973, Rippa used 2-deoxy-6-PG as an alternative substrate for sheep liver 6PGDH. The 2-deoxy-3-keto intermediate is released from the enzyme since the next step, decarboxylation, is slow, and the decarboxylation only occurs in the presence of NADPH (*22*). This result is consistent with the proposed step-wise mechanism with

hydride transfer preceding decarboxylation.

The proton inventory method was utilized to obtain information on the number and fractionation factor for proton(s) being transferred in the rate-limiting transition states. Primary solvent deuterium, multiple solvent deuterium/substrate deuterium and multiple solvent/^{13}C isotope effects were measured and suggest the presence of a significant medium effect in a step preceding hydride transfer, likely a conformational change, and the presence of a kinetic solvent deuterium isotope effect on hydride transfer, indicating that proton transfer and hydride transfer occur in the same step (*23*).

1.2.2 Substrate Specificity.

6PGDH is specific for NADP. Sheep liver 6PGDH has a K_{NADP} of about 5μM. NAD has been shown to be a poor substrate for the *C. utilis* enzyme with a K_m 1000 times that for NADP (*10*). In addition, NAD 3'-phosphate is also a poor substrate. Thus, the 2'-phosphate of NADP is critical for optimum binding and/or catalysis. Changes at the adenine ring, such as with nicotinamide hypoxanthine dinucleotide 2'-phosphate and ε–NADP, have little effect on activity. Changes in the nicotinamide ring, such as with 3-acetylpyridine adenine dinucleotide 2'-phosphate (APADP) and thio-NADP give slight changes in V/E_t and $V/K_{cofactor}\,E_t$.

6PGDH is relatively specific for the 6PG/Ru5P substrate/product pair. The best

alternative substrate is 2-deoxy-6PG, in which a proton substitutes the 2-hydroxyl group of 6PG. The V/E_t in this case is down about 100 fold and the immediate product of the reaction is 2-deoxy-3-keto-6PG (3Kd6PG) (*22*). The *C. utilis* enzyme can use 6-phosphomannonic acid (with the stereochemistry at C2 reversed compared to 6PG) as a substrate, but with a V/E_t 1,000 fold lower than that obtained with 6PG (*10*). Data obtained with these two analogs show the importance of the 2-hydroxyl group in the reaction. Changes in the stereochemistry of C3, C4 positions, e.g. 6-phosphoallonate and 6-phosphogalactonate, as well as changes in the 6-phosphate group, e.g. 6-sulfogluconate, eliminate substrate activity. This suggests that these positions are critical for optimum enzyme activity.

1.2.3 Chemical Mechanism.

6PGDH is classed as a pyridine nucleotide linked dehydrogenase. A general acid- general base mechanism has been proposed for this class of enzyme. Since 6PGDH is slightly different from the typical enzymes in this class by being metal ion independent, it became interesting to Cook and his coworkers.

The hypothesis of a Schiff-base intermediate mechanism was ruled out by studies carried out previously (*24*). In their experiment, $H_2{}^{18}O$ was used as a solvent exchange probe for the forward reaction direction and [2-^{18}O] Ribulose-5-phosphate was prepared as a substrate for the reverse reaction direction. If a Schiff-base

intermediate is involved in the decarboxylation step, solvent exchange will occur with the C-2 oxygen of the 3-keto intermediate. However, they observed a complete retention of the labeled oxygen for the reductive carboxylation and the product of the oxidative decarboxylation remained unlabeled. This result excludes the possibility of a Schiff-base mechanism.

The pH dependence of the kinetic parameters of the *C. utilis* enzyme has been investigated and a general acid-general base chemical mechanism has been proposed (*11*) (Figure 1-3). In this mechanism, an active site general base is required to accept a proton from the 3-hydroxyl group of 6PG concomitant with a hydride transferring from C-3 of 6PG to the coenzyme. The resulting 3-keto-6-PG intermediate is decarboxylated to produce the enediol of Ru5P. The same general base shuttles the proton between itself and the sugar oxygen throughout the reaction, and ultimately accepts it as ribulose is formed. A general acid is needed to assist the tautomerization of the enediol of Ru5P to the keto product by protonating the C-1 of the enediol of Ru5P. Price and Cook performed the same studies on sheep liver 6PGDH and came to a similar conclusion.

From the crystal structures of sheep liver 6PGDH, the completely conserved K183 and Glu190 have been proposed to be the best candidate for general base and general acid, respectively (*12*, *25*). The pH profiles yield pK values of about 6 and 8

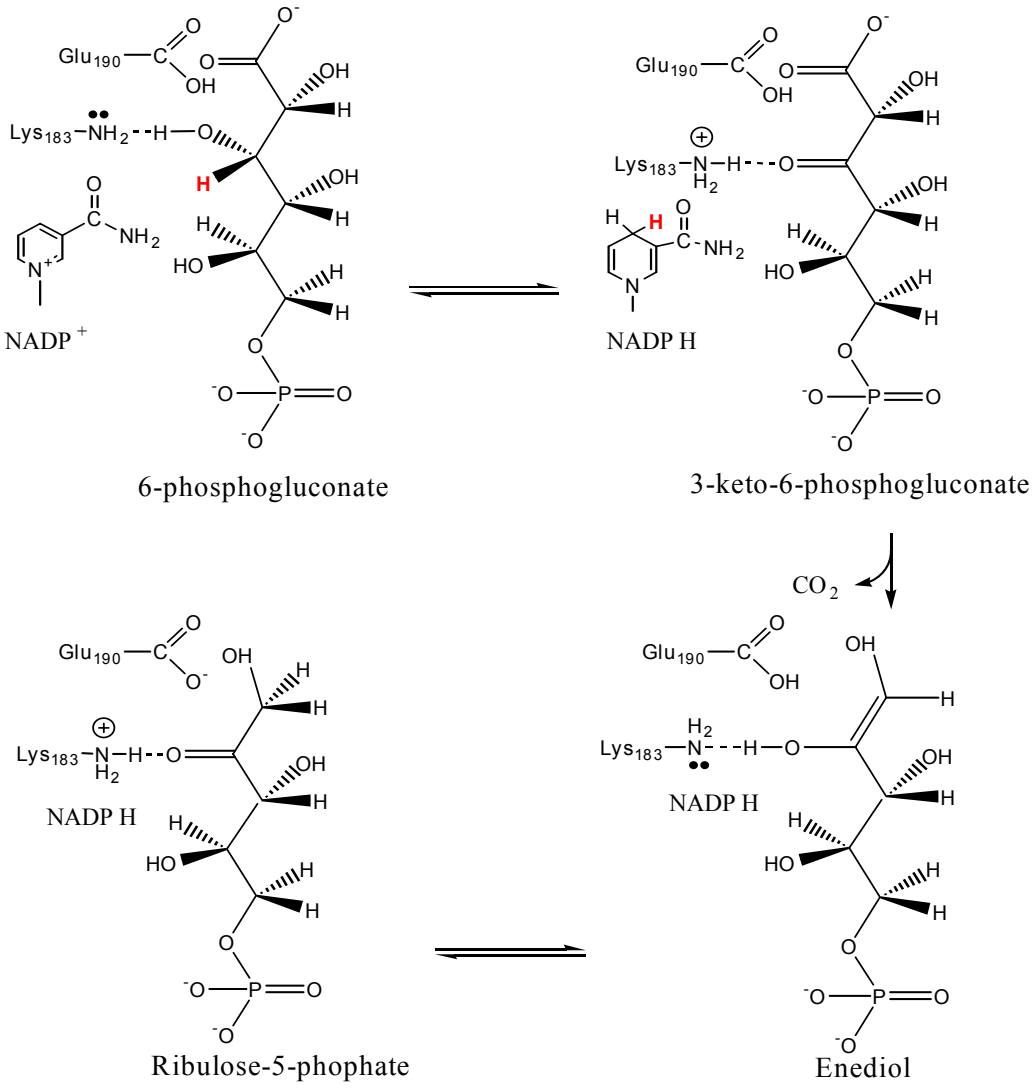

Figure 1-3. The proposed general acid-general base chemical mechanism of 6-Phosphogluconate Dehydrogenase.

(*12*). If the assignment of acid-base catalytic groups is correct, then K183 should have a pK of 8 even though it has to be unprotonated, while E190 has a pK of 6 even though it has to be protonated. Therefore Price and Cook proposed reverse protonation states between the general acid and the general base for the sheep liver 6PGDH (*12*) and this hypothesis is in agreement with the unionized form of Glu190 hydrogen bonding to the 1-carboxylate of 6PG (*25*). Although the solution pK of lysine and glutamate side chain is 10.5 and 4.5, respectively, the hydrophobic environment of the active site will favor neutral species, which will make the observed pK possible.

1.2.4 Structure of 6-Phosphogluconate Dehydrogenase.

The three-dimensional structures of 6PGDH from several sources, including sheep liver, *Trypanosoma brucei*, and *Lactococcus lactis*, have been solved by X-ray crystallography (*15*, *25*, and *26*).

The crystal structures of sheep liver 6PGDH, including the apo-enzyme, enzyme-6PG, enzyme-NADPH binary complexes as well as enzyme-substrate analogs have been solved (*25*). Sheep liver 6PGDH is a homodimer with a subunit molecular weight of 51,000. The dimer has molecular two fold symmetry. Each subunit is comprised of 482 amino acids and can be divided into three domains: the dinucleotide binding domain, the helical domain and the C-terminal tail. The monomeric enzyme

structure is depicted in Figure 1-4.

The dinucleotide binding domain is also called the N-terminal β-α-β domain (residues 1-176). This domain has a typical Rossman-fold, which is often found in dinucleotide binding protein, followed by a short helix and an additional β-α-β unit antiparallel to the first one. The second domain (residues 177-434) is the largest domain and it has a repeated five-helix motif, which is almost identical in structure. The C-terminal tail (residues 435-482) has a single helix and it penetrates into the second subunit. Beyond Gly473, the tail is disordered. The active site resides in the bottom of the cleft formed by the first two domains and consists of residues from all three domains: the dinucleotide binding domain, the helical domain and the C-terminal tail from the other subunit (Figure 1-5), which is not common to other β-hydroxyacid oxidative decarboxylases.

According to the crystallographic studies, there may be conformational changes upon binding coenzyme and substrate. By comparing the positional parameters between the apo-enzyme and the protein in E:Nbr^{8}ADP (nicotinamide-8-bromo-adenine dinucleotide phosphate, the active NADP analog), E:2'AMP and E:6PG complexes, Adams et al. suggested that there is little protein movement required to accommodate the coenzyme (*25*). The most prominent change is the ordering of the side chain of Arg33, which is disordered in the native enzyme,

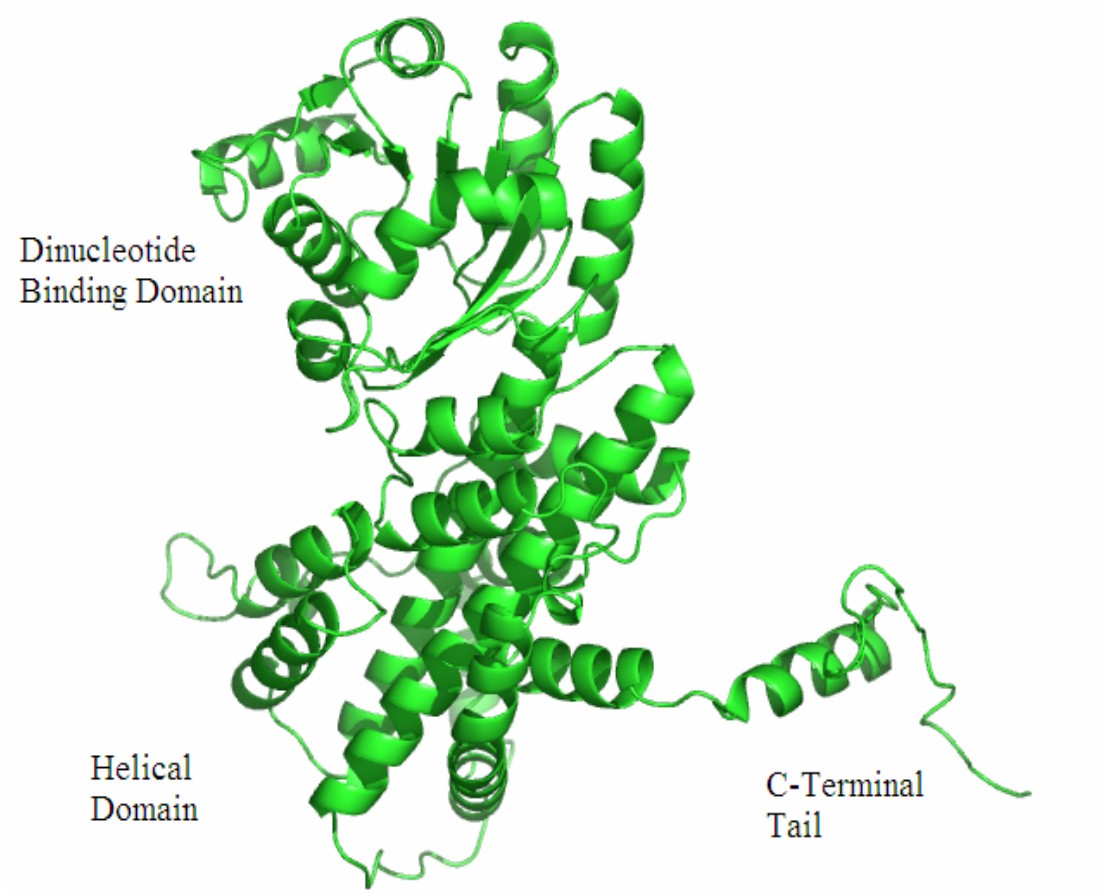

Figure 1-4. Structure of a Monomer of Sheep Liver 6-Phosphogluconate Dehydrogenase. Each monomer has three domains: a dinucleotide binding domain, a large helical domain, and a C-terminal tail.

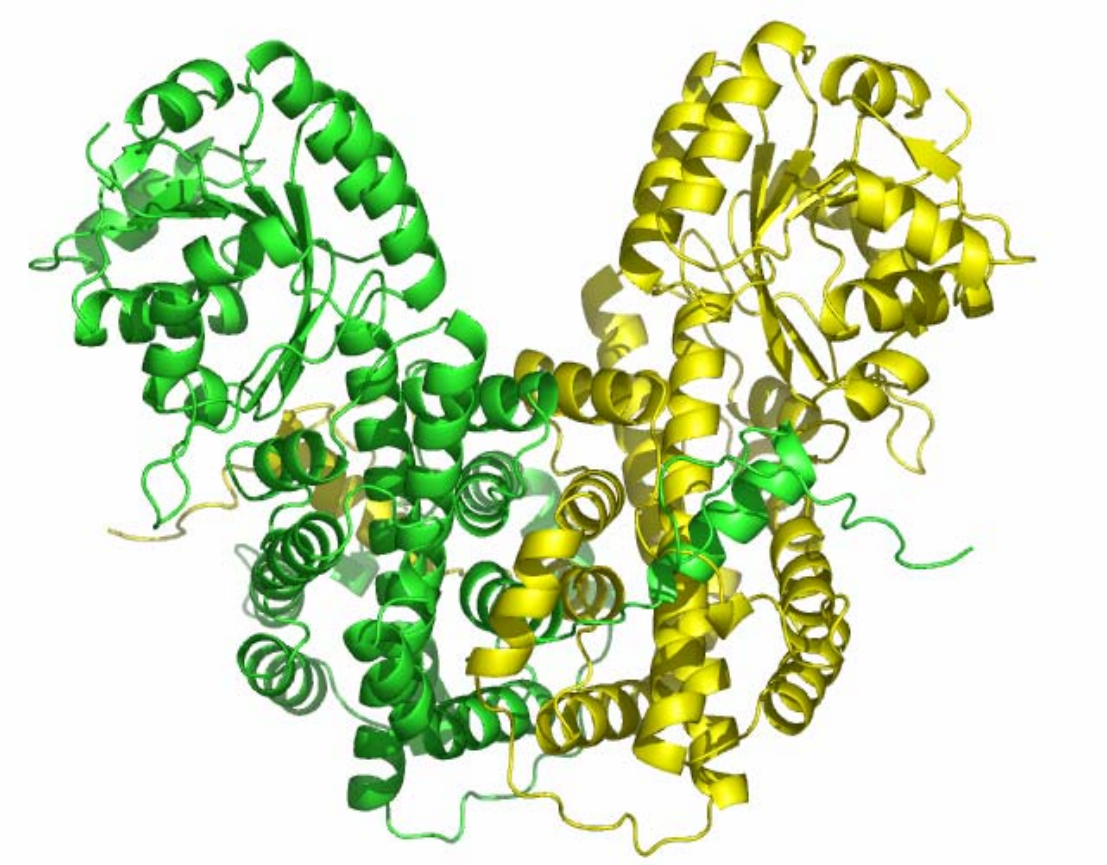

Figure 1-5. Structure of the dimer of Sheep Liver 6-Phosphogluconate Dehydrogenase.

but is visible in all coenzyme difference maps. A small movement of some of the residues in two loops: 73-78 and 130-133 is also detected. Upon binding coenzyme, the solvent accessibilities of several residues in the binding site are decreased and hydrophobic residues are more exposed, which contribute to an exposed hydrophobic patch. In the 6PG complex, the substrate binds to the protein with only a small movement of protein residues. The removal of the two sulphates and four waters in the active site pocket is the most important change. It is suggested that the coenzyme undergoes a conformational change upon hydride transfer. The evidence for this hypothesis is that the conformations of Nbr^8ADP, the active NADP analog, and of NADPH differs remarkably when they are in the enzyme. The conformations of the adenine, adenine ribose and 2'-phosphate are very similar in the E: Nbr^8ADP, E:2'AMP and E:NADPH structures and the difference essentially comes from the nicotinamide ring. The nicotinamide ring in the E: Nbr^8ADP complex is very close to *syn* conformation, while in the E:NADPH structure, the nicotinamide ring flips over. This change brings the nicotinamide ring of NADPH closer to the substrate binding domain and therefore may affect the binding mode of 6PG.

The oxidized coenzyme makes contacts only with residues in the coenzyme domain, while the reduced coenzyme makes large number of hydrogen bond contacts with the protein, including those residues that interact with substrate in the E:6PG

complex. If the locations of the nicotinamide rings of Nbr^8ADP and NADPH represent the positions of the coenzyme prior and after the hydride transfer (*27*), then upon hydride transfer the less bonded NADP is brought to the position where more hydrogen bonds could be made. And since the new interactions of the coenzyme are with the same protein residues that bind 6PG, then it may displace the substrate and therefore facilitate decarboxylation or produce release. This may also explain that why the E:NADPH:reduced 6PG ternary complex can not be obtained (*25*). More recently, Cervellati et al. mutated Met13 of sheep liver 6PGDH to valine, isoleucine, cysteine, phenylalanine, and glutamine. All the resulting mutant enzymes have a decreased affinity for NADP, but not for NADPH (*28*), with the exception of the cysteine mutant. This experiment proved that the binding mode of NADP is different from that of NADPH, therefore the flipping of the nicotinamide ring of the coenzyme observed from the crystallographic study is real, i.e. the rotation is on the reaction pathway, but not due to crystallization effect. Therefore, a modified mechanism with hydride transfer accompanied by the rotation of the nicotinamide ring around the N-glycosidic bond is proposed (*28*, Figure 1-6).

Similar phenomenon that different conformers of bound oxidized and reduced coenzyme has been observed in two other NAD-dependent aldehyde dehydrogenases and NAD-malic enzyme (*29-32*). Cervellati et al. proposed that this mechanism may

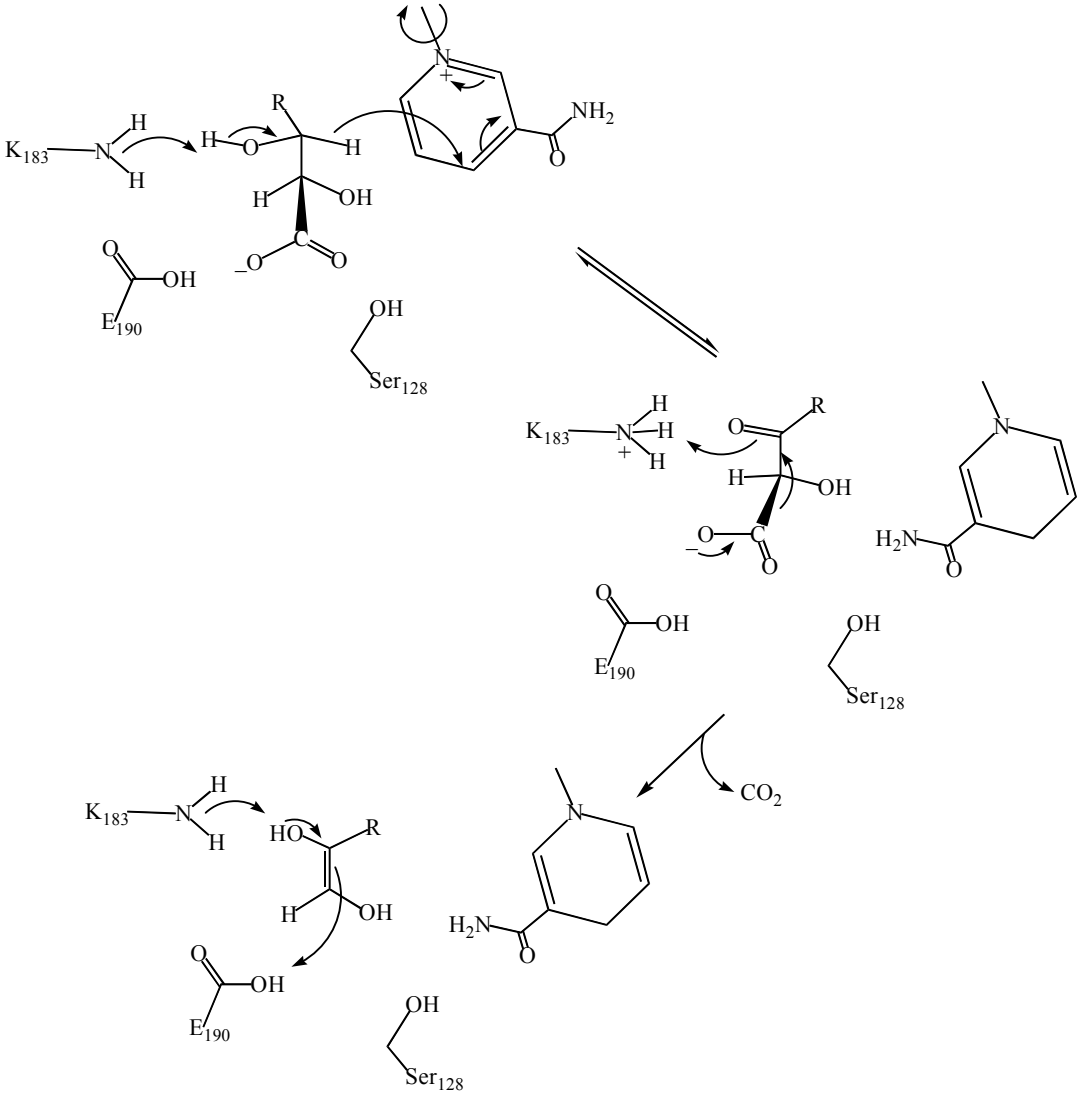

Figure 1-6. Modified Chemical Mechanism for 6-Phosphogluconate Dehydrogenase.

be common for the pyridine nucleotide-linked oxidative decarboxylases (*28*).

1.2.5 Theory on 6-Phosphogluconate Dehydrogenase.

6PGDH from human erythrocytes has been used to study its mechanism (*8*). Binding studies shows that 1 molecule of the dimeric enzyme binds 2 molecules of NADP, but only 1 molecule of NADPH per molecule of enzyme. The binding of oxidized and reduced coenzyme are mutually exclusive. The initial velocity kinetic and inhibition studies shows a negative co-operativity, which is proposed to be the result of the half-site reactivity for 6PGDH. In 1992, Hanau et al. carried out experiments with sheep liver 6PGDH, using 2-deoxy-6PG and 1,6-NADPH as substrate analogs (*33*). They suggested that NADPH plays a role in activating the decarboxylation reaction. The reason being: (i) the decarboxylation of 3Kd6PG does not occur with the enzyme alone, (ii) it does not occur when the concentration of NADPH is low or when NADPH is recycled, (iii) it occurs when NADPH is formed or added. Then they used periodate-oxidized NADP (oNADP) to inactivate the enzyme (*33*). In the presence of substrate, the inactivation is faster and almost complete after the labeling of only one subunit. They proposed that these results not only confirm the hypothesis of a ‘half-of-the-sites’ mechanism of action of the enzyme, but also suggest that the formation of the ternary complex in one subunit causes a conformational change that inactive the other subunit.

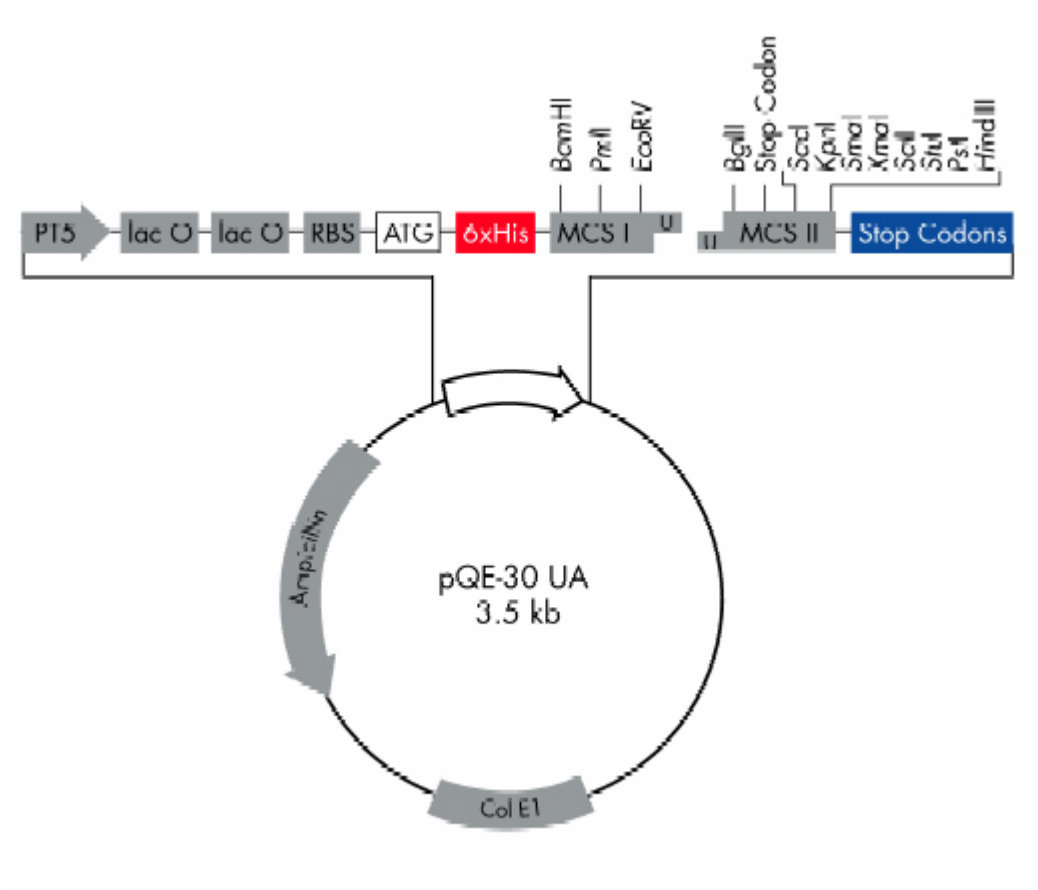

Figure 1-7. Map of pQE30 vector. The insertion a 1.5 kb 6-Phosphogluconate Dehydrogenase cDNA is between the *EcoR* I-*Bam H*I sites.

1.2.6 Cloning, Sequencing, Expression, and Purification of 6-Phosphogluconate Dehydrogenase.

Previously, several attempts to isolate a cDNA clone of 6PGDH were unsuccessful. The cDNA sequence, however, was obtained by PCR amplification and a family of overlapping cDNA clones encoding a mature protein of 482 amino acids was generated (*34*). A cDNA of the gene that encode the enzyme from sheep liver was obtained using RT-PCR and cloned it into a pBluescript phagemid. An expression vector, pKK223-3, was used to subclone the cDNA. Expression and purification resulted in copurification of the host 6PGDH (*Escherichia coli*) with the sheep liver recombinant enzyme. Therefore, the cDNA was subcloned into pQE-30, which adds a 6-membered histidine tag to the N-terminus of 6PGDH (Figure 1-7). The pQE plasmids contain an optimized, regulatable promoter/operator element, including the *E. coli* phage T5 promoter and two *lac* operator sequences. Expression from this system is highly efficient and only high level of *lac* repressor can prevent it. M15[pREP4] is used as the host strain, which contains multiple copies of the plasmid pREP4, carrying the *lacI* gene encoding the *lac* repressor. Expression of the recombinant protein from pQE vectors is achieved by addition of isopropylthio-β-D-galactoside (IPTG), which physically mimics lactose and can bind to the lac repressor, preventing it from binding the lac operator, and therefore induces

the expression of the protein. The purification system uses a metal chelate adsorbent, Ni-NTA (nitrilo-tri-acetic acid), resin that has extremely high affinity for proteins containing several consecutive histidine residues (*35*). The binding capacity of the Ni-NTA resin is approximately 5-10 mg protein per ml of resin. The purified enzyme has been characterized and the kinetic parameters within error are identical to those measured for the native sheep liver 6PGDH (*36*).

1.3 Specific Goals of This Study.

Although the kinetic and chemical mechanism of sheep liver 6PGDH has been proposed, the mechanism is not completely understood and the functions of some of the important residues still remain unclear. The purpose of this research is to investigate the functions of these residues and quantitate their contributions, which can help us better understand the mechanism of sheep liver 6PGDH.

Three groups of active site residues are discussed here. They are Asn32, Arg33, and Thr34, hydrogen bonding to the 2'-phosphate of NADP; Tyr191, Lys260, Thr262, Arg287 and Arg446, hydrogen bonding to and lining the binding site of 6PG; And Ser128, hydrogen bonding to the 1-carboxylate of 6PG; Asn187, responsible for binding the 3-hydroxyl group of 6PG and together with His186, Ser128 and Asn187 hydrogen bonding to the nicotinamide of NADPH. In this research, each of these

identified residues was mutated to alanine, one at a time, to eliminate their interactions with the coenzyme/substrate.

The hypothesis of this research can be divided into three parts according to the three groups of active site residues and they are:

1. Asn32, Arg33 and Thr34 are important in providing the binding energy and determining the specificity of the enzyme for the cofactor.
2. Tyr191, Lys260, Thr262, Arg287 and Arg446 are important in binding the substrate and/or in catalysis.
3. Ser128, His186 and Asn187 are important in binding 6PG, NADPH and catalysis.

1.4 References.

1. Voet D. and Voet J. G. (1995) The Pentose Phosphate Pathway. In *Biochemistry* (2nd ed.), pp. 617-625, John Wiley and Sons, Inc, USA.

2. Luzzato, L. and Mehta, A. (1989) *Glucose-6-Phosphate Dehydrogenase Deficiency. In The Metabolic Basis of Inherited Disease* (6th ed., Scriver, C. R. Beudet, A., Sly, W. S., and Valle, D., Eds.), pp. 2237-2265, McGraw-Hill, Inc., USA.

3. Ganea, E., and Harding, J. J. (1996) Inhibition of 6-Phosphogluconate Dehydrogenase by Carbamylation and Protection by Alpha-Crystallin, a Chaperone-like Protein. *Biochem. Biophys. Res. Commun.* 222, 626-631.

4. Hanau, S., Rippa, M., Bertelli, M., Dallocchio, F., and Barrett, M. P. (1996) 6-Phosphogluconate Dehydrogenase from *Trypanosoma brucei*. Kinetic Analysis and Inhibition by Trypanocidal Drugs. *Eur. J. Biochem.* 240, 592-599.

5. Siebert, G., Carsiotis, M., and Plaut, G. W. E. (1957) The Enzymatic Properties of Isocitric Dehydrogenase. *J. Biol. Chem.* 226, 977-991.

6. Pntremoli, S., de Flora, A., Grazi, E., Mangiarotti, G., Bondignore, A., and Horecker, B. L. (1961) Crystalline D-Gluconate 6-Phosphate Dehydrogenase. *J. Biol. Chem.* 236, 2975-2980.

7. Dyson, J. E. D., D'Orazio, R. E., and Hanson, W. H. (1973) Sheep Liver 6-Phosphogluconate Dehydrogenase: Isolation Procedure and Effect of pH, Ionic Strength, and Metal Ions on the Kinetic Parameters. *Arch. Biochem. Biophys.* 154, 623-625.

8. Dallocchio, F., Matteuzzi, M., and Bellini, T. (1985) Half-Site Reactivity in 6-Phosphogluconate Dehydrogenase from Human Erythrocytes. *Biochem. J.* 227, 305-310.

9. Yoon, H, Anderson, C. D., and Anderson, B. M. (1989) Kinetic Studies of *Haemophilus influenzae* 6-Phosphogluconate Dehydrogenase. *Biochem. Biophys. Acta.* 994, 75-80.

10. Berdis, A. J. and Cook, P. F. (1993a) Overall Kinetic Mechanism of 6-Phosphogluconate Dehydrogenase from Candida utilis. *Biochemistry* 32, 2036-2040.

11. Berdis, A. J. and Cook, P. F. (1993b) Chemical Mechanism of 6-Phosphogluconate Dehydrogenase from Candida utilis from pH studies. *Biochemistry* 32, 2041-2046.

12. Price, N. E. and Cook, P. F. (1996) Kinetic and Chemical Mechanism of the Sheep Liver 6-Phosphogluconate Dehydrogenase. *Arch. Biochem. Biophys.* 336, 215-223.

13. Niehuas, W. G., Richardson, S. B. and Wolz, R. L. (1996) Slow-Binding Inhibition of 6-Phosphogluconate Dehydrogenase by Zinc Ion. *Arch. Biochem. Biophys.* 333, 333-337.

14. Tsai, C. S. and Chen, Q. (1998) Purification and Kinetic Characterization of 6-Phosphogluconate Dehydrogenase from *Schizosaccharomyces pombe*. *Biochem.*

Cell. Biol. 76, 637-644.

15. Tetaud, E., Hanau, S., Wells, J. M., Le Page, R. W., Adams, M. J., Arkinson, S. and Barrett, M. P. (1999) 6-Phosphogluconate Dehydrogenase from *Lactococcus lactis*: A Role for Arginine Residues in Binding Substrate and Coenzyme. *Biochem. J.* 338, 55-60.

16. Cook, P. F. and Cleland, W. W. (1981) Mechanistic Deduction from Isotope Effects for Bi-reactant Enzyme Reactions. *Biochemistry* 20, 1790-1796.

17. Rendina, A. R. Hermes, J. D. and Cleland, W. W. (1984) Use of Multiple Isotope Effects to Study the Mechanism of 6-Phosphogluconate Dehydrogenase. Biochemistry 23, 6257-6262.

18. Hermes, J. D., Roeske, C. A., O'Leary, M. H. and Cleland, W. W. (1982) Use of Multiple Isotope Effects to Determine Enzyme Mechanisms and Intrinsic Isotope Effects, Malic Enzyme and Glucose-6-Phosphate Dehydrogenase. *Biochemistry* 21, 5106-5114.

19. Hwang, C-C., Berdis, A. J., Karsten, W. E., Cleland, W. W. and Cook, P. F. (1998) Oxidative Decarboxylation of 6-Phosphogluconate by 6-Phosphogluconate Dehydrogenase Proceeds by a Stepwise Mechanism with NADP and APADP as Oxidants. *Biochemistry* 37, 12596-12602.

20. Westheimer F. H. (1961) *Chem. Rev.* 61, 265-273.

21. Sühnel, J. and Schowen, R. L. in *Enzyme Mechanism from Isotope Effects* (Cook, P. F. ed., 1991), pp. 3-35, Boca Raton, FL:CRC.

22. Rippa, M., Signorini, M. and Dallocchio, F. (1973) A Multiple Role for the Coenzyme in the Mechanism of Action of 6-Phosphogluconate Dehydrogenase. *J. Biol. Chem.* 248, 4920-4925.

23. Hwang, C-C. and Cook, P. F. (1998) Multiple Isotope Effects as a Probe of Proton and Hydride Transfer in the 6-Phosphogluconate Dehydrogenase Reaction. *Biochemistry* 37, 15698-15702.

24. Topham, C. M. and Dalziel, K. (1986) The Chemical Mechanism of Sheep Liver 6-Phosphogluconate Dehydrogenase. A Schiff-base Intermediate Is Not Involved.

Biochem. J. 234, 671-677.

25. Adams, M. J., Ellis, G. H., Cover, S., Naylor, C. E. and Phillips, C. (1994) Crystallographic Study of Coenzyme, Coenzyme Analogue and Substrate Binding in 6-Phosphogluconate Dehydrogenase: Implications for NADP Specificity and the Enzyme Mechanism. *Structure* 2, 651-668.

26. Phillips, C., Dohnalek, J., Cover, S., Barrett, M. P. and Adams, M. J. (1998) A 2.8 Å Resolution Structure of 6-Phosphogluconate Dehydrogenase from the Protozoan Parasite Trypanosoma brucei: Comparison with the Sheep Enzyme Accounts for Difference in Activity with Coenzyme and Substrate Analogues. *J. Mol. Biol.* 282, 667-681.

27. Zhang, L., Chooback, L. and Cook, P. F. (1999) Lysine 183 Is the General Base in the 6-Phosphogluconate Dehydrogenase-Catalyzed Reaction. *Biochemistry* 38, 11231-11238.

28. Cervellati, C., Dallocchio, F., Bergamini, C. M. and Cook, P. F. (2005) Role of Methionine-13 in the Catalytic Mechanism of 6-Phosphogluconate Dehydrogenase from Sheep Liver. *Biochemistry* 44, 2432-2440.

29. Hammen, P. K., Alliali-Hassani, A., Hallenga, K., Hurley, T. D. and Weiner, H. (2002) Multiple Conformations of NAD and NADH When Bound to Cytosolic and Mitochondrial Aldehyde Dehydrogenase. *Biochemistry* 41, 7156-7168.

30. Coleman, D. E., Rao, G. S. J., Goldsmith, E. J., Cook, P. F. and Harris, B. G. (2002) Crystal Structure of the Malic Enzyme from *Ascaris suum* Complexed with Nicotinamide Adenine Dinucleotide at 2.3 Å Resolution. *Biochemistry* 41, 6928-6938.

31. Perez-Miller, S. J. and Hurley, T. D. (2003) Coenzyme Isomerization Is integral to Catalysis in Aldehyde Dehydrogenase. *Biochemistry* 42, 7100-7109.

32. Rao, G. S. J., Coleman, D. E., Karsten, W. E., Cook, P. F. And Harris, B. G. (2003) Crystallographic Studies on *Ascaris suum* NAD-Malic Enzyme Bound to Reduced Cofactor and Identification of an Effector Site. *J. Biol. Chem.* 278, 38051-38058.

33. Hanau, S., Dallocchio, F. and Rippa, M. (1992) NADPH Activates a Decarboxylation Reaction Catalyzed by Lamb Liver 6-Phoaphogluconate

Dehydrogenase. *Biochem. Biophys. Acta.* 1122, 273-277.

34. Somers, D., Medd, S. M., Walker, J. E. and Adams, M. J. (1992) Sheep 6-Phosphogluconate Dehydrogenase: Revised Protein Sequence Based upon the Sequences of cDNA Clones Obtained with the Polymerase Chain Reaction. *Biochem. J.* 288, 1061-1067.

35. Hochuli, E., Döbeli, H. and Schacher, A. (1987) New Metal Chelate Adsorbents Selective for Proteins and Peptide Containing Neighboring Histidine Residues. *J. Chromatography* 411, 177-184.

36. Chooback, L., Price, N. E., Karsten, W. E., Nelson, J., Sundstrom, P. R. and Cook, P. F. (1998) Cloning, Expression, Purification, and Characterization of the 6-Phosphogluconate Dehydrogenase from Sheep Liver. *Protein Expression and Purification* 13, 251-258.

CHAPTER 2

IMPORTANCE OF THE 2'-PHOSPHATE OF NADP

2.1 Introduction.

6-Phosphogluconate dehydrogenase (6PGDH1; EC 1.1.1.44) catalyzes the reversible oxidative decarboxylation of 6-phosphogluconate (6PG), producing ribulose-5-phosphate (Ru5P) and CO_2 with the concomitant reduction of NADP to NADPH. The kinetic mechanism is rapid equilibrium random on the basis of a complete kinetic characterization of the enzymes from sheep liver and *Candida utilis* (*1, 2*). The pH dependence of kinetic parameters indicates a general acid-general base chemical mechanism (*1, 2*), and site-directed mutagenesis studies suggest that K183 and E190 are likely the general base and the general acid, respectively (*3, 4*). In this mechanism, the general base (K183) is required to accept a proton from the 3-hydroxyl group of 6PG concomitant with hydride transfer from C-3 of 6PG to the coenzyme. Reduction of the nicotinamide ring is accompanied by rotating around the N-glycosidic bond such that the ring occupies the position formerly occupied by the 1-carboxylate of the substrate (*5*). The resulting 3-keto-6-phosphogluconate intermediate is decarboxylated to produce the enediol of Ru5P with the general base used to protonate the carboxyl oxygen. A general acid (E190) is needed to facilitate the tautomerization of the enediol of Ru5P to the keto product (Figure 1-6).

6PGDH is specific for the substrate 6PG; the best alternative substrate is 6-phosphomannonate, which has a V/E_t 10^3-fold lower, and a $V/K_{6PM}E_t$ 10^5-fold lower than values obtained with 6PG (*21*). The enzyme also has a very high specificity toward its cofactor NADP; the $V/K_{NAD}E_t$ is 10^5-fold lower than that obtained with NADP (*7*). Most of the direct interactions between the protein and the cofactor are made to the 2'-phosphate (*6*). Removal of the 2'-phosphate of NADP decreases the affinity more than 1,000-fold (*7*). In the structure of the E:Nbr^{8}ADP (the active NADP analog) binary complex, the 2'-phosphate interacts with three active-site residues that are within hydrogen-bond distance: N32, R33 and T34 (*6*). Multiple sequence alignment of 6PGDH shows that N32 is completely conserved, while R33 is replaced by tyrosine in the *Bacillus Licheniformis* and *Bacillus subtilis* sequences, which can use NAD as a cofactor, and T34 is replaced by serine in some species (Figure 2-1). Data indicate that identical hydrogen-bond potential can be retained at residues 32 and 34, while the ionic interaction at residue 33 is likely important for binding the 2'-phosphate.

At least four hydrogen-bonds have been proposed between the 2'-phosphate and the three residues discussed above, two of which are contributed by R33; Figure 2-2 shows these residues in the protein environment. Mutation of R34 in the 6PGDH from *Lactococcus lactis* (the homolog is R33 in sheep liver 6PGDH) to tyrosine gave

Species				N32	R33	T34			
Ovis aries	·····	A	F	**N**	**R**	**T**	V	S	·····
Homo sapiens	·····	A	F	**N**	**R**	**T**	V	S	·····
Drosophila melanogaster	·····	A	Y	**N**	**R**	**T**	V	A	·····
Ceratitis capitata	·····	A	Y	**N**	**R**	**T**	V	E	·····
Cunninghamella elegans	·····	A	Y	**N**	**R**	**T**	T	S	·····
Saccharomyces	·····	A	Y	**N**	**R**	**T**	Q	S	·····
Haemophilus influenzae	·····	A	Y	**N**	**R**	**T**	T	S	·····
Treponema pallidum	·····	V	F	**N**	**R**	**T**	T	T	·····
Chlamydia trachomatis	·····	V	Y	**N**	**R**	**S**	P	E	·····
Escherichia coli	·····	I	F	**N**	**R**	**S**	R	E	·····
Shigella flexneri	·····	I	F	**N**	**R**	**S**	R	E	·····
Salmonella typhimurium	·····	V	F	**N**	**R**	**S**	R	E	·····
Klebsiella pneumoniae	·····	V	F	**N**	**R**	**S**	R	E	·····
Yersinia	·····	I	F	**N**	**R**	**S**	S	D	·····
Burkholderia	·····	V	Y	**N**	**R**	**S**	R	A	·····
Lactobacillus lactis	·····	I	F	**N**	**R**	**T**	G	A	·····
Staphylococcus	·····	V	F	**N**	**R**	**S**	S	E	·····
Bacillus licheniformis	·····	V	Y	**N**	**Y**	**T**	R	D	·····
Bacillus subtilis	·····	V	Y	**N**	**Y**	**T**	R	D	·····
Mycobacterium leprae	·····	L	H	**N**	**R**	**S**	I	A	·····
Zea mays	·····	V	Y	**N**	**R**	**T**	T	S	·····
Rhodopirellula	·····	V	Y	**N**	**R**	**T**	T	S	·····
Synechococcus sp.	·····	V	Y	**N**	**R**	**T**	Y	A	·····
Trypanosoma brucei	·····	V	F	**N**	**R**	**T**	Y	S	·····

Figure 2-1. Multiple Sequence Alignment of 6-Phosphogluconate Dehydrogenase Sequences Around Position N32-T34.

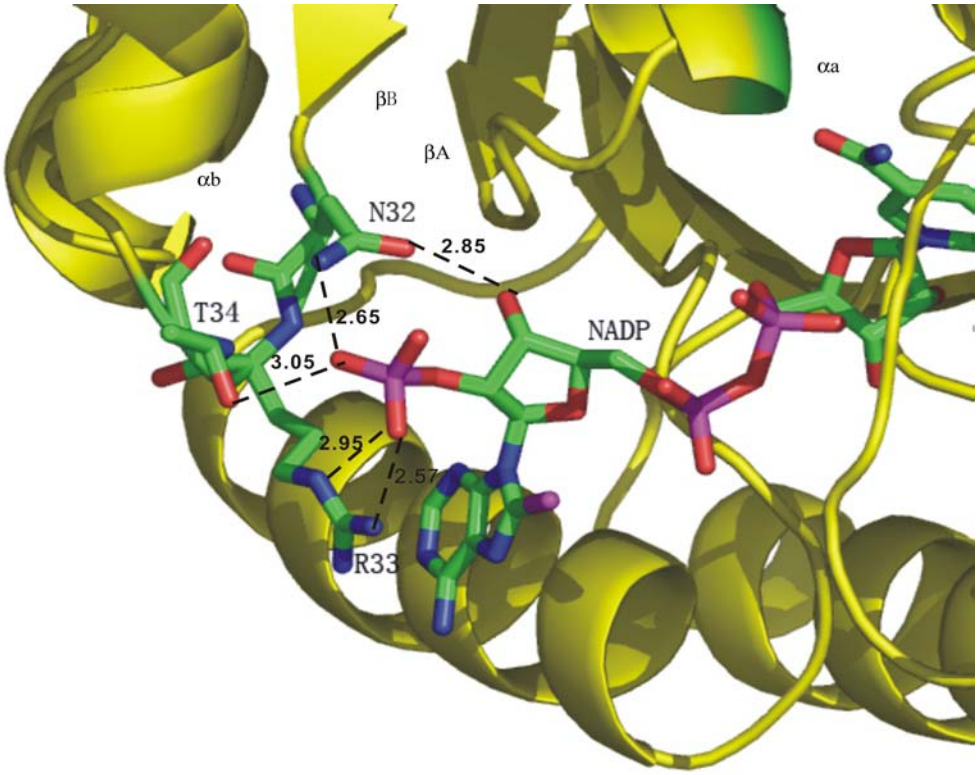

Figure 2-2. Residues in the Binding Site of 2'-Phosphate of NADP in Sheep Liver 6-Phosphogluconate Dehydrogenase. In the figure C is green, N is blue, O is red, and P is magenta. The dashed lines represent potential hydrogen bonds between the residues of interest and the cofactor. The numbers above the dashed lines are the distances in Å between the hydrogen bond donors. The figure was created using PyMOL from DeLano Scientific LLC (www.pymol.org). The accession number in the PDB is 1PGN for the E:Nbr^{8}ADP structure.

a mutant enzyme that lost most of its affinity for NADP (700-fold decrease), and used NAD as a cofactor, but very poorly (*8*). In addition to the three residues discussed above, a helix dipole is positioned 5 Å away from the 2'-phosphate and is proposed to provide an additional electrostatic interaction with the 2'-phosphate (*6*).

In this paper we investigate the role of each of the residues that interact with the 2'-phosphate of NADP. Site-directed mutagenesis was used to change N32, R33 and T34 to A, one at a time. Initial velocity and isotope effects studies were carried out to characterize the mutant enzymes. Data are consistent with the hypothesis that these residues are important in providing the binding energy for the 2'-phsophate of NADP. They also play a role in catalysis in the 6PGDH reaction as a result of properly orientating the cofactor as well as 6PG.

2.2 Material and Methods.

2.2.1. Chemicals and Reagents.

Oligonucleotide primers for mutagenesis and sequencing were from Biosynthesis, GibcoBRL and Invitrogen. The QuikChange® Site-Directed Mutagenesis kit and Pfu polymerase were from Stratagene. The Geneclean® II kit was from Bio 101, Inc. The PerfectPrep® Plasmid Mini kit was from Eppendorf. The DNA molecular ladder was from New England Biolabs. Restriction endonucleases, deoxynucleoside

triphosphates, and protein molecular mass markers were purchased from Gibco-BRL.

Acetaldehyde, acetate kinase, ADP-agarose resin, ATP, ampicillin, glucose-6-phosphate dehydrogenase (G6PDH), hexokinase, kanamycin, lithium potassium acetyl phosphate, the trisodium salt of 6PG, NADP, and pyrophosphate were from Sigma-Aldrich, Co. β–D-(3-deutero)-glucose (98 atom %D) was from Omicron Biochemicals, Inc. Ni-NTA agarose resin was purchased from QIAGEN. Glycerol and sulfuric acid were from Fisher-Scientific, Co. IPTG was from Gold Bio Technology (GBT). Hepes, Bis-Tris, and Ches buffers were from Research Organics, Inc. D_2O (99 atom %D) was from Cambridge Isotope Laboratories, Inc. All other chemicals were the highest quality available.

2.2.2 Bacterial Strain and Plasmids.

The *Escherichia coli* strain XL1-Blue was used to transform the mutated plasmid and M15[pREP4] was the host strain for expression of the mutant proteins. The plasmid pQE-30 was used as both mutagenesis and expression vector.

2.2.3 Site-Directed Mutagenesis.

The QuikChange® Site-Directed Mutagenesis kit from Stratagene was used to perform site-directed mutagenesis. Double-stranded DNA prepared from recombinant plasmid pPGDH.LC4 (*8*) was used as a template and the synthetic oligonucleotide primers are listed in Table 2-1. Whole gene sequencing was

$N32A_f$	GTGGTCTGTGCTTTT**GCT**AGG
$N32A_r$	GGAGACTGTCCT**AGC**AAAAGC
$R33A_f$	GTCTGTGCTTTTAAT**GCG**ACAGTCTCCAAAG
$R33A_r$	CTTTGGAGACTGT**CGC**ATTAAAAGCACAGAC
$T34A_f$	GCTTTTAATAGG**GCA**GTCTCCAAAGTTG
$T34A_r$	CAACTTTGGAGAC**TGC**CCTATTAAAAGC

Table 2-1. Sequence of Oligonucleotide Primers at the 2'-Phosphate Site. Subscripts f and r represent forward and reverse primers. Mutated codons are in bold.

performed for every mutation at the Laboratory for Genomics and Bioinformatics of the University of Oklahoma Health Science Center in Oklahoma City. The resulting sequence was compared to that of the wild type 6PGDH using BLAST. Successfully mutated plasmids were transformed into M15[pREP14] competent cells, the expression host. Frozen stocks of strains harboring plasmid were stored in LB/ampicillin/kanamycin medium containing 15% glycerol at -80 ^{o}C.

2.2.4 Growth and Purification Conditions.

The bacterial strain containing the mutated plasmid was first grown in 50-200 mL LB medium, containing 100 μg/mL ampicillin and 25 μg/mL kanamycin at 37 ^{o}C, overnight in a water-bath shaker. The next day, this culture was transferred into 2-10 liters of LB/Amp/Kan medium and was incubated at 25 ^{o}C for 8 hours or until the A_{600} reached 0.6. IPTG was then added to a final concentration of 1 mM to initiate expression. After 16 hours of growth at 25 ^{o}C with shaking, the cells were harvested by centrifugation at 5,000 *g* for 30 minutes. The cell pellet was resuspended in 4 volumes of Buffer A (50 mM triethanolamine, 2 mM β–mercaptoethanol, pH 7.5), sonicated on ice for 3 minutes, (pulsing 30 seconds with 30 seconds rest) using a MISONIX Sonicator® XL, and centrifuged at 25,000 *g* for 30 minutes. The supernatant was combined with 2-10 mL of Ni-NTA resin pre-equilibrated with Buffer A and stirred at 4 ^{o}C for 2 hours. The mixture was then loaded onto a 25 mL

column, and the column was washed with 5 volumes of Buffer A containing 20 mM imidazole. Elution made use of an imidazole gradient (0.2-0.4 M, depends upon the freshness of the resin). Protein concentrations were measured for all fractions using the method of Bradford (*10*). Fractions containing protein were pooled and applied to an ADP agarose affinity column, which takes advantage of the NAD/NADP binding site in the protein. Pooled fractions from the Ni-NTA column were applied to the ADP agarose column directly, with a flow rate of 2 mL/min. The column was then washed with 10 volumes of Buffer A and protein was eluted with 150 mM pyrophosphate buffer, pH 7.5, containing 1 mM EDTA and 2 mM β–mercaptoethanol. Fractions were collected and protein concentration was determined by reading the absorbance at 280 nm (ε = 62,160 M^{-1} cm^{-1} for 6-His tagged 6PGDH). Fractions containing protein were again pooled and concentrated using an Amicon ultrafiltration apparatus with a PM-30 semipermeable membrane. SDS-PAGE was performed for wild type and all mutant enzymes to analyze the purity of the protein.

The wild type and mutant proteins were purified in an identical manner, and all enzymes were stored at 4 ^{o}C in the same buffer used for elution from the ADP agarose column.

2.2.5 Synthesis of 3-d-6PG.

3-*deutero*-glucose was converted to 3-*deutero*-glucose 6-phosphate enzymatically

using hexokinase as described previously (*11*). The extent of conversion to the product of the reaction was determined by end-point assay using glucose-6-phosphate dehydrogenase. Upon completion of the reaction, the pH of the solution was adjusted to 4.5 to denature the enzymes in the mixture and Amicon ultrafiltration was used to remove the enzymes. The resulting solution was treated with acid-washed and heat-activated charcoal, stirred for 1 hour and filtered to remove nucleotides and Dowex 50W-H^+ resin was then used to remove Mg^{2+}. The solution, containing 3-*d*-glucose 6-phosphate, was bromine oxidized to yield the final product 3-*d*-6PG, which was purified as described previously (*5*). ^{1}H-NMR confirmed deuteration at the 3-position.

2.2.6 Initial Velocity Studies.

Initial velocity studies were performed using a Beckman DU640 UV/Vis spectrophotometer. The appearance of NADPH (ε_{340} = 6.22 mM^{-1} cm^{-1}) was monitored over time using 1 cm pathlength semi-micro quartz cuvettes. The temperature was maintained at 25 ^oC using a Beckman Temperature Controller. Initial velocity patterns were measured for all mutant and wild type enzymes in 100 mM Hepes, pH 7.5, using variable concentrations of 6PG (15-500 μM) and NADP (1-3000 μM) dependent on the mutant enzyme. Initial velocity studies were also performed with NAD as the cofactor at saturating concentration of 6PG (40 K_m).

2.2.7 Primary Deuterium Isotope Effects.

The concentrations of 3-*h*-6PG and 3-*d*-6PG were determined enzymatically in triplicate via end-point assay using wild type 6PGDH. The concentrations from three determinations were in agreement within 2%. Primary deuterium isotope effects with 3-*d*-6PG were obtained for all the mutant enzymes as well as for the wild type enzyme by direct comparison of initial velocities (*12*). ^{D}V and $^{D}(V/K_{6PG})$ were measured in triplicate varying 3-*h*-6PG or 3-*d*-6PG at saturating concentrations of NADP.

2.2.8 pH Studies.

Initial velocity data were obtained as a function of pH under conditions in which NADP was varied while 6PG was fixed at saturating level (40 K_m). The pH was maintained using the following buffers at 100 mM concentrations: Bis-Tris, 5-6.5; Hepes, 6.5-8.5; Ches, 8.5-9.5. Sufficient overlap was obtained upon changing buffers to eliminate buffer effects. The pH was determined before and after the initial velocity measurements.

2.2.9 ^{13}C Kinetic Isotope Effect.

Isotope effects were measured using the natural abundance of ^{13}C at the C-1 position of 6PG (*13*). Both high conversion (100% reaction, which represents $^{12}C/^{13}C$ in the substrate 6PG) and low conversion samples were used to measure the

$^{12}C/^{13}C$ isotope ratios in the CO_2 produced from the reaction of 3-*h*-6PG or 3-*d*-6PG. From these ratios, the ^{13}C-kinetic isotope effect was calculated (*14*).

For high conversion samples, in 40 mL, the reaction mixtures contained 2 mM 3-*h*-6PG or 3-*d*-6PG, 0.5 mM $NADP^+$ and 10 mM oxidized glutathione. The low conversion reactions contain 6.5 mM 3-*h*-6PG or 3-*d*-6PG. The $NADP^+$ concentration was 0.25 mM for the wild type and the T34A mutant enzymes or 2 mM for the N32A and R33A mutant enzymes. All low conversion samples contained 5 mM oxidized glutathione in a final volume of 40 mL. The pH of the reaction solutions was titrated to 7.6, followed by sparging with CO_2-free nitrogen overnight. Before starting the reactions, aliquots were withdrawn to determine the initial concentrations of 6PG by end-point assay in triplicate. Then the reactions were initiated by the addition of 2 units of 6PGDH and 100 units of glutathione reductase to recycle NADP for both high and low conversion samples.

The high conversion samples were allowed to proceed for more than 16 hours and end-point assays were used to confirm the completion of the reaction. For the low conversion samples, extents of reaction were monitored by end-point, assaying the remaining 6PG. Reactions were quenched when 50 μmole of CO_2 were produced. For both high and low conversion samples, 0.2 mL of concentrated sulfuric acid was added to quench the reactions and the generated CO_2 was isolated by vacuum

distillation (*15*). Aliquots of the samples were withdrawn after CO_2 isolation and incubated at pH 8 overnight. The next day, end-point assays were performed in triplicate to determine the exact extent of the low conversion reactions. Isotopic composition of the CO_2 was measured on a Finnigan Delta E isotope-ratio mass spectrometer in the laboratory of Dr. Michael Engel, Department of Geophysics, University of Oklahoma. All ratios were corrected for ^{17}O according to Craig (*16*).

2.2.10 Data Processing.

Double reciprocal plots were used to analyze the data and all plots and replots were linear. Data were fitted using the appropriate rate equations and programs developed by Cleland (*17*). Data for substrate saturation curves obtained at a fixed concentration of the second substrate were fitted using eq. 1. Initial velocity patterns were fitted using eq. 2. Deuterium kinetic isotope effect data were fitted using eq. 3. In eqs. 1 and 2, v is the initial velocity, V is the maximum velocity, A and B are reactant concentrations, K_a and K_b are the Michaelis constants for NADP and 6PG, respectively, and K_{ia} is the dissociation constant for E:NADP. In eq. 3, F_i is the fraction of deuterium label in the substrate, and E_V and $E_{V/K}$ are the isotope effects minus 1 on V and V/K. The pH dependence of V/K was fitted using eq. 4, while that for V was fitted using eq. 5. In eqs. 4 and 5, y is V or V/K, C is the pH independent value of y, H is the hydrogen ion concentration, and K_1 and K_2 are the

acid dissociation constants for enzyme or substrate groups important in a given protonation state for optimal binding and/or catalysis.

Calculation of ^{13}C-kinetic isotope effects was performed according to eq. 6, where f is the fraction of completion of the reaction, R_p and R_∞ are the $^{12}C/^{13}C$ isotopic ratios for CO_2 at partial and complete conversion, respectively. Isotope ratios, given as $\delta^{13}C$, were calculated from eq. 7, where R_{smp} and R_{std} are $^{12}C/^{13}C$ isotopic ratios for sample and standard, respectively. The standard for CO_2 was calibrated from Pee Dee Belemnite with a $^{12}C/^{13}C$ of 0.0112372 (*16*).

$$v = \frac{VA}{K_a + A} \quad [1]$$

$$v = \frac{VAB}{K_{ia}K_b + K_aB + K_bA + AB} \quad [2]$$

$$v = \frac{VA}{K_a\left(1 + F_iE_{V/K}\right) + A\left(1 + F_iE_V\right)} \quad [3]$$

$$\log y = \log\left[\frac{C}{1 + H/K_1 + K_2/H}\right] \quad [4]$$

$$\log y = \log\left[\frac{C}{1 + H/K_1}\right] \quad [5]$$

$$^{13}(V/K) = \frac{\log(1-f)}{\log\left(1 - f\left[R_p/R_\infty\right]\right)} \quad [6]$$

$$\delta(^{13}C) = \left(\frac{R_{smp}}{R_{std}} - 1\right) x\, 10^3 \quad [7]$$

2.3 Results.

2.3.1 Spectral Properties of Mutant Enzymes.

Far UV CD spectra were recorded for all mutant and wild type enzymes, and all were identical after adjusting for protein concentration (data not shown). In addition, identical tryptophan fluorescence emission spectra were obtained for all mutant and wild type enzymes upon excitation at 298 nm, indicating that the microenvironment of tryptophan residues of the proteins is the same for all enzymes (data not shown). There are 16 tryptophan residues in 6PGDH spread throughout the protein structure. As a result, there are no major changes in the overall structure of the enzyme resulting from the mutation, and changes are restricted to the local area within the active site.

2.3.2 Kinetic Parameters of the Mutant Enzymes.

Initial velocity patterns were obtained by measuring the initial rate at pH 7.5 using variable concentrations of 6PG (15-500 μM) and NADP (1-1000 μM) dependent on the mutant enzyme. Data are summarized in Table 2-2. No significant change was observed in K_{6PG} or in the V/E_t for all three mutant enzymes with respect to the values of the wild type enzyme. K_{NADP} increased from 6-fold to 80-fold for all mutations, resulting in a 6- to 80-fold decrease in $V/K_{NADP}E_t$. Data indicate elimination of either asparagine or arginine impairs cofactor binding more than it does when the threonine is replaced.

With NAD as the cofactor, K_{NAD} increases by more than 1,000-fold compared to K_{NADP}; in fact saturation by NAD cannot be achieved, and only $V/K_{NAD}E_t$ can be estimated. For the wild type enzyme, a value of 6.6 $\mu M^{-1}min^{-1}$ is obtained for V/K_{NAD} E_t, while for the N32A, R33A and T34A mutant enzymes, values of 0.46 $\mu M^{-1}min^{-1}$, 0.29 $\mu M^{-1}min^{-1}$ and 2.2 $\mu M^{-1}min^{-1}$, respectively, are estimated. Data suggest that substitution of the three residues by alanine do not improve the ability of the enzyme to use NAD as a cofactor.

2.3.3 Kinetic Primary Deuterium Isotope Effects.

The kinetic isotope effects on V and V/K_{6PG} were measured at saturating NADP (40 K_m) (Table 2-3). The isotope effects are smaller than the values obtained with the wild type enzyme in all cases, and within error equal to each other, consistent with the proposed rapid equilibrium random kinetic mechanism (*1*).

2.3.4 ^{13}C-Kinetic Isotope Effects.

Data for ^{13}C-kinetic isotope effects obtained with 3-*h*-6PH and 3-*d*-6PG are shown in Table 2-3. For all of the mutant enzymes, the value of $^{13}(V/K_{6PG})_H$ minus 1 is at least 7-fold higher than that of the wild type protein. Deuteration of 6PG decreases the observed ^{13}C-kinetic isotope effects in all cases and the equality for a stepwise mechanism with oxidation preceding decarboxylation is satisfied within error (*14*).

	wt	N32A	R33A	T34A
V/E_t (sec^{-1})	9.4 ± 0.4	9.3 ± 0.8	10.4 ± 0.1	9.9 ± 0.3
K_{NADP} (μM)	5 ± 1	310 ± 60	383 ± 9	30.0 ± 0.3
Fold increase		62	77	6
K_{6PG} (μM)	28 ± 4	57 ± 1	33.0 ± 0.5	11.0 ± 0.1
Fold increase		2	1	0.5
$V/K_{NADP}E_t$ ($M^{-1}s^{-1}$)	1.9×10^6	3×10^4	2.7×10^4	3.3×10^5
Fold decrease		63	70	6
ΔG^o (kcal $mole^{-1}$)[b]	-7.2	-4.8	-4.7	-6.2
$\Delta\Delta G^o$ (kcal $mole^{-1}$)[b]		2.4	2.5	1.0

Table 2-2. Summary of the Kinetic Parameters for 6PGDH Wild Type and Mutant Enzymes[a] at the 2'-Phosphate Site.
[a]Values are ± S.E.
[b]Values are calculated from K_{NADP}, using $\Delta G^o = -RT\ln K_{NADP}$.

	wt	N32A	R33A	T34A
^{D}V	1.9 ± 0.1[b]	1.43 ± 0.03	1.43 ± 0.02	1.4 ± 0.1
$^{D}(V/K_{6PG})$	1.9 ± 0.1[b]	1.5 ± 0.1	1.5 ± 0.1	1.6 ± 0.1
$^{13}(V/K_{6PG})_{H}$	1.0028	1.0192	1.0183	1.0213
	(0.0007)[c]	(0.0003)	(0.0003)	(0.0007)
$^{13}(V/K_{6PG})_{D}$	1.0017	1.017	1.015	1.016
	(0.0005)	(0.002)	(0.002)	(0.002)
pK_a (V)[d]	6.40 ± 0.04	6.18 ± 0.03	5.92 ± 0.08	6.05 ± 0.05
[d]	-	9.39 ± 0.05	9.6 ± 0.1	-
pK_a (V/K)[e]	6.2 ± 0.2	7.3 ± 0.2	6.9 ± 0.1	7.03 ± 0.06
[e]	8.5 ± 0.1	7.7 ± 0.2	8.3 ± 0.1	8.56 ± 0.07

Table 2-3. Summary of Isotope Effects and pK_a Values for Wild Type and Mutant 6PGDH[a] at the 2'-Phosphate Site.
[a]Values are ± S.E. [b]From ref 9.
[c]Values in parenthesis are standard errors for the ^{13}C-kinetic isotope effects. [d]pKa from the V pH profile.
[e]pKa from the (V/ K) pH profile.

2.3.5 pH Dependence of Kinetic Parameters.

The pH dependence of the kinetic parameters was measured by varying NADP at saturating level of 6PG (40 K_m). All of the mutant and the wild type enzymes are stable from pH 5.5 to pH 9.5. For all of the mutant enzymes, a bell shaped pH-rate profile with limiting slopes of 1 and -1 was obtained for V/K_{6PG}. The pH-rate profile for V is bell shaped in the case of the N32A and R33A mutant enzymes, while that of the wild type and T34A mutant enzymes, decreases only at low pH. The pK_a values are summarized in Table 2-3. The pH-rate profiles for the wild type and R33A mutant enzyme are shown in Figure 2-3 and Figure 2-4.

2.4 Discussion.

The main aim of this research was to determine the importance of residues N32, R33 and T34, which interact with the 2'-phosphate of NADP, and their roles in providing binding energy. Site-directed mutagenesis was used to change N32, R33 and T34 to alanine one at a time to eliminate the interaction between each of the residues and the 2'-phosphate of NADP. Steady-state kinetic parameters and isotope effects were measured to determine the effect of the substitutions on 6PGDH's ability to use NADP as a cofactor.

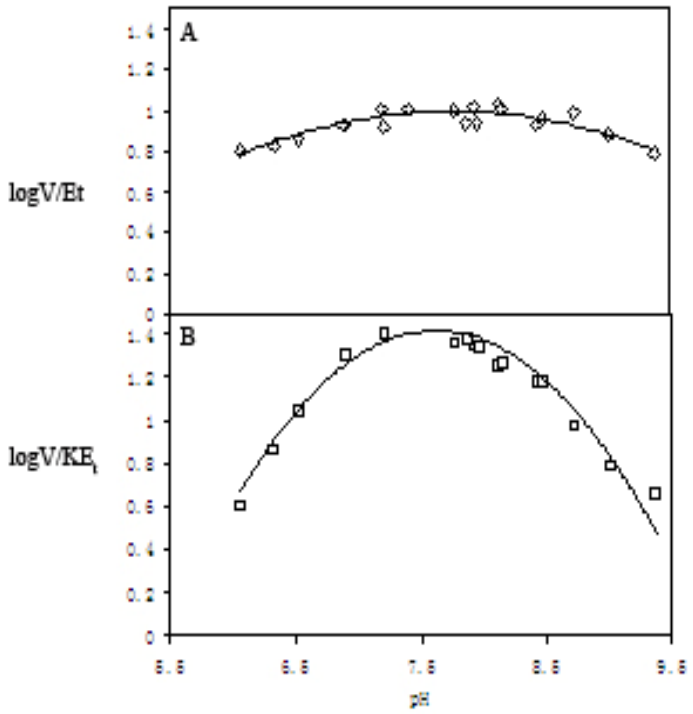

Figure 2-3. pH Dependence of Kinetic Parameters for R33A Mutant Enzyme. Data were obtained for V (A) and V/K_{NADP} (B). The points shown are the experimentally determined values and the curves are theoretical based on the using eq. 4 for V/K and 5 for V.

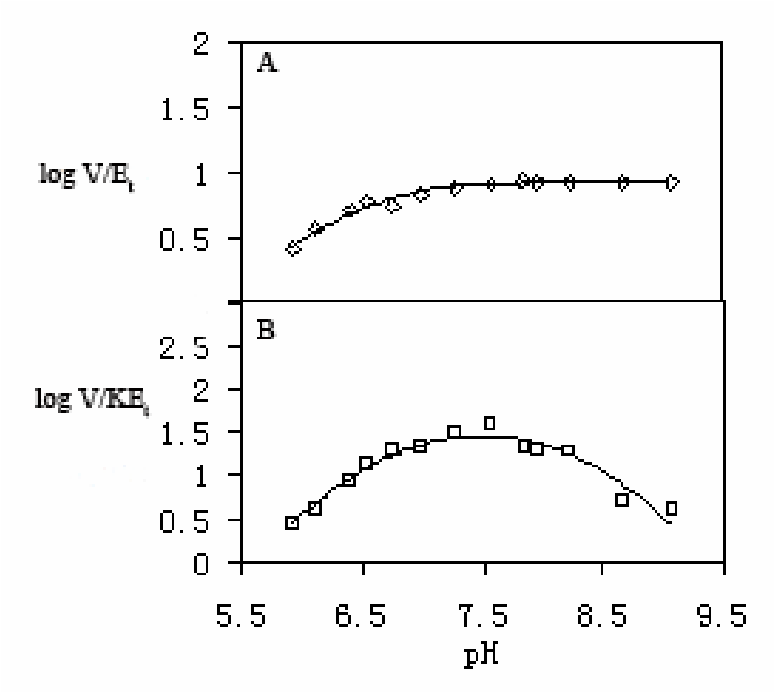

Figure 2-4. pH Dependence of Kinetic Parameters for Wild Type 6-PGDH. Data were obtained for V (A) and V/K_{NADP} (B). The points shown are the experimentally determined values and the curves are theoretical based on the using eq. 4 for V/K and 5 for V.

Theory for interpretation of kinetic parameters and isotope effects in the 6PGDH reaction has been developed previously and equations are reproduced here for aid in data interpretation (*5, 11*). The oxidative decarboxylation reaction catalyzed by 6PGDH is stepwise with oxidation preceding decarboxylation as suggested by multiple deuterium/^{13}C kinetic isotope effect studies (*11*). Multiple solvent deuterium/^{13}C kinetic isotope effect and proton inventory studies indicate the presence of an isomerization of the enzyme complex prior to hydride transfer and decarboxylation (*18*). The kinetic mechanism of 6PGDH can be written:

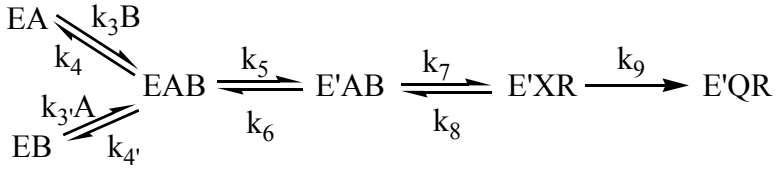

[8]

where A and B represent NADP and 6PG, respectively, and X, Q, and R represent 3-keto-6PG, ribulose 5-phosphate, and NADPH, respectively. The rate constants k_3 and k_4 are for binding and dissociation of 6PG and $k_{3'}$ and $k_{4'}$ are for binding and dissociation of NADP, k_5 and k_6 are for an isomerization of E:NADP:6PG complex, k_7 and k_8 are for forward and reverse hydride transfer, and k_9 is the rate constant for decarboxylation of the 3-keto intermediate and release of CO_2.

Given the rapid equilibrium nature of the mechanism, central complex interconversion is rate-limiting (steps included from EAB to E'QR), and thus k_4, $k_{4'}$ >

k_5.

The following expressions have been developed.

$$V = \frac{\frac{k_7}{1+\frac{k_6}{k_5}}}{1+c_{Vf}+c_r} \qquad [9]$$

$$\frac{V}{K_{6PG}} = \frac{\frac{k_3 k_5 k_7}{k_4 k_6}}{1+c_f+c_r} \qquad [10]$$

$$\frac{V}{K_{NADP}} = \frac{\frac{k_{3'} k_5 k_7}{k_{4'} k_6}}{1+\frac{k_7}{k_6}+\frac{k_8}{k_9}} \quad \frac{V}{K_{6PG}} = \frac{\frac{k_{3'} k_5 k_7}{k_{4'} k_6}}{1+c_f+c_r} \qquad [11]$$

where $c_{Vf} = \frac{k_7\left(\frac{1}{k_5}+\frac{1}{k_9}\right)}{1+\frac{k_6}{k_5}}$, $c_f = \frac{k_7}{k_6}$, and $c_r = \frac{k_8}{k_9}$.

A kinetic deuterium isotope effect is observed on the hydride transfer step, depicted by $^{D}k_7$ and $^{D}k_8$, which can be related by the equilibrium isotope effect, $^{D}K_{eq} = {}^{D}k_7 / {}^{D}k_8$. Expressions for the primary kinetic deuterium isotope effects are given in eqs. 12 and 13.

$$^{D}V = \frac{^{D}k_7 + c_{Vf} + \left(^{D}K_{eq}\right)c_r}{1 + c_{Vf} + c_r} \quad [12]$$

$$^{D}\left(\frac{V}{K_{6PG}}\right) = \frac{^{D}k_7 + c_f + \left(^{D}K_{eq}\right)c_r}{1 + c_f + c_r} \quad [13]$$

Since $^{D}V = {}^{D}(V/K)$ (Table 3), $c_f = c_{vf}$ and the equation for the isotope effect on V (eq.12) is equal to that on V/K, i.e., eq.13. The rate constant k_9 will reflect a ^{13}C-kinetic isotope effect given by $^{13}k_9$. Expressions for the primary kinetic ^{13}C-kinetic isotope and the multiple ^{13}C/D multiple isotope effect, i.e., the ^{13}C-kinetic isotope effect with 3-d-6PG, are given in eqs. 14 and 15.

$$^{13}\left(\frac{V}{K_{6PG}}\right)_H = \frac{^{13}k_9 + \frac{1 + c_f}{c_r}}{1 + \frac{1 + c_f}{c_r}} \quad [14]$$

$$^{13}\left(\frac{V}{K_{6PG}}\right)_D = \frac{^{13}k_9 + \left(\frac{^{D}k_7}{c_r\left(^{D}K_{eq}\right)}\right)\left(1 + \frac{c_f}{^{D}k_7}\right)}{1 + \left(\frac{^{D}k_7}{c_r\left(^{D}K_{eq}\right)}\right)\left(1 + \frac{c_f}{^{D}k_7}\right)} \quad [15]$$

where $^{D}k_7$ is the intrinsic deuterium isotope effect on the hydride transfer step, and $^{D}K_{eq}$ is the equilibrium isotope effect on hydride transfer (1.18 for oxidation of a

secondary alcohol (*20*)).

Since K_{6PG} is the ratio of V and V/K_{6PG}, and K_{NADP} is the ratio of V and V/K_{NADP} and taking into account $c_f = c_{vf}$

$$K_{6PG} = \left(\frac{k_4}{k_3}\right)\left(\frac{k_6}{k_5 + k_6}\right) = K_{d\,6PG} \qquad [16]$$

$$K_{NADP} = \left(\frac{k_{4'}}{k_{3'}}\right)\left(\frac{k_6}{k_5 + k_6}\right) = K_{d\,NADP} \qquad [17]$$

where k_4/k_3 is the K_d of 6PG and $k_{4'}/k_{3'}$ is the K_d of NADP for the E:NADP:6PG complex and $k_6/(k_5 + k_6)$ corrects for the distribution of the central complexes between E:NADP:6PG and E':NADP:6PG. Therefore, K_{6PG} is the equilibrium constant for dissociation of 6PG from E:NADP:6PG and E':NADP:6PG and K_{NADP} is the equilibrium constant for dissociation of NADP from E:NADP:6PG and E':NADP:6PG. Using the above rate equations, we discuss the results for each of the mutant enzyme.

The key to interpretation of the data obtained for the mutant enzymes lies in changes in K_{NADP}, $^{D}(V/K_{6PG})$ and $^{13}(V/K_{6PG})$. The decrease in K_{NADP} likely results from an increase in the net off-rate for NADP from E':NADP:6PG, $k_{4'}k_6/(k_5 + k_6)$, suggesting an increase in $k_{4'}$, k_6, or both. However, since $k_6/(k_5 + k_6)$ is present in

both K_{NADP} and K_{6PG}, and no change is observed in the latter, it is k_4, that is increased.

2.4.1 Kinetic Parameters.

A significant increase in K_{NADP} has been obtained for all three mutant enzymes. The positively charged arginine side chain is thought to help to neutralize the charge on the 2'-phosphate; it is also responsible for all the contacts to one face of the adenine ring and thus forms one side of its binding pocket, shielding it from solvent (*6*). Changing arginine to alanine, not surprisingly, decreases the affinity of the mutant enzyme for NADP by >70-fold. A similar phenomenon has been observed for glutathione reductase (*19*), indicating that this interaction may be one of the solutions to the problem of determining the specificity of the enzyme for NADP.

In the case of N32, the amide side chain donates a hydrogen bond to the 2'-phosphate, and it also interacts with the 3'-hydroxyl of the adenine ribose. The amide of N32 bridges two turns between βA-αa and βB-αb (Figure 2-2), and is also within hydrogen-bonding distance of the main chain nitrogen of L10 and the main chain carbonyl of T34, forming a hydrogen-bond network (*6*). Substitution of asparagine with alanine eliminates all of the above interactions, and thus a 60-fold decrease in the affinity to NADP is not unexpected. Similar binding energy is provided by residues N32 and R33 (2.4 kcal/mole and 2.5 kcal/mole, respectively). T34A exhibits the smallest change in K_{NADP}, indicating this residue does not

contribute as much as N32 and R33 in providing the binding energy to NADP. If a simple sum of $\Delta\Delta G^o$ values could accurately be used to give the overall ΔG^o of NADP binding, the three residues together contribute about 78% of the total binding energy to NADP, with about 68% derived from N32 and R33. Although the simple sum is not valid, data are consistent with significant roles of N32, R33 and T34 in providing the binding energy of NADP.

2.4.2 pH Studies.

The pH dependence of the kinetic parameters measured for the wild type enzyme in this study is slightly different than the data reported previously. The maximum velocity exhibits a single pK of 6.4, while two pK values of 5.8 and 8.8 were suggested in an earlier study, although the decrease at high pH was slight (*1, 3*). The difference may reflect the difference in purity and stability of the enzyme after ADP agarose affinity chromatography, a step not carried out in the earlier study.

In the V pH-rate profile of the N32A and R33A mutant enzymes, the pK value of K183 is shifted to lower pH, 6-6.2, compared to 6.4 for the wt enzyme. The V/K pH-rate profile of all the three mutant enzymes exhibits two pK values, one on the acid side and one on the basic side, as observed for the wt enzyme (*3*). However, the pK values are closer together in the case of the mutant enzymes, largely a result of an increase in the observed pK of the group with the pK on the acid side of the profile.

The pK values are attributed to E190 (acid side) and K183 (basic side), which serve as general acid and general base, respectively, that is, the two groups exist in reverse protonation states. It is suggested that the local environment of the general acid and the general base in the mutant enzymes is more hydrophobic than they are in the wild type enzyme. It is difficult to explain the change in the hydrophilicity of the local environment unless the structures of the mutant enzymes are available.

2.4.3 Kinetic Isotope Effects.

A small decrease in ^{D}V and $^{D}(V/K)$ is obtained, while $^{13}(V/K_{6PG})_H$ minus 1 is increased about 6-fold compared to the wt enzyme (Table 3). Data suggest an increase in the reverse rate of the hydride transfer step and a decrease in the rate of decarboxylation step. Using eqs. 12-14, to have a decreased ^{D}V, $^{D}(V/K)$, and an increased $^{13}(V/K)$, the reverse commitment to catalysis c_r (k_8/k_9) has to increase, that is the partition ratio of the 3-keto-6-phosphogluconate changes to favor 6PG. Given the increase in c_r, and in order that V for the mutant enzymes remains unchanged compared to that of the WT enzyme, another rate process must increase to compensate. The obvious choice is k_7 since k_7/k_8 determines the equilibrium constant for the hydride transfer step, which is unlikely to change as a result of any of the mutations.

We have recently provided evidence that reduction of the nicotinamide is

accompanied by rotation of the ring about the *N*-glycosidic bond to a position that was occupied by the 1-carboxylate of 6PG (Fig. 1, *5*). The end result would be elimination of the interaction between E190 and the 1-carboxylate, facilitating decarboxylation, and resulting in the *re* face of the nicotinamide ring being exposed to the active site (the stereochemistry of hydride transfer is to the *si* face). It is possible that changing the interaction with the 2'-phosphate by eliminating the side chain of N32, R33, or T34, decreases the ability of the nicotinamide ring to rotate. This would result in a stabilization of the nicotinamide ring in the optimum position for hydride transfer, increasing the partitioning of the 3-keto-6PG toward 6PG compared to ribulose 5-phosphate. This aspect will require further experimentation.

In retrospect, the results are not surprising, because the three residues mutated provide most of the binding energy for NADP. Removal of any of the three residues may result in a positional change of the bound NADP, which may reorientate the nicotinamide ring of NADP to a position that disfavors ring rotation, but favors hydride transfer.

In conclusion, the 2'-phosphate of NADP is critical for making most of the interactions between the protein and the cofactor, helping position the cofactor for hydride transfer and participating in the rotational isomerization of the cofactor after reduction, probably by holding the cofactor in position so that the nicotinamide ring

can flip into the right location. Destroying the interactions between the 2'-phosphate and the protein results in a slower or less efficient rotation.

2.5 Reference.

1. Price, N., and Cook, P. F. (1996) Kinetic and Chemical Mechanisms of the Sheep Liver 6-Phosphogluconate Dehydrogenase. *Arch. Biochem. Biophys. 336*, 215-223.

2. Berdis, A. J., and Cook, P. F. (1993) Overall Kinetic Mechanism of 6-Phosphgluconate Dehydrogenase from *Candida utilis*. *Biochemistry 32*, 2036-2040.

3. Karsten, W. E., Chooback, L., and Cook, P. F. (1998) Glutamate 190 Is a General Acid Catalyst in the 6-Phosphogluconate Dehydrogenase-Catalyzed Reaction. *Biochemistry 37*, 15691-15697.

4. Zhang, L., Chooback, L., and Cook, P. F. (1999) Lysine 183 Is the General Base in the 6-Phosphogluconate Dehydrogenase-Catalyzed Reaction. *Biochemistry 38*, 11231-11238.

5. Cervellati, C., Dallocchio, F., Bergamini, C. M., and Cook, P. F. (2005) Role of Methionine-13 in the Catalytic Mechanism of 6-Phosphogluconate Dehydrogenase from Sheep Liver. *Biochemistry 44*, 2432-2440.

6. Adams, J. M., Grant, H. E., Gover, S., Naylor, C. E., and Philips, C. (1994) Substrate Binding in 6-Phosphogluconate Dehydrogenase: Implications for NADP Specificity and the Enzyme Mechanism. *Structure 2*, 651-668.

7. Berdis, A. J., and Cook, P. F. (1993) The 2'-Phosphate of NADP is Critical for Optimum Productive Binding to the 6-Phosphogluconate Dehydrogenase from *Candida utilis. Arch. Biochem. Biophys.* 305, 551-558.

8. Tetaud, E., Hanau, S., Wells, J. M., Page, R. W. F., Adams, J. M., Arkinson, S.,

and Barrett, M. P. (1999) 6-Phosphogluconate Dehydrogenase from *Lactococcus lactis*: A Role of Arginine Residues in Binding Substrates and Coenzyme. *Biochem. J. 338*, 55-60.

9. Chooback, L., Price, N. E., Karsten, W. E., Nelson, J., Sundstrom, P., and Cook, P. F. (1998) Cloning, Expression, Purification, and Characterization of the 6-Phosphogluconate Dehydrogenase from Sheep Liver. *Protein Expression Purif. 13*, 251-258.

10. Bradford, M. M. (1976) A Rapid and Sensitive Method for the Quantitation of Microgram Quantities of Protein Utilizing the Principle of Protein-dye Binding. *Anal. Biochem. 72*, 248-254.

11. Hwang, C. C., Berdis, A. J., Karsten, W. E., Cleland, W. W., and Cook, P. F. (1998) Oxidative Decarboxylation of 6-Phosphgluconate by 6-Phosphogluconate Dehydrogenase Proceeds by a Stepwise Mechanism with NADP and ADADP as Oxidants. *Biochemistry 37*, 12596-12602.

12. Parkin, D. W. (1991) *Enzyme Mechanism from Isotope Effects* (Cook, P. F., Ed.), CRC Press, Inc., Boca Raton, FL, pp. 284-285.

13. O'Leary, M. H. (1980) Determination of Heavy-atom Isotope Effects on Enzyme-catalyzed Reactions. *Methods Enzymol*. *64B*, 83-104.

14. Hermes, J. D., Roeske, C. A., O'Leary, M. H., and Cleland, W. W. (1982) Use of Multiple Isotope Effects to Determine Enzyme Mechanisms and Intrinsic Isotope Effects. Malic Enzyme and Glucose 6-Phosphate Dehydrogenase. *Biochemistry 21*, 5106-5114.

15. Weiss P. M. (1991) *Enzyme Mechanism from Isotope Effects* (Cook P. F., Ed.), CRC Press, Inc., Boca Raton, FL, pp. 291-311.

16. Craig, N. (1957) Isotopic standards for carbon and oxygen and correction factors for mass-spectrometric analysis of carbon dioxide. *Geochim. Cosmochim. Acta 12*, 133-149.

17. Cleland, W. W. (1979) Statistical Analysis of Enzyme Kinetic Data. *Methods Enzymol. 63*, 103-108.

18. Hwang, C. C. and Cook, P. F. (1998) Multiple Isotope Effects as a Probe of Proton and Hydride Transfer in the 6-Phosphogluconate Dehydrogenase Reaction. *Biochemistry 37*, 15698-15702.

19. Karplus, P. and Schulz, G. (1989) Substrate Binding and Catalysis by Glutathione Reductase as Derived from Refined Enzyme:Substrate Crystal Structure at 2 Å Resolution. *J. Mol. Biol.* 210, 163-180.

20. Cook, P. F., Blanchard, J. S. and Cleland, W. W. (1980) Primary and Secondary Deuterium Isotope Effects on the Equilibrium Constant for Enzyme Catalyzed Reactions. *Biochemistry 19*, 4853-4858.

21. Berdis, A. J., and Cook, P. F. (1993) Chemical Mechanism of 6-Phosphgluconate Dehydrogenase from *Candida utilis* from pH Studies. *Biochemistry 32*, 2041-2046.

CHAPTER 3

IMPORTANCE OF THE 6-PHOSPHATE OF 6PG

3.1 Introduction.

6-Phosphogluconate dehydrogenase (6PGDH1; EC 1.1.1.44) catalyzes the reversible oxidative decarboxylation of 6-phosphogluconate (6PG), producing ribulose-5-phosphate (Ru5P) and CO_2 with the concomitant reduction of NADP to NADPH. The kinetic mechanism is rapid equilibrium random on the basis of a complete kinetic characterization of the sheep liver enzyme and *Candida utilis* (*1, 2*). The pH dependence of kinetic parameters indicates a general acid-general base chemical mechanism (*1, 2*), and site-directed mutagenesis (*3, 4*) studies suggest that K183 and E190 are likely the general base and the general acid, respectively. In this mechanism, the general base (K183) is required to accept a proton from the 3-hydroxyl group of 6PG concomitant with hydride transfer from C-3 of 6PG to the coenzyme. Reduction of the nicotinamide ring is accompanied by rotating around the N-glycosidic bond such that the ring occupies the position formerly occupied by the 1-carboxylate of the substrate (*5*). The resulting 3-keto-6-phosphogluconate intermediate is decarboxylated to produce the enediol of Ru5P with the general base used to protonate the carboxyl oxygen. A general acid (E190) is needed to facilitate

the tautomerization of the enediol of Ru5P to the keto product (Figure 1-3).

In the E:6PG binary complex, the 6-phosphate of 6PG is surrounded by five active-site residues that are within hydrogen-bond distance: Y191, K260, T262, R287 and R446 (*6*). Multiple sequence alignment of 6PGDH shows that these five residues are completely conserved (Figure 3-1) and Figure 3-2 shows these residues in the protein environment. Notably, Lys260 donates a hydrogen bond to the 6-phosphate from its backbone NH and also provides significant hydrophobic interaction to substrate via its side chain. Arginine 446 is from the C-terminal tail of the second subunit and together with Arg287, balances the charge of the phosphate and may contribute most to anchoring the substrate. Mutations were made at Arg447 in 6PGDH from *Lactococcus lactis* (*7*) (the homolog is Arg446 in sheep liver 6PGDH) and all the mutants were devoid of enzyme activity, indicating that this residue is critical for activity. Interestingly, Arg287 participates in a hydrogen-bond network through water 528 to Glu190 and the 1-carboxyl of 6PG. It is suggested that this network is important in defining the bound conformation of 6PG (*6*).

In this chapter we investigate the role of each of the residues that interact with the 6-phosphate of 6PG. Site-directed mutagenesis was used to change Y191, K260, T262, R287 and R446 to A, one at a time. Initial velocity and isotope effects studies were carried out to characterize the mutant enzymes. Data are consistent with the

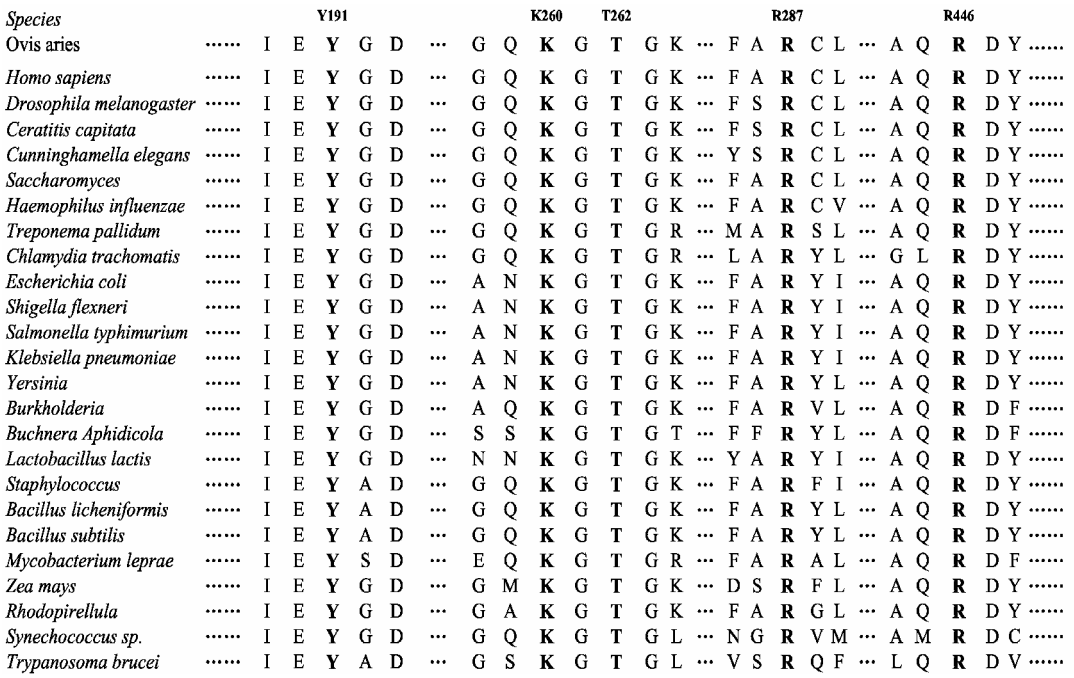

Figure 3-1. Multiple Sequence Alignment of 6-Phosphogluconate Dehydrogenase at Y191, K260, T262, R287 and R446 Positions.

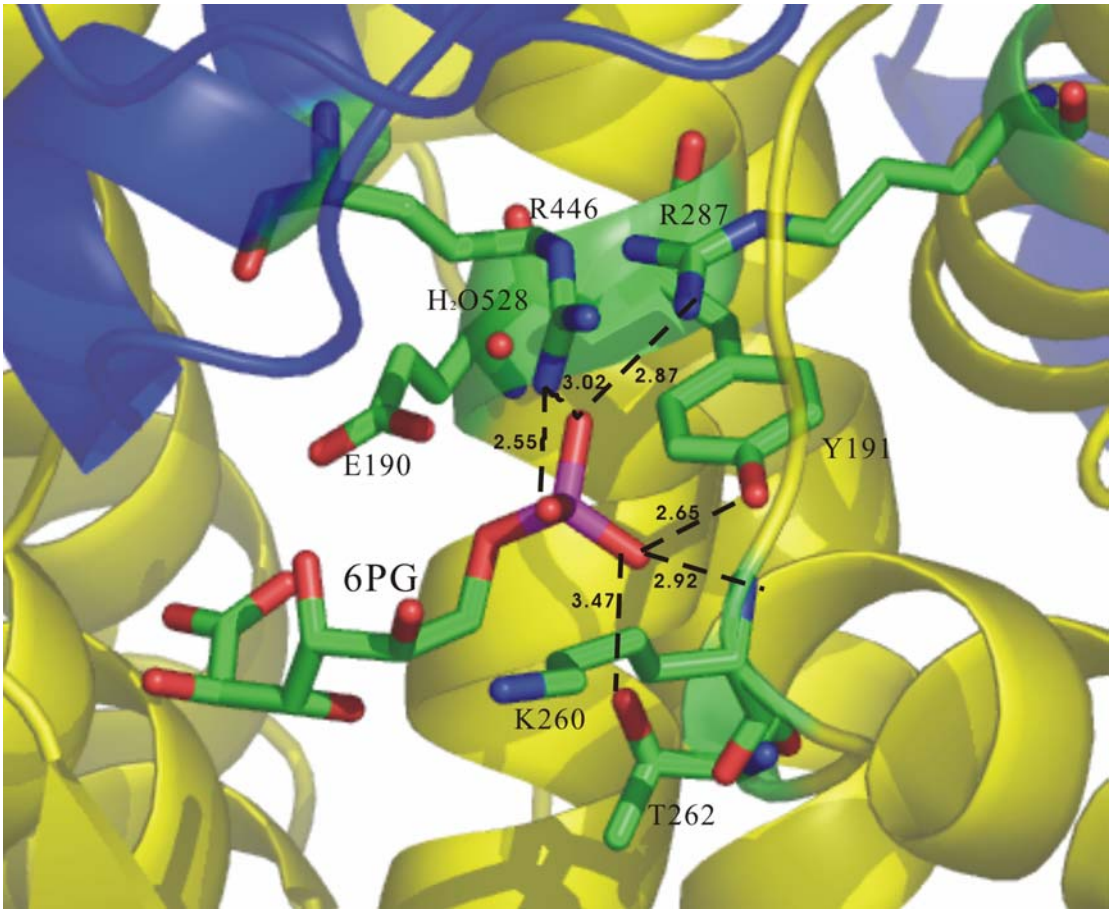

Figure 3-2. Residues in the 6-Phosphate Binding Site of 6PG in Sheep Liver 6-Phosphogluconate Dehydrogenase. One subunit is shown in blue and the second subunit is shown in yellow. The dashed lines represent potential hydrogen bonds between the residues of interest and the cofactor. The numbers above the dashed lines are the distances between the hydrogen bond donors. The figure was created using PyMOL from DeLano Scientific LLC (www.pymol.org). The accession number in the PDB is 1PGN for the E:Nbr^{8}ADP structure.

hypothesis that these residues are important in providing the binding energy for the 6-phosphate of 6PG. They also play a role in catalysis in the 6PGDH reaction as a result of properly orientating the substrate.

3.2 Material and Methods.

3.2.1 Chemicals and Reagents.

Oligonucleotide primers for mutagenesis and sequencing were from Biosynthesis, GibcoBRL and Invitrogen. The QuikChange® Site-Directed Mutagenesis kit and Pfu polymerase were from Stratagene. The Geneclean® II kit was from Bio 101, Inc. The PerfectPrep® Plasmid Mini kit was from Eppendorf. The DNA molecular ladder was from New England Biolabs. Restriction endonucleases, deoxynucleoside triphosphates, and protein molecular mass markers were purchased from Gibco-BRL.

Acetaldehyde, acetate kinase, ADP-agarose resin, ATP, ampicillin, glucose-6-phosphate dehydrogenase (G6PDH), hexokinase, kanamycin, lithium potassium acetyl phosphate, the trisodium salt of 6PG, NADP, and pyrophosphate were from Sigma-Aldrich, Co. β–D-(3-deutero)-glucose (98 atom% D) was from Omicron Biochemicals, Inc. Ni-NTA agarose resin was purchased from QIAGEN. Glycerol and sulfuric acid were from Fisher-Scientific, Co. IPTG was from Gold

Bio Technology (GBT). Hepes, Bis-Tris, and Ches buffers were from Research Organics, Inc. Deuterium oxide (99 atom% D) was from Cambridge Isotope Laboratories, Inc. All other chemicals were the highest quality available.

3.2.2 Bacterial Strain and Plasmids.

The *Escherichia coli* strain XL1-Blue was used to transform the mutated plasmid and M15[pREP4] was the host strain for expression of the mutant proteins. The plasmid pQE-30 was used as both mutagenesis and expression vector.

3.2.3 Site-Directed Mutagenesis.

The QuikChange® Site-Directed Mutagenesis kit from Stratagene was used to perform site-directed mutagenesis. Double-stranded DNA prepared from recombinant plasmid pPGDH.LC4 (*8*) was used as a template and the synthetic oligonucleotide primers are listed in Table 3-1. Whole gene sequencing was performed for every mutation at the Laboratory for Genomics and Bioinformatics of the University of Oklahoma Health Science Center in Oklahoma City. The resulting sequence was compared to that of the wild type 6PGDH using BLAST. Successfully mutated plasmids were transformed into M15[pREP14] competent cells, the expression host. Frozen stocks of strains harboring plasmid were stored in LB/ampicillin/kanamycin medium containing 15% glycerol at -80 ^{o}C.

3.2.4 Growth and Purification Conditions.

$Y191A_f$	GCACAACGGCATAGAG**GCC**CGGGGACATGCAGC
$Y191A_r$	GCTGCATGTCCCC**GGC**CTCTATGCCGTTGTGC
$K260A_f$	GGACAGCGCAGGGCAG**GCG**GGCACCGGGAAGTGG
$K260A_r$	CCACTTCCCGGTGCC**CGC**CTGCCCTGCGCTGTCC
$T262A_f$	GGGCAGAAGGGC**GCC**CGGGAAGTGGACC
$T262A_r$	GGTCCACTTCCC**GGC**GCCCTTCTGCCC
$R287A_f$	GCTGTCTTCGCG**GCA**TGCTTATCATC
$R287A_r$	GATGATAAGCA**TGC**CGCGAAGACAGC
$R446A_f$	CCTCATCCAGGCTCAG**GCC**GACTACTTTGGGGCG
$R446A_r$	CGCCCCAAAGTAGTC**GGC**CTGAGCCTGGATGAGG

Table 3-1. Sequences of Oligonucleotide Primers at the 6-Phosphate Site. Subscripts f and r represent forward and reverse primers. Mutated codons are in bold.

The bacterial strain containing the mutated plasmid was first grown in 50-200 mL LB medium, containing 100 μg/mL ampicillin and 25 μg/mL kanamycin at 37 ^{o}C, overnight in a water-bath shaker. The next day, this culture was transferred into 2-10 liters of LB/Amp/Kan medium and was incubated at 25 ^{o}C for 8 hours or until the A_{600} reached 0.6. IPTG was then added to a final concentration of 1 mM to initiate expression. After 16 hours of growth at 25 ^{o}C with shaking, the cells were harvested by centrifugation at 5,000 *g* for 30 minutes. The cell pellet was resuspended in 4 volumes of Buffer A (50 mM triethanolamine, 2 mM β–mercaptoethanol, pH 7.5), sonicated on ice for 3 minutes, (pulsing 30 seconds with 30 seconds rest) using a MISONIX Sonicator® XL, and centrifuged at 25,000 *g* for 30 minutes. The supernatant was combined with 2-10 mL of Ni-NTA resin pre-equilibrated with Buffer A and stirred at 4 ^{o}C for 2 hours. The mixture was then loaded onto a 25 mL column, and the column was washed with 5 volumes of Buffer A containing 20 mM imidazole. Elution made use of an imidazole gradient (0.2-0.4 M, dependent on the freshness of the resin). Protein concentrations were measured for all fractions using the method of Bradford (*9*). Fractions containing protein were pooled and applied to an ADP-agarose affinity column, which takes advantage of the NADP binding site in the protein. Pooled fractions from the Ni-NTA column were applied to the ADP-agarose column directly, with a flow rate of 2 mL/min. The column was then

washed with 10 volumes of Buffer A and protein was eluted with 150 mM pyrophosphate buffer, pH 7.5, containing 1 mM EDTA and 2 mM β–mercaptoethanol. Fractions were collected and protein concentration was determined by reading the absorbance at 280 nm (ε = 62,160 $M^{-1}cm^{-1}$ for 6-His tagged 6PGDH). Fractions containing protein were again pooled and concentrated using an Amicon ultrafiltration apparatus with a PM-30 semipermeable membrane. SDS-PAGE was performed for wild type and all mutant enzymes to analyze the purity of the protein.

The wild type and mutant proteins were purified in an identical manner, and all enzymes were stored at 4 ^{o}C in the same buffer used for elution from the ADP-agarose column.

3.2.5 Synthesis of 3-d-6PG.

3-*deutero*-glucose was converted to 3-*deutero*-glucose 6-phosphate enzymatically using hexokinase as described previously (*10*). The extent of conversion to the product of the reaction was determined by end-point assay using glucose-6-phosphate dehydrogenase. Upon completion of the reaction, the pH of the solution was adjusted to 4.5 to denature the enzymes in the mixture and Amicon ultrafiltration was used to remove the enzymes. The resulting solution was treated with acid-washed and heat-activated charcoal, stirred for 1 hour and filtered to remove nucleotides and then Dowex 50W-H^{+} resin was used to remove Mg^{2+}. The

solution, containing 3-*d*-glucose 6-phosphate, was bromine oxidized to yield the final product 3-*d*-6PG, which was purified as described previously (*5*).

3.2.6 Initial Velocity Studies.

Initial velocity studies were performed using a Beckman DU640 UV/Vis spectrophotometer. The appearance of NADPH (ε_{340} = 6.22 mM^{-1} cm^{-1}) was monitored over time using 1 cm pathlength semi-micro quartz cuvettes. The temperature was maintained at 25 ^{o}C using a Beckman Temperature Controller. Initial velocity patterns were measured for all mutant and wild type enzymes in 100 mM Hepes, pH 7.5, using variable concentrations of 6PG (15-500 μM) and NADP (1-1000 μM) dependent on the mutant enzyme.

3.2.7 pH Studies.

Initial velocity data were obtained as a function of pH under conditions in which 6PG was varied while NADP was fixed at saturating level (40 K_m). The pH was maintained using the following buffers at 100 mM concentrations: Bis-Tris, 5-6.5; Hepes, 6.5-8.5; Ches, 8.5-9.5. Sufficient overlap was obtained upon changing buffers to eliminate buffer effects. The pH was determined before and after the initial velocity measurements.

3.2.8 Primary Deuterium Kinetic Isotope Effects.

The concentrations of 3-*h*-6PG and 3-*d*-6PG were determined enzymatically in

triplicate by end-point assay using wild type 6PGDH. The concentrations from three determinations were in agreement within 2%. Primary deuterium isotope effects with 3-*d*-6PG were obtained for all the mutant enzymes as well as for the wild type enzyme by direct comparison of initial velocities (*11*). ^{D}V and $^{D}(V/K_{NADP})$ were obtained in triplicate by varying NADP at saturating levels of either 3-*h*-6PG or 3-*d*-6PG (20 K_m), while ^{D}V and $^{D}(V/K_{6PG})$ were measured in triplicate varying 3-*h*-6PG or 3-*d*-6PG at saturating concentrations of NADP (40 K_m).

3.2.9 Solvent Deuterium Kinetic Isotope Effects.

Initial velocities for the wild type and mutant enzymes were measured in both H_2O and D_2O solutions. Substrates (NADP, 3-*h*-6PG and 3-*d*-6PG) and buffers used in D_2O solutions were first dissolved in small volume of D_2O and lyophilized overnight to remove exchangeable protons. The lyophilized powders were then dissolved in D_2O to give the desired concentrations and pD was adjusted using either DCl or NaOD. Primary solvent deuterium isotope effects were obtained by direct comparison of initial velocities in the pH/pD independent region.

3.2.10 ^{13}C-Kinetic Isotope Effects.

These effects were measured using the natural abundance of ^{13}C at the C-1 position of 6PG (*12*). Both high conversion (100% reaction, which represents $^{12}C/^{13}C$ in substrate) and low conversion samples were used to measure the $^{12}C/^{13}C$

isotope ratios in the CO_2 produced from the reaction of 3-*h*-6PG or 3-*d*-6PG. From these ratios, the ^{13}C-kinetic isotope effect was calculated (*13*).

For high conversion samples, in 40 mL of H_2O or D_2O, the reaction mixtures contained 2 mM 3-*h*-6PG or 3-*d*-6PG, 0.5 mM NADP and 10 mM oxidized glutathione. The low conversion reactions contain 6.5 mM 3-*h*-6PG or 3-*d*-6PG for the enzymes that have a K_{6PG} close to that of the wild type 6PGDH (28 μM), or 15 mM, if K_{6PG} was higher. The NADP concentration was 0.25 mM for enzymes with a K_{NADP} about 2 μM or 1mM if K_{NADP} was higher (greater than 20 μM). All low conversion samples contained 5 mM oxidized glutathione in a final volume of 40 mL. The pH(D) of the reaction solutions was titrated to 7.6, followed by sparging with CO_2-free nitrogen overnight. Before starting the reactions, aliquots were withdrawn to determine the initial concentrations of 6PG by end-point assay in triplicate. Then the reactions were initiated by the addition of 2 units of 6PGDH and 100 units of glutathione reductase to recycle NADP for both high and low conversion samples.

The high conversion samples were allowed to proceed for more than 16 hours and end-point assays were used to confirm the completion of the reaction. For the low conversion samples, extents of reaction were monitored by end-point, assaying the remaining 6PG. Reactions were quenched when 50 μmole of CO_2 were produced. For both high and low conversion samples, 0.2 mL of concentrated

sulfuric acid was added to quench the reactions and the generated CO_2 was isolated by vacuum distillation (*14*). Aliquots of the samples were withdrawn after the CO_2 isolation and incubated at pH 8 overnight. The next day, end-point assays were performed in triplicate to determine the exact extent of the low conversion reactions. Isotopic composition of the CO_2 was measured on a Finnigan Delta E isotope-ratio mass spectrometer in the laboratory of Dr. Michael Engel, Department of Geophysics, University of Oklahoma. All ratios were corrected for ^{17}O according to Craig (*15*).

3.2.11 Nomenclature.

Isotope effects are expressed using the nomenclature developed by Northrop (*20*) and Cook and Cleland (*21*). Deuterium, ^{13}C, and solvent deuterium kinetic isotope effects are written with a leading superscript D, 13, or D_2O, e.g. a primary deuterium isotope effect on V/K is written $^{D}(V/K)$. Multiple isotope effects are written with a leading superscript to depict the isotope varied, and a following subscript to depict the fixed isotope, e.g. a solvent deuterium isotope effect measured with deuterated 6PG would be written $^{D2O}(V/K)_D$.

3.2.12 Data Processing.

Double reciprocal plots were used to analyze the data and all plots and replots were linear. Data were fitted using the appropriate rate equations and programs developed by Cleland (*16*). Data for substrate saturation curves obtained at a fixed

concentration of the second substrate were fitted using eq. 1. Initial velocity patterns were fitted using eq. 2. Deuterium kinetic isotope effect data in H_2O and D_2O were fitted using eq. 3. In eqs. 1 and 2, v is the initial velocity, V is the maximum velocity, A and B are reactant concentrations, K_a and K_b are the Michaelis constants for NADP and 6PG, respectively, and K_{ia} is the dissociation constant for NADP. In eq. 3, F_i is the fraction of deuterium label in the substrate or solvent, and E_V and $E_{V/K}$ are the isotope effects minus 1 on V and V/K. The pH dependence of V and V/K were fitted using eq. 4, in which y is V or V/K, C is the pH independent value of y, H is the hydrogen ion concentration, and K_1 and K_2 are the acid dissociation constants for enzyme or substrate groups important in a given protonation state for optimal binding and/or catalysis.

Calculation of ^{13}C-kinetic isotope effects was performed according to eq. 5, where f is the fraction of completion of the reaction, R_p and R_∞ are the $^{12}C/^{13}C$ isotopic ratios for CO_2 at partial and complete conversion, respectively. Isotope ratios, given as $\delta^{13}C$, were calculated from eq. 6, where R_{smp} and R_{std} are $^{12}C/^{13}C$ isotopic ratios for sample and standard, respectively. The standard for CO_2 was calibrated from Pee Dee Belemnite with a $^{12}C/^{13}C$ of 0.0112372 (*15*).

$$v = \frac{VA}{K_a + A} \qquad [1]$$

$$v = \frac{VAB}{K_{ia}K_b + K_aB + K_bA + AB} \quad [2]$$

$$v = \frac{VA}{K_a(1 + F_iE_{V/K}) + A(1 + F_iE_V)} \quad [3]$$

$$\log y = \log\left[\frac{C}{1 + H/K_1 + K_2/H}\right] \quad [4]$$

$$^{13}(V/K) = \frac{\log(1-f)}{\log(1 - f[R_p/R_\infty])} \quad [5]$$

$$\delta(^{13}C) = \left(\frac{R_{smp}}{R_{std}} - 1\right) x\, 10^3 \quad [6]$$

3.3 Results.

3.3.1 Spectral Properties of Mutant Enzymes.

There are 16 tryptophan residues in 6PGDH spread throughout the protein structure. Identical tryptophan fluorescence emission spectra were obtained for all mutant and wild type enzymes, upon excitation at 298 nm (data not shown), indicating that the microenvironment of tryptophan residues of the proteins is the same for all enzymes. As a result, there are no major changes in the overall structure of the enzyme resulting from the mutation. Changes are restricted to the local area within the active site.

3.3.2 Kinetic Parameters of the Mutant Enzymes.

Initial velocity patterns were obtained by measuring the initial rate at pH 7.5

	wt	Y191A	K260A	T262A	R287A	R446A
V/E_t (sec^{-1})	9.4 ± 0.4	11.0 ± 0.4	0.43 ± 0.05	3.1 ± 0.3	0.015 ± 0.001	0.03 ± 0.01
Fold decrease		-	22	3	627	303
K_{NADP} (μM)	5 ± 1	14 ± 2	16 ± 3	4.2 ± 0.5	73 ± 10	64 ± 6
Fold increase		2.8	3.2	-	15	13
K_{6PG} (μM)	28 ± 4	1,040 ± 60	150 ± 8	24 ± 1	23000 ± 2000	3,400 ± 400
Fold increase		37	5.4	0.9	814	120
$V/K_{6PG}E_t$ ($M^{-1}s^{-1}$)	3.4×10^5	1.1×10^4	2.8×10^3	1.3×10^5	0.6	9.2
Fold decrease		31	121	2.6	5.7×10^5	3.7×10^4
ΔG^o (kcal $mole^{-1}$)[b]	-6.2	-4.1	-5.2	-6.3	-2.2	-3.4
$\Delta\Delta G^o$ (kcal $mole^{-1}$)[b]		2.1	1.0	-	4.0	2.8

Table 3-2. Summary of the Kinetic Parameters for 6PGDH Wild Type and Mutant Enzymes[a] at the 6-Phosphate Site. [a]Values are ± S.E.
[b]Values are calculated from K_{6PG}, using $\Delta G^o = RT\ln K_{6PG}$.

	wt	Y191A	K260A	T262A
^{D}V	1.9 ± 0.1[b]	1.06 ± 0.02	1.24 ± 0.09	1.25 ± 0.07
$^{D}(V/K_{6PG})$	1.9 ± 0.1[b]	1.05 ± 0.02	1.48 ± 0.23	1.19 ± 0.10
$^{13}(V/K_{6PG})_{H}$	1.0028 (0.0007)[c]	1.0269 (0.0005)	1.0397 (0.0007)	1.0325 (0.0005)
$^{13}(V/K_{6PG})_{D}$	1.0017 (0.0005)	N.D.[d]	1.0290 (0.0007)	1.030 (0.001)
$^{13}(V/K_{6PG})_{D2O}$	- -	1.0116 (0.0005)	- -	1.0206 (0.0003)
$^{D2O}V_{H}$	2.10 ± 0.05	1.58 ± 0.06	1.22 ± 0.04	1.15 ± 0.04
$^{D2O}(V/K_{6PG})_{H}$	1.9 ± 0.2	1.6 ± 0.1	1.25 ± 0.09	0.76 ± 0.06
$^{D2O}(V)_{D}$	2.3 ± 0.1	-	1.22 ± 0.10	1.29 ± 0.04
$^{D2O}(V/K_{6PG})_{D}$	2.28 ± 0.02	-	0.94 ± 0.10	0.77 ± 0.04
pK_a (V)[f]	6.40 ± 0.04[e]	6.2 ± 0.1	-	-
[f]	-	9.1 ± 0.1	-	-
pK_a (V/K)[g]	6.2 ± 0.2[e]	6.6 ± 0.2	-	-
[g]	8.5 ± 0.1[e]	8.0 ± 0.1	-	-

Table 3-3. Summary of Isotope Effects for 6PGDH Wild Type and Mutant Enzymes[a] at the 6-Phosphate Site. [a]Values are ± S.E.

[b]From Hwang, et al *Biochemistry* 1998.

[c]Values in parenthesis are standard errors for the ^{13}C-kinetic isotope effects.

[d]Not determined as a result of the deuterium isotope effect near 1.

[e]From Li and Cook (*19*).

[f]pKa from the V pH profile.

[g]pKa from the (V/ K) pH profile.

using variable concentrations of 6PG (15-500 μM) and NADP (1-1000 μM) dependent on the mutant enzymes. Data are summarized in Table 3-2.

K_{NADP} increased for all but T262 mutation, which showed no change compared to that of wild type enzyme. The increase in K_{NADP} for Y191A and K260A is about 3-fold, while more than an order of magnitude increase is observed for R287A and R446A mutant enzymes. Data suggest that changes in the 6PG binding site somehow affect the binding of NADP, i.e., there is a linkage between the two sites. In comparison, the value of $V/K_{6PG}E_t$ for the R287A and R446A mutant enzymes is decreased 10^4-10^5 fold, and V/E_t is decreased by at least two orders of magnitudes with respect to the wild type enzyme. Data indicate that elimination of either of the arginine residues dramatically impairs enzyme activity. On the other hand, $V/K_{6PG}E_t$ is decreased 30- and 120-fold, respectively, compared to the wild type enzyme, for Y191A and K260A mutant enzymes. Changes in V/E_t are smaller with no change in the case of Y191A, and a 20-fold change in the case of K260A. The T262A mutant enzyme exhibits a 3-fold change in V/E_t and $V/K_{6PG}E_t$, reflecting the 3-fold change in the former.

3.3.3 Kinetic Primary Deuterium Isotope Effects.

The kinetic deuterium isotope effects on V and V/K_{6PG} were measured at saturating NADP (40 K_m) (Table 3-3). The isotope effects on both kinetic

parameters are small in all cases, and within error equal to one another, consistent with the proposed rapid equilibrium random kinetic mechanism (*1*). Isotope effects on R287A and R446A were not measured because of the very low activity.

3.3.4 Solvent Deuterium Kinetic Isotope Effects.

The solvent deuterium kinetic isotope effects on V and V/K_{6PG} were measured at saturating NADP (40 K_m), comparing the rates in H_2O and D_2O (Table 3-3). Equal isotope effects on the two parameters were obtained for the wild type enzyme, Y191A and K260A mutations, while for the T262A mutant enzyme $^{D2O}(V/K) < {}^{D2O}V$. For all three mutant enzymes, the isotope effects are smaller than those observed for the wild type protein. Multiple primary deuterium / solvent deuterium isotope effects were measured for K260A and T262A mutant enzymes at saturating level NADP (40 K_m) (Table 3-3). For the K260A mutant enzyme $^{D}V_{D2O}$, within error, is equal to ^{D}V, while $^{D}(V/K)_{D2O}$ is slightly smaller than $^{D}(V/K)$. In the case of T262A mutation, $^{D}V_{D2O}$ is within error equal to ^{D}V, and an inverse value of $^{D}(V/K)_{D2O}$ is obtained.

3.3.5 ^{13}C-Kinetic Isotope effects.

Data for ^{13}C-kinetic isotope effects obtained with 3-*h*-6PG and 3-*d*-6PG are shown in Table 3. For all of the mutant enzymes, the value of $^{13}(V/K_{6PG})_H$ minus 1 is at least an order of magnitude higher than that of the wild type enzyme. Deuteration of 6PG decreases the observed ^{13}C-kinetic isotope effects for the wild

type enzyme as well as that for K260A and T262A, and in all cases the equality for a stepwise mechanism with oxidation preceding decarboxylation is satisfied within error (*13*). ^{13}C-kinetic isotope effects were also measured in H_2O and D_2O to determine the multiple solvent deuterium/^{13}C isotope effects, as summarized in Table 3-3. Note that there is a decrease in the ^{13}C-kinetic isotope effects when measured in D_2O.

3.3.6 pH Dependence of Kinetic Parameters.

The pH dependence of the kinetic parameters of the mutant enzyme Y191A was measured by varying 6PG at saturating level of NADP (40 K_m). Bell shaped pH-rate profiles with limiting slopes of 1 and -1 was obtained for V/K_{6PG} and V. The pK_a values are summarized in Table 3-3. The pH-rate profiles for the Y191A mutant enzyme is shown in Figure 3-3.

3.4 Discussion.

The main aim of this research was to determine the importance of residues Y191, K260, T262, R287 and R446, which interact with the 6-phosphate of 6PG, and their role in providing binding energy and proper orientation of the substrate. On the basis of the crystal structure of the E:6PG binary complex, interactions between each of the five residues listed and the 6-phosphate of 6PG is suggested. A multiple

sequence alignment of 6PGDHs from a variety of species from bacteria to man indicates a complete conservation of all of the residues considered (Figure 3-1). Site-directed mutagenesis was used to change Y191, K260, T262, R287 and R446 to alanine one at a time to eliminate the interaction between each of the residues and the 6-phosphate of 6PG. Steady-state kinetic parameters and isotope effects were measured to determine the effect of the substitutions on the ability of 6PGDH to use 6PG as a substrate.

Theory for interpretation of kinetic parameters and isotope effects in the 6PGDH reaction has been developed previously and equations are reproduced here for aid in data interpretation (*5, 10*). The oxidative decarboxylation reaction catalyzed by 6PGDH is stepwise with oxidation preceding decarboxylation as suggested by multiple deuterium/^{13}C kinetic isotope effect studies (*10*). Multiple solvent deuterium kinetic isotope effect and proton inventory studies indicate the presence of an isomerization of the enzyme complex prior to hydride transfer and decarboxylation (*17*). The kinetic mechanism of 6PGDH at saturating NADP can be written:

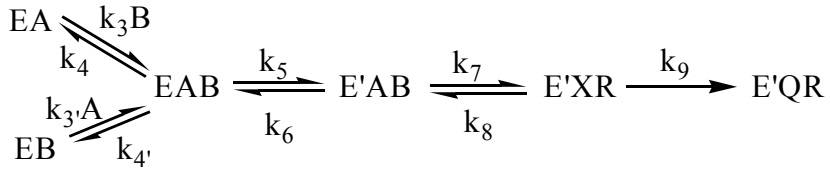

[7]

where A, B, X, Q, and R represent NADP, 6PG, 3-keto-6PG, ribulose 5-phosphate,

and NADPH, respectively. The rate constants k_3 and k_4 are for binding and dissociation of 6PG and $k_{3'}$ and $k_{4'}$ are for binding and dissociation of NADP, k_5 and k_6 are for an isomerization of E:NADP:6PG complex, k_7 and k_8 are for forward and reverse hydride transfer, and k_9 is the rate constant for decarboxylation of the 3-keto intermediate and release of CO_2. The deuterium sensitive step, hydride transfer, may exhibit an isotope effect upon deuteration of 6PG at the 3-poisition, depicted by $^{D}k_7$ and $^{D}k_8$, which can be related by the equilibrium isotope effect, $^{D}K_{eq} = {}^{D}k_7/{}^{D}k_8$. The ^{13}C-kinetic sensitive step, k_9, may exhibit a primary isotope effect, $^{13}k_9$.

Given the rapid equilibrium nature of the mechanism, central complex interconversion is rate-limiting (steps included from EAB to E'QR, and thus $k_4, k_{4'} > k_5$, while k_{11}, $k_{13} > k_7$. Finally, since the kinetic isotope effects on V and V/K are equal to one another for the wild type and each of the mutant enzymes, $k_6 = (1 + k_6/k_5)/(1/k_5 + 1/k_9)$.

It is possible that the kinetic mechanism of the enzyme changed upon making the mutations discussed above. However, the kinetic mechanism is equilibrium random for the wt enzyme (*1*, *2*), and in all of the mutant enzymes with the exception of the Y191A mutant enzyme V is decreased. The only real possibility for a change in kinetic mechanism for the remaining mutant enzymes is to an equilibrium ordered addition of reactants, and this would have been observed when initial velocity

patterns were performed (the K_m for one of the reactants would be zero). In the case of the Y191A mutant enzyme, the V/K values for both reactants decrease, and this would be difficult to rationalize for other than an equilibrium mechanism.

On the basis of the above, the following expressions have been developed.

$$V = \frac{\dfrac{k_7}{1+\dfrac{k_6}{k_5}}}{1+\dfrac{k_7\left(\dfrac{1}{k_5}+\dfrac{1}{k_9}\right)}{1+\dfrac{k_6}{k_5}}+\dfrac{k_8}{k_9}} \qquad [8]$$

$$\frac{V}{K_{6PG}} = \frac{\dfrac{k_3 k_5 k_7}{k_4 k_6}}{1+\dfrac{k_7}{k_6}+\dfrac{k_8}{k_9}} \qquad [9]$$

$${}^{D}V = \frac{{}^{D}k_7+\dfrac{k_7\left(\dfrac{1}{k_5}+\dfrac{1}{k_9}\right)}{1+\dfrac{k_6}{k_5}}+\left({}^{D}K_{eq}\right)\left(\dfrac{k_8}{k_9}\right)}{1+\dfrac{k_7\left(\dfrac{1}{k_5}+\dfrac{1}{k_9}\right)}{1+\dfrac{k_6}{k_5}}+\dfrac{k_8}{k_9}} \qquad [10]$$

$${}^{D}\left(\frac{V}{K_{6PG}}\right) = \frac{{}^{D}k_7+\dfrac{k_7}{k_6}+\left({}^{D}K_{eq}\right)\left(\dfrac{k_8}{k_9}\right)}{1+\dfrac{k_7}{k_6}+\dfrac{k_8}{k_9}} \qquad [11]$$

$${}^{13}\left(\frac{V}{K_{6PG}}\right)_H = \frac{{}^{13}k_9+\left(k_9/k_8\right)\left(1+k_7/k_6\right)}{1+\left(k_9/k_8\right)\left(1+k_7/k_6\right)} \qquad [12]$$

$$^{13}\left(\frac{V}{K_{6PG}}\right)_D = \frac{^{13}k_9 + \left(^Dk_7k_9/k_8{}^DK_{eq}\right)\left(1 + k_7/k_6{}^Dk_7\right)}{1 + \left(^Dk_7k_9/k_8{}^DK_{eq}\right)\left(1 + k_7/k_6{}^Dk_7\right)} \quad [13]$$

Since K_{6PG} is the ratio of V and V/K_{6PG}, and taking into account $k_6 = (1 + k_6/k_5)/(1/k_5 + 1/k_9)$

$$K_{6PG} = \left(\frac{k_4}{k_3}\right)\left(\frac{k_6}{k_5 + k_6}\right) \quad [14]$$

where k_4/k_3 is the K_d of 6PG for the E:NADP:6PG complex and $k_6/(k_5 + k_6)$ corrects for the distribution of the central complexes between E:NADP:6PG and E':NADP:6PG. Therefore, K_{6PG} is the equilibrium constant for dissociation of 6PG from E:NADP:6PG and E':NADP:6PG. Using the above rate equations, we discuss the results for each of the mutant enzyme.

The key to interpretation of the data obtained for the mutant enzymes lies in the change in K_{6PG}, $^D(V/K_{6PG})$, and $^{13}(V/K_{6PG})$. The increase in K_{6PG} and K_{NADP} likely results from an increase in the net off-rates for 6PG and NADP from E':NADP:6PG, $k_4k_6/(k_5 + k_6)$ ($k_4'k_6/(k_5 + k_6)$ in the case of NADP), suggesting an increase in k_4, k_6, or both. Since the K_m values of both substrates are affected, it is likely to be both. The conformational change that precedes the catalytic steps represented by k_5 and k_6 in mechanism 7, requires both reactants bound as suggested by a superposition of the

E:Nbr^{8}ADP and E:6PG complexes (*6*), which gives a hydride transfer distance of 5.3 Å, which is much too long. Therefore a conformational change that brings the two substrates close together is required.

3.4.1 The R287A and R446A Mutant Enzymes.

As shown in Table 2, K_{6PG} increases by about 800-fold and 120-fold for R287A and R446A, respectively, compared to the value of the wild type enzyme. In addition, V/E_t decreases about 600- and 300-fold respectively, resulting in a $V/K_{6PG}E_t$ more than 10,000 times lower than that of the wild type protein. Because of the very low activity, no further characterization was carried out on the two mutant enzymes. On the basis of the measured kinetic parameters, the affinity of the mutant enzymes for their substrate 6PG decreases substantially ($\Delta\Delta G^o$ 3.95 and 2.81 kcal/mol for R287A and R446A, respectively), and the ability of the mutant enzymes to catalyze reaction is severely impaired, as a result of eliminating hydrogen-bonding and ionic interactions contributed by the arginine residues. Given the expression for K_{6PG}, eq. 14, the net rate constant for release of 6PG is increased. Since there is also an observed greater than10-fold increase in K_{NADP} it is likely, as suggested above, that part of the increase results from a change in the equilibrium position of the conformational change that precedes the hydride transfer step to favor EAB, mechanism 7.

3.4.2 The Y191A Mutant Enzyme.

Data for replacement of Y191 with A are interesting in that V/E_t is increased by about 20% (1.17 ± 0.06, Table 2). One would thus not expect much change in the isotope effects. This is not the case, and significant changes in the magnitude of the isotope effects are observed. The V and V/K_{6PG} pH-rate profiles for the Y191A mutant enzyme exhibits pK values that are closer together than those observed for the wt enzyme, Table 3-3. (The phenomenon is easier to see and explain using the V/K profiles. The same phenomenon is apparent for the V pH-rate profiles, but one of the pK values is too high to be observed in the case of the wt enzyme.) The V/K_{6PG} pH-rate profiles reflect reverse protonation states between the K183 general base and the E190 general acid (*4*), and thus the amount of active enzyme can be estimated from the antilog of the difference between the acid and base pK values. In the case of the wt enzyme, the fraction of active enzyme is 0.5%, while in the case of the Y191A enzyme the value is 4%, representing a 8-fold increase, i.e. a value of 70 s^{-1} would be expected compared to the value of the wt enzyme, Table 3-2. The observed value of V/E_t for the Y191A mutant enzyme, therefore, reflects an 8-fold decrease in the actual value of V/E_t. The tyrosine donates a single hydrogen bond to the phosphate, Figure 3-3. Changing Y to A, results in a 40-fold decrease in affinity.

In the wt enzyme, the ^{13}C kinetic isotope effect is 1.0028, while when it is

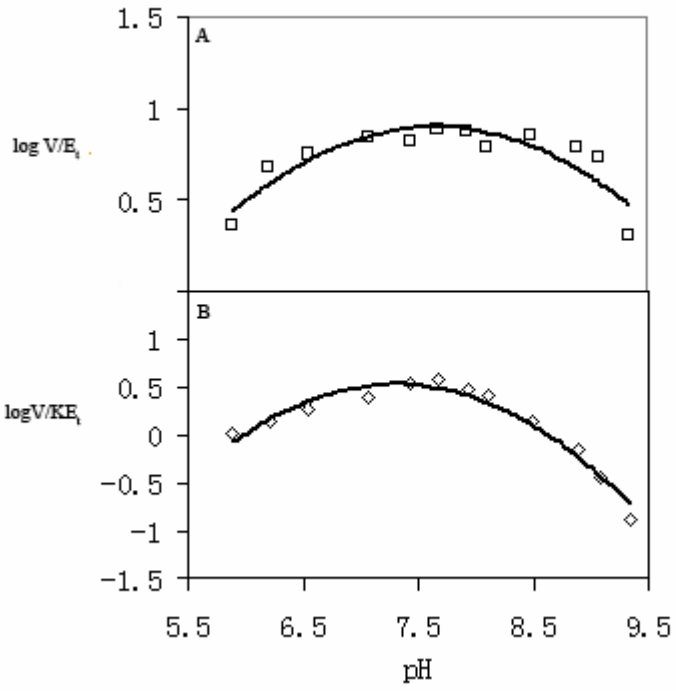

Figure 3-3. pH Dependence of Kinetic Parameters for the Y191A Mutant of 6-PGDH. Data were obtained for V (A) and V/K_{6PG} (B). The points shown are the experimentally determined values and the curves are from a fit of the data using eq.4.

measured in D_2O, the number decreases to 1, indicating that under D_2O condition, the decarboxylation step is not rate limiting at all. Given the solvent deuterium isotope effect about 2 on both V and V/K_{6PG} and the primary deuterium isotope effect about 1.9 on V and V/K_{6PG}, it is suggested that in the wt enzyme rate-limitation arises mostly from the isomerization and the hydride transfer step. In the Y191A mutant enzyme, the value of $^{13}(V/K_{6PG})$ has increased to 1.0269, concomitant with a decrease in ^{D}V and $^{D}(V/K_{6PG})$ to a small finite value. Data suggest a decrease in the rate of the decarboxylation step relative to hydride transfer. The solvent deuterium isotope effect is finite, but slightly lower in value compared to the wt enzyme, and the multiple ^{13}C/solvent deuterium effect indicates some of this is on a step other than decarboxylation. Since the effect is normal and not inverse, the hydride transfer step likely contributes part of the effect (see T262A below, *17*). Therefore, in the Y191A mutant enzyme, decarboxylation is predominantly rate-limiting. Isomerization and hydride transfer also contribute to rate-limitation. In addition to the large increase in K_{6PG}, the mutant enzyme exhibits a 3-fold increase in K_{NADP} suggesting a change in the rate of the conformational change that precedes hydride transfer. Data further suggest that occupancy of the 6-phosphate-binding site is needed to generate the enzyme's optimum catalytic conformation.

3.4.3 The T262A Mutant Enzyme.

Only in the case of the T262A mutant enzyme is there no observed change in K_{6PG}, suggesting no significant binding energy is provided by this side chain. This is not surprising, given the 3.7 Å distance from the T side chain to the 6-phosphate (*6*) (Figure 3-2). However, a 3-fold decrease in V/E_t is observed and the isotope effects differ significantly from those obtained for the wild type enzyme. The large value of $^{13}(V/K_{6PG})$, 1.0325, indicates the decarboxylation step has become predominantly rate-limiting overall, and the primary kinetic deuterium isotope effects is close to the value of the equilibrium deuterium isotope effect of 1.18 on the hydride transfer step (*18*). The multiple deuterium/^{13}C isotope effect is decreased slightly consistent with the small deuterium isotope effect. The increase in the ^{13}C isotope effect to 1.0325 (the effect for wt is 1.0028) can be used to estimate the partition ratio for the 3-keto-6PG intermediate in the case of the wt enzyme. Substituting 1.0325 for $^{13}k_9$ in eq. 11 and 1.0028 for $^{13}(V/K_{6PG})$, gives a value of 10.6 for k_9/k_8. Thus, in order to see the increased value of $^{13}(V/K_{6PG})$ the partition ratio for the 3-keto-6PG intermediate must decrease by a factor of 10. The change in partition ratio is much greater than the observed decrease in V/E_t (3-fold), and thus it is likely that the fraction of enzyme that is catalytically competent has increased in the case of the mutant enzyme as suggested above for the Y191A mutant enzyme, or that a step within the catalytic pathway has increased in rate (this would most likely be k_7 since

it is included in both V and V/K).

An inverse solvent deuterium kinetic isotope effect is observed on V/K, and this likely reflects a medium effect on the conformation change that precedes hydride transfer (*17*). Deuteration of the substrate has no significant effect on the inverse solvent effect on V/K; this is not surprising given the small value of ^{D}(V/K). Of interest, the solvent deuterium isotope effect on V is normal, and this may be indicative of some rate-limitation by tautomerization of the enediol of ribulose 5-phosphate, but this will require additional study.

3.4.4 The K260A Mutant Enzyme.

Lysine 260 donates a hydrogen bond from its backbone NH to the 6-phosphate, and also provides van der Waals interactions via its side chain and the backbone of 6PG. Changing K260 to alanine gives a greater than 5-fold decrease in the affinity of 6PGDH for 6PG. This change in binding energy likely reflects the van der Waals interactions since the backbone NH will still be present (although it may not be in position to donate a hydrogen bond). As stated above, the increase in both K_{NADP} and K_{6PG} suggest a decrease in the rate of the conformational change to set the active site up for catalysis. Data further suggest either a requirement for occupancy of the 6-phosphate site or proper binding of 6PG to generate an optimum catalytic conformation, that is, utilization of the binding energy of 6PG to catalyze the

reaction.

The 20-fold decrease in V likely results from a decrease in the rate of the decarboxylation step, k_9, consistent with the estimated 13-fold decrease in k_9/k_8, calculated as above for the T262A mutant enzyme. The largest value of $^{13}(V/K_{6PG})$ is observed for this mutant enzyme. The decreased value of the deuterium isotope effects is also consistent with the increased rate-limitation of the decarboxylation step. However, the values of ^{D}V and $^{D}(V/K_{6PG})$ are greater than $^{D}K_{eq}$ suggesting a small contribution to rate-limitation by the hydride transfer step. In agreement, the values of ^{D2O}V and $^{D2O}(V/K_{6PG})$ are finite and normal, suggesting a contribution from either hydride transfer, decarboxylation, or both (*17*). The observed decrease in the solvent isotope effect to a value of 1 is consistent with a decrease in the observed solvent isotope effects on decarboxylation, as a result of the inverse effect on the conformational change preceding hydride transfer. The finite value of the effect on V may again suggest a contribution from the tautomerization step. Data are also consistent with the structural data of Adams (*6*), which show that the alkyl side chain of K260 rests against the backbone of 6PG. The effect of removing the lysine side chain could introduce a significant positional change of the bound substrate, resulting in a poorly orientated 6PG, a subsequent decrease in the rate of the conformational change to establish the catalytic conformation and decrease the rate of

decarboxylation.

3.4.5 Evidence for Interaction Between the Two Substrates Binding Sites.

A summation of the $\Delta\Delta G^o$ values estimated from all of the mutations greatly exceeds the total binding energy of 6PG. It is apparent that the 6-phosphate of 6PG is a very important binding determinant for the substrate. Occupancy of the 6-phosphate binding site appears to be critical for proper positioning of the substrate for the subsequent catalytic steps, most importantly decarboxylation (see above). Another way of putting this is that occupancy of the 6-phosphate binding site is important for the reaction, likely to induce the conformational change in enzyme preceding catalysis. In agreement with this suggestion, there is an increase in K_{NADP} for all the mutant enzymes, with the exception of T262A, ranging from 3-fold to 15-fold. According to the crystal structures of wild type protein with ligands bound, the coenzyme binding pocket is separated from the 6PG binding site (*6*). Since all of the mutations reside in the 6PG-binding site and no significant change in the overall structure of the mutant enzymes was detected, it is suggested that the two sites are linked, likely via the induced conformational change. To this point, there is no direct evidence to suggest where and how the two sites are linked. In addition, a ternary complex of 6PGDH with both substrates bound is not available. An overlay of the two binary complexes (E: Nbr^8ADP and E:6PG) (*5*) can be used as a starting

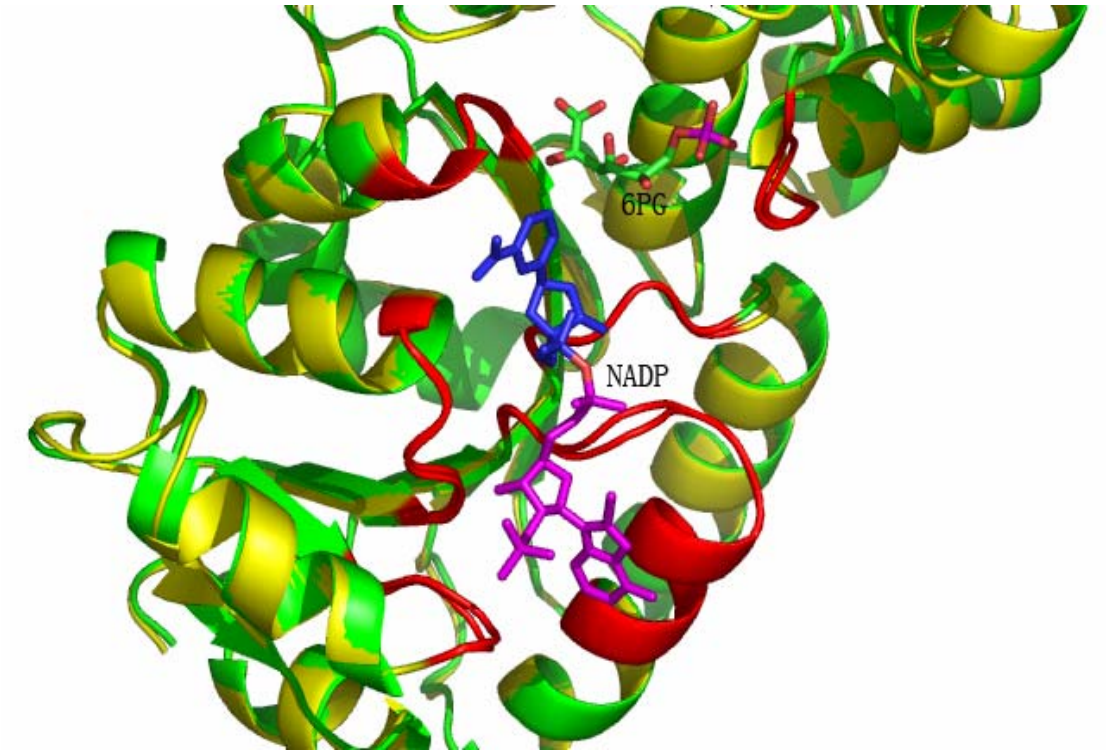

Figure 3-4. Possible Linkage Between the Cofactor and Substrate Binding Sites. In the figure C is green, N is blue, O is red, and P is magenta. The structure of E:6PG complex is shown in green and the structure of E:Nbr^{8}ADP complex is shown yellow. The highlighted region (red) represents the proposed linkage that connects the two sites. The figure was created using PyMOL from DeLano Scientific LLC (www.pymol.org). Accession numbers in the PDB are 1PGN and 1PGP for the E:Nbr^{8}ADP and E:6PG structures, respectively.

point for identification of a proposed pathway that connects the sites, as shown in Figure 3-4. The green colored structure is from the E:6PG binary complex and the yellow colored structure is the E: Nbr^{8}ADP complex. The highlighted region (red) including loops (residue 8-12, 31-34, 73-78, 100-103, 128-131 and 258-261) and a helix (residue 79-83) on both sides of the dinucleotide provides a possible linkage. Further experiments including site-directed mutagenesis in the proposed region and structure analysis will help to test the putative linkage between sites.

However, one of the things we anticipated is that the bound substrate would change in its position within its binding site in the mutant enzymes compared to the wild type enzyme. This is likely what has occurred in most cases given the change in the relative rates of hydride transfer and decarboxylation. Care must be taken in interpreting data for mutant enzymes when alanine is substituted for a residue with a larger volume side chain, since the position of the bound reactant can change when large changes are made by site-directed mutagenesis. Isotope effects and multiple isotope effects, when they can be measured, greatly facilitate the interpretation of the data.

3.4.6 Note Added in Proof.

Consistent with the suggestion that decarboxylation is rate-limiting for the mutant enzymes, we have recently measured pre-steady state time courses following the

appearance of NADPH, mixing enzyme with both substrates. A rapid burst is observed followed by a slow steady state rate that is equivalent to V/E_t. The burst amplitude is equal to E_t in the case of the K260A and T262A mutant enzymes.

3.5 References.

1. Price, N., and Cook, P. F. (1996) Kinetic and Chemical Mechanisms of the Sheep Liver 6-Phosphogluconate Dehydrogenase. *Arch. Biochem. Biophys. 336*, 215-223.

2. Berdis, A. J., and Cook, P. F. (1993) Overall Kinetic Mechanism of 6-Phosphgluconate Dehydrogenase from *Candida utilis*. *Biochemistry 32*, 2036-2040.

3. Karsten, W. E., Chooback, L., and Cook, P. F. (1998) Glutamate 190 Is a General Acid Catalyst in the 6-Phosphogluconate Dehydrogenase-Catalyzed Reaction. *Biochemistry 37*, 15691-15697.

4. Zhang, L., Chooback, L., and Cook, P. F. (1999) Lysine 183 Is the General Base in the 6-Phosphogluconate Dehydrogenase-Catalyzed Reaction. *Biochemistry 38*, 11231-11238.

5. Cervellati, C., Dallocchio, F., Bergamini, C. M., and Cook, P. F. (2005) Role of Methionine-13 in the Catalytic Mechanism of 6-Phosphogluconate Dehydrogenase from Sheep Liver. *Biochemistry 44*, 2432-2440.

6. Adams, J. M., Grant, H. E., Gover, S., Naylor, C. E., and Philips, C. (1994) Substrate Binding in 6-Phosphogluconate Dehydrogenase: Implications for NADP Specificity and the Enzyme Mechanism. *Structure 2*, 651-668.

7. Tetaud, E., Hanau, S., Wells, J. M., Page, R. W. F., Adams, J. M., Arkinson, S., and Barrett, M. P. (1999) 6-Phosphogluconate Dehydrogenase from *Lactococcus lactis*: A Role of Arginine Residues in Binding Substrates and Coenzyme. *Biochem. J. 338*, 55-60.

8. Chooback, L., Price, N. E., Karsten, W. E., Nelson, J., Sundstrom, P., and Cook, P. F. (1998) Cloning, Expression, Purification, and Characterization of the 6-Phosphogluconate Dehydrogenase from Sheep Liver. *Protein Expression Purif. 13*, 251-258.

9. Bradford, M. M. (1976) A Rapid and Sensitive Method for the Quantitation of Microgram Quantities of Protein Utilizing the Principle of Protein-dye Binding. *Anal. Biochem. 72*, 248-254.

10. Hwang, C. C., Berdis, A. J., Karsten, W. E., Cleland, W. W., and Cook, P. F. (1998) Oxidative Decarboxylation of 6-Phosphgluconate by 6-Phosphogluconate Dehydrogenase Proceeds by a Stepwise Mechanism with NADP and ADADP as Oxidants. *Biochemistry 37*, 12596-12602.

11. Parkin, D. W. (1991) *Enzyme Mechanism from Isotope Effects* (Cook, P. F., Ed.), CRC Press, Inc., Boca Raton, FL, pp. 284-285.

12. O'Leary, M. H. (1980) Determination of Heavy-atom Isotope Effects on Enzyme-catalyzed Reactions. *Methods Enzymol*. *64B*, 83-104.

13. Hermes, J. D., Roeske, C. A., O'Leary, M. H., and Cleland, W. W. (1982) Use of Multiple Isotope Effects to Determine Enzyme Mechanisms and Intrinsic Isotope Effects. Malic Enzyme and Glucose 6-Phosphate Dehydrogenase. *Biochemistry 21*, 5106-5114.

14. Weiss P. M. (1991) *Enzyme Mechanism from Isotope Effects* (Cook P. F., Ed.), CRC Press, Inc., Boca Raton, FL, pp. 291-311.

15. Craig, N. (1957) Isotopic standards for carbon and oxygen and correction factors for mass-spectrometric analysis of carbon dioxide. *Geochim. Cosmochim. Acta 12*, 133-149.

16. Cleland, W. W. (1979) Statistical Analysis of Enzyme Kinetic Data. *Methods Enzymol. 63*, 103-108.

17. Hwang, C. C. and Cook, P. F. (1998) Multiple Isotope Effects as a Probe of Proton and Hydride Transfer in the 6-Phosphogluconate Dehydrogenase Reaction. *Biochemistry 37*, 15698-15702.

18. Cook, P. F., Blanchard, J. S., Cleland, W. W. (1980) Primary and Secondary Deuterium Isotope Effects on Equilibrium Constants for Enzyme-Catalyzed Reactions. *Biochemistry 19*, 4853-4858.

19. Northrop, D. B. (1977) in *Isotope effects on Enzyme-Catalyzed Reactions* (Cleland, W. W., O'Leary, M. H. & Northrop, D. B., Eds.) p 122, University Park Press, Baltimore, MD.

20. Cook, P. F., and Cleland, W. W. (1981) Mechanistic Deductions from Isotope Effects in Multireactant Enzyme Mechanisms. *Biochemistry 20*, 1790-1796.

Chapter 4

Roles of S128, H186 and N187

4.1 Introduction

6-Phosphogluconate dehydrogenase (6PGDH[1]; EC 1.1.1.44) catalyzes the reversible oxidative decarboxylation of 6-phosphogluconate (6PG), giving ribulose-5-phosphate (Ru5P) and CO_2 with the concomitant production of NADPH. The kinetic mechanism is rapid equilibrium random on the basis of a complete kinetic characterization of the enzymes from sheep liver and *Candida utilis* (*1, 2*). The pH dependence of kinetic parameters indicates a general acid-general base chemical mechanism (*1, 2*), and site-directed mutagenesis studies suggest that K183 and E190 are the general base and the general acid, respectively (*3, 4*). In this mechanism, the general base (K183) is required to accept a proton from the 3-hydroxyl group of 6PG concomitant with hydride transfer from C-3 of 6PG to the coenzyme. The resulting 3-keto-6-phosphogluconate intermediate is decarboxylated to produce the enediol of Ru5P with the general base used to protonate the carboxyl oxygen. A general acid (E190) is needed to facilitate the tautomerization of the enediol of Ru5P to the keto product (Figure 1-6).

Previous studies suggest that NADPH play a non-redox role in the 6PGDH

catalyzed reaction (*5* - *9*). It has been suggested that after hydride transfer, the nicotinamide ring of NADPH rotates around the *N*-glycosidic bond to a position that was occupied by the 1-carboxylate of 6PG to facilitate decarboxylation (*10*). The structures of the E:6PG and E:NADPH binary complexes indicate that residue S128 and N187 are within hydrogen-bonding distance to the 1-carboxyl group and 3-hydroxyl group of 6PG, respectively, prior to hydride transfer and are interacting with NADPH after hydride transfer. Histidine 186 interacts with the nicotinamide of NADPH in the E:NADPH binary complex, but is within hydrogen-bonding distance to S128 and N187 in the E:6PG binary complex (Figures 4-1 and 4-2) (*11*). Multiple sequence alignment of 6PGDHs from a number of species from bacteria to man shows that S128, H186 and N187 are completely conserved (Figure 4-3). Data suggest that the residues may be important in binding of 6PG prior to hydride transfer and anchoring the nicotinamide ring of NADPH to facilitate decarboxylation after rotation of the nicotinamide ring.

In this chapter we investigate the role of each of the three residues play along the reaction pathway. Site-directed mutagenesis was used to change S128, H186 and N187 to A, one at a time. Initial velocity, pH and isotope effects studies were carried out to characterize the mutant enzymes. Data are consistent with the roles for S128, H186 and N187 in binding of 6PG and NADPH, and in guiding the rotation

of the nicotinamide ring after hydride transfer.

4.2. Material and Methods

4.2.1 Chemicals and Reagents.

Oligonucleotide primers for mutagenesis and sequencing were from Biosynthesis, GibcoBRL and Invitrogen. The Altered site II in vitro mutagenesis system was purchased from Promega. The Geneclean® II kit was from Bio 101, Inc. The PerfectPrep® Plasmid Mini kit was from Eppendorf. The DNA molecular ladder was from New England Biolabs. Restriction endonucleases, deoxynucleoside triphosphates, and protein molecular mass markers were purchased from Gibco-BRL. Acetaldehyde, acetate kinase, ADP-agarose resin, ATP, ampicillin, glucose-6-phosphate dehydrogenase (G6PDH), hexokinase, kanamycin, lithium potassium acetyl phosphate, the trisodium salt of 6PG, NADP, and pyrophosphate were from Sigma-Aldrich, Co. β–D-(3-deutero)-glucose (98 atom% D) was from Omicron Biochemicals, Inc. Ni-NTA agarose resin was purchased from QIAGEN. Glycerol and sulfuric acid were from Fisher-Scientific, Co. IPTG was from Gold Bio Technology (GBT). Hepes, Bis-Tris, and Ches buffers were from Research Organics, Inc. Deuterium oxide (99 atom% D) was from Cambridge Isotope Laboratories, Inc. All other chemicals were the highest quality available.

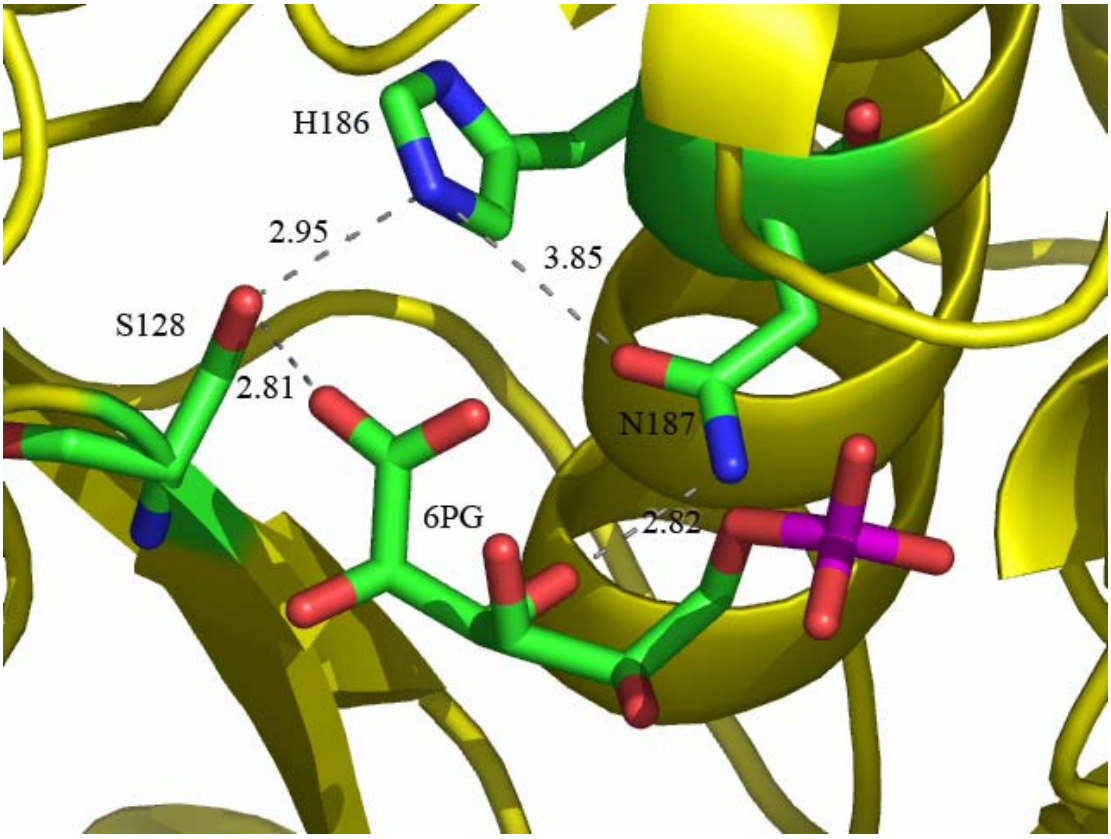

Figure 4-1. S128, H186 And N187 in the E:6PG binary complex. In the figure C is green, N is blue, O is red, and P is magenta. The dashed lines represent potential hydrogen bonds between the residues of interest and the substrate. The numbers above the dashed lines are the hydrogen bond distances in Å. The figure was created using PyMOL from DeLano Scientific LLC (www.pymol.org). The accession number in the PDB is 1PGP for the E:6PG structure.

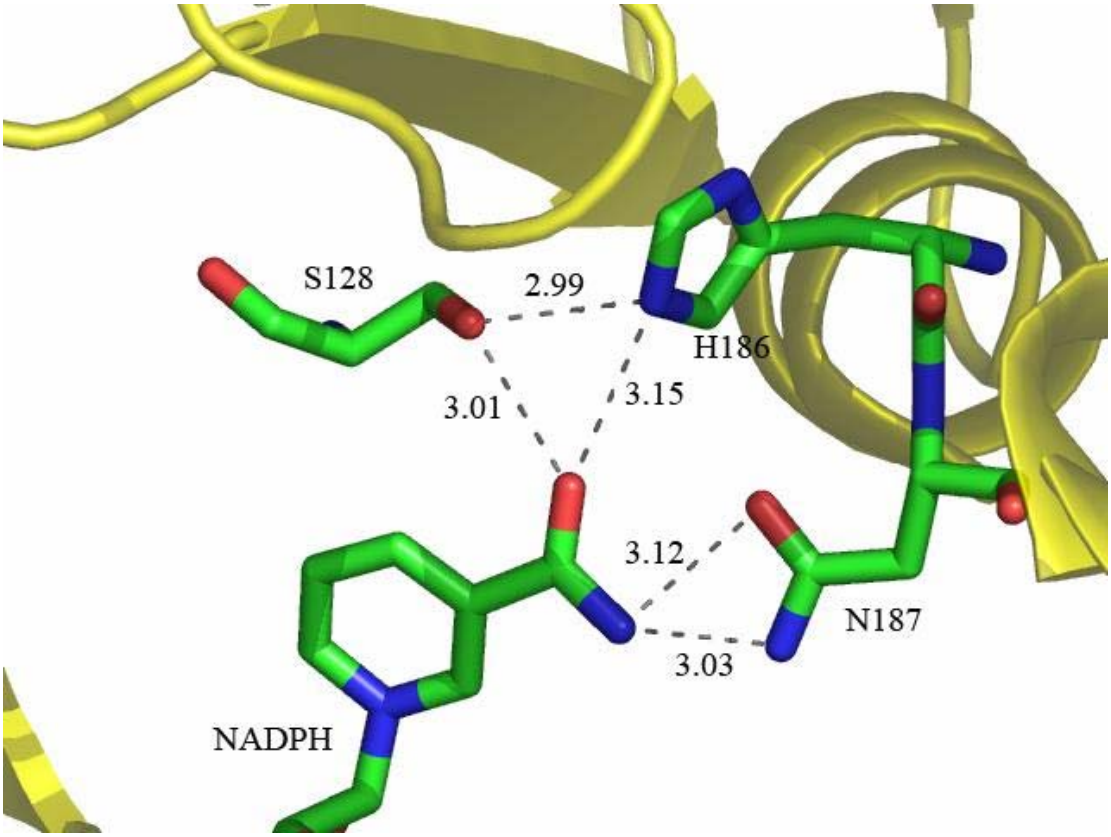

Figure 4-2. S128, H186 And N187 in the E:NADPH binary complex. In the figure C is green, N is blue, and O is red. The dashed lines represent potential hydrogen bonds between the residues of interest and the cofactor. The numbers above the dashed lines are the hydrogen bond distances in Å. The figure was created using PyMOL from DeLano Scientific LLC (www.pymol.org). The accession number in the PDB is 1PGO for the E:NADPH structure.

Species				S128						H186	N187			
Ovis aries	·····	G	V	S	G	G	·····	M	V	H	N	G	I	·····
Homo sapiens	·····	G	V	S	G	G	·····	M	V	H	N	G	I	·····
Drosophila melanogaster	·····	G	V	S	G	G	·····	M	V	H	N	G	I	·····
Ceratitis capitata	·····	G	V	S	G	G	·····	M	V	H	N	G	I	·····
Cunninghamella elegans	·····	G	V	S	G	G	·····	M	V	H	N	G	I	·····
Saccharomyces	·····	G	V	S	G	G	·····	M	V	H	N	G	I	·····
Haemophilus influenzae	·····	G	V	S	G	G	·····	M	V	H	N	G	I	·····
Treponema pallidum	·····	G	V	S	G	G	·····	M	I	H	N	G	I	·····
Chlamydia trachomatis	·····	G	V	S	G	G	·····	A	V	H	N	G	I	·····
Escherichia coli	·····	G	V	S	G	G	·····	M	V	H	N	G	I	·····
Shigella flexneri	·····	G	V	S	G	G	·····	M	V	H	N	G	I	·····
Salmonella typhimurium	·····	G	V	S	G	G	·····	M	V	H	N	G	I	·····
Klebsiella pneumoniae	·····	G	V	S	G	G	·····	M	V	H	N	G	I	·····
Yersinia	·····	G	V	S	G	G	·····	M	V	H	N	G	I	·····
Burkholderia	·····	G	V	S	G	G	·····	M	V	H	N	G	I	·····
Buchnera Aphidicola	·····	G	F	S	G	G	·····	M	V	H	N	G	I	·····
Lactobacillus lactis	·····	G	V	S	G	G	·····	M	V	H	N	G	I	·····
Staphylococcus	·····	G	V	S	G	G	·····	M	V	H	N	G	I	·····
Bacillus licheniformis	·····	G	I	S	G	G	·····	M	V	H	N	G	I	·····
Bacillus subtilis	·····	G	I	S	G	G	·····	M	V	H	N	G	I	·····
Mycobacterium leprae	·····	G	I	S	G	G	·····	M	V	H	N	G	I	·····
Zea mays	·····	G	V	S	G	G	·····	M	V	H	N	G	I	·····
Rhodopirellula	·····	G	V	S	G	G	·····	M	V	H	N	G	I	·····
Synechococcus sp.	·····	G	V	S	G	G	·····	T	V	H	N	G	I	·····
Trypanosoma brucei	·····	G	I	S	G	G	·····	M	Y	H	N	S	G	·····

Figure 4-3. Multiple Sequence Alignment of 6-Phosphogluconate Dehydrogenase Sequences Around Position S128, H186 and N187.

4.2.2 Bacterial Strain and Plasmids.

The *Escherichia coli* strain XL1-Blue was used to transform the mutated plasmid and M15[pREP4] was the host strain for expression of the mutant proteins. The plasmid pQE-30 was used as both mutagenesis and expression vector.

4.2.3 Site-Directed Mutagenesis.

The Altered site II in vitro mutagenesis system from Promega was used to perform site-directed mutagenesis. Single-stranded DNA prepared from recombinant plasmid pPGDH.LC5 (*12*) was used as a template and the synthetic oligonucleotide primers are listed in Table 4-1. Newly synthesized DNA was recovered from the recipient strain ES1301 *mutS* and subsequently transformed into JM109. Gene sequencing was performed for every mutation at the Laboratory for Genomics and Bioinformatics of the University of Oklahoma Health Science Center in Oklahoma City. The resulting sequence was compared to that of the wild type 6PGDH using BLAST. Two synthesized oligonucleotides containing the desired restriction sites were constructed (Table 1). One primer creates a *Sph*I restriction site at the start of the gene, and the other one contains a *Hind*III site at the end of the gene. The two sites were introduced into the gene containing the desired mutation using polymerase chain reaction (PCR). The PCR product was subcloned into the pQE30 vector via the corresponding restriction sites. Successfully mutated plasmids

were transformed into M15[pREP14] competent cells, the expression host. Frozen stocks of strains harboring plasmid were stored in LB/ampicillin/kanamycin medium containing 15% glycerol at -80 ^{o}C.

4.2.4 Growth and Purification Conditions.

The bacterial strain containing the mutated plasmid was first grown in 50-200 mL LB medium, containing 100 μg/mL ampicillin and 25 μg/mL kanamycin at 37 ^{o}C, overnight in a water-bath shaker. The next day, this culture was transferred into 2-10 liters of LB/Amp/Kan medium and was incubated at 25 ^{o}C for 8 hours or until the A_{600} reached 0.6. IPTG was then added to a final concentration of 1 mM to initiate expression. After 16 hours of growth at 25 ^{o}C with shaking, the cells were harvested by centrifugation at 5,000 *g* for 30 minutes. The cell pellet was resuspended in 4volumes of Buffer A (50 mM triethanolamine, 2 mM β–mercaptoethanol, pH 7.5), sonicated on ice for 3 minutes, (pulsing 30 seconds with 30 seconds rest) using a MISONIX Sonicator® XL, and centrifuged at 25,000 *g* for 30 minutes. The supernatant was combined with 2-10 mL of Ni-NTA resin pre-equilibrated with Buffer A and stirred at 4 ^{o}C for 2 hours. The mixture was then loaded into a 25 mL column, and the column was washed with 5 volumes of Buffer A containing 20 mM imidazole. Elution made use of an imidazole gradient (0.2-0.4 M, dependent on the freshness of the resin). Protein concentrations were measured for all fractions using

S128A	GGGAGCGGAGTT**GCT**GGTGGAGAGGA
H186	GTGAAGATGGTG**GCC**AACGGCATAGAG
N187A	AAGATGGTGCAC**GCC**GGCATAGAGTAC

Table 4-1. Sequence of Oligonucleotide Primers for mutation S128A, H186A and N187A. Mutated codons are in bold.

the method of Bradford (*13*). Fractions containing protein were pooled and applied to an ADP-agarose affinity column, which takes advantage of the NADP binding site in the protein. Pooled fractions from the Ni-NTA column were applied to the ADP-agarose column directly, with a flow rate of 2 mL/min. The column was then washed with 10 volumes of Buffer A and protein was eluted with 150 mM pyrophosphate buffer, pH 7.5, containing 1 mM EDTA and 2 mM β–mercaptoethanol. Fractions were collected and protein concentration was determined by reading the absorbance at 280 nm (ε = 62,160 $M^{-1}cm^{-1}$ for 6-His tagged 6PGDH). Fractions containing protein were again pooled and concentrated using an Amicon ultrafiltration apparatus with a PM-30 semipermeable membrane. SDS-PAGE was performed for wild type and all mutant enzymes to analyze the purity of the protein.

The wild type and mutant proteins were purified in an identical manner, and all enzymes were stored at 4 ^{o}C in the same buffer used for elution from the ADP-agarose column.

4.2.5 Synthesis of 3-d-6PG.

3-*deutero*-glucose was converted to 3-*deutero*-glucose 6-phosphate enzymatically using hexokinase as described previously (*14*). The extent of conversion to the product of the reaction was determined by end-point assay using glucose-6-phosphate dehydrogenase. Upon completion of the reaction, the pH of the

solution was adjusted to 4.5 to denature the enzymes in the mixture and Amicon ultrafiltration was used to remove the enzymes. The resulting solution was treated with acid-washed and heat-activated charcoal, stirred for 1 hour and filtered to remove nucleotides and then Dowex 50W-H^+ resin was used to remove Mg^{2+}. The solution, containing 3-*d*-glucose 6-phosphate, was bromine oxidized to yield the final product 3-*d*-6PG, which was purified as described previously (*10*).

4.2.6 Initial Velocity Studies.

Initial velocity studies were performed using a Beckman DU640 UV/Vis spectrophotometer. The appearance of NADPH (ε_{340} = 6.22 mM^{-1} cm^{-1}) was monitored over time using 1 cm pathlength semi-micro quartz cuvettes. The temperature was maintained at 25 ^oC using a Beckman Temperature Controller. Initial velocity patterns were measured for all mutant and wild type enzymes in 100 mM Hepes, pH 7.5, using variable concentrations of 6PG and NADP dependent on the mutant enzyme.

The K_i for NADPH as an inhibitor competitive vs NADP was measured with 6PG equal to its K_m (E:NADP) and at saturating ($20K_m$) concentration (E:NADP:6PG). Data were obtained for the wild-type and mutant enzymes as above at pH 7.5.

4.2.7 pH Studies.

Initial velocity data were measured as a function of pH under conditions in which 6PG was varied while NADP was fixed at saturation (40 K_m). The pH was maintained using the following buffers at 100 mM concentrations: Bis-Tris, 5-6.5; Hepes, 6.5-8.5; Ches, 8.5-9.5. Sufficient overlap was obtained upon changing buffers to eliminate inhibition buffer effects. The pH was determined before and after the initial velocity measurements.

4.2.8 Primary Deuterium Kinetic Isotope Effects.

The concentrations of 3-*h*-6PG and 3-*d*-6PG were determined enzymatically in triplicate by end-point assay using wild type 6PGDH. The concentrations from three determinations were in agreement within 2%. Primary deuterium isotope effects with 3-*d*-6PG were obtained for all the mutant enzymes as well as for the wild type enzyme by direct comparison of initial velocities (*15*). ^{D}V and $^{D}(V/K_{NADP})$ were obtained in triplicate by varying NADP at saturating levels of either 3-*h*-6PG or 3-*d*-6PG (20 K_m), while ^{D}V and $^{D}(V/K_{6PG})$ were measured in triplicate varying 3-*h*-6PG or 3-*d*-6PG at saturating concentrations of NADP (40 K_m).

4.2.9 Solvent Deuterium Kinetic Isotope Effects.

Initial velocities for the wild type and mutant enzymes were measured in both H_2O and D_2O solutions. Substrates (NADP and 3-*h*-6PG) and buffers used in D_2O solutions were first dissolved in small volume of D_2O and lyophilized overnight to

remove exchangeable protons. The lyophilized powders were then dissolved in D_2O to give the desired concentrations and pD was adjusted using either DCl or NaOD. Primary solvent deuterium isotope effects were obtained by direct comparison of initial velocities in the pH/pD independent region.

4.2.10 ^{13}C-Kinetic Isotope Effect.

These effects were measured using the natural abundance of ^{13}C at the C-1 position of 6PG (*16*). Both high conversion (100% reaction, which represents $^{12}C/^{13}C$ in substrate) and low conversion samples were used to measure the $^{12}C/^{13}C$ isotope ratios in the CO_2 produced from the reaction of 3-*h*-6PG or 3-*d*-6PG. From these ratios, the ^{13}C-kinetic isotope effect was calculated (*17*).

For high conversion samples, in 40 mL of H_2O or D_2O, the reaction mixtures contained 2 mM 3-*h*-6PG or 3-*d*-6PG, 0.5 mM NADP and 10 mM oxidized glutathione. The low conversion reactions contain 6.5 mM 3-*h*-6PG or 3-*d*-6PG for the enzymes that have a K_{6PG} close to that of the wild type 6PGDH (28 μM), or 15 mM, if K_{6PG} was higher. The NADP concentration was 0.25 mM for enzymes with a K_{NADP} about 2 μM or 1mM if K_{NADP} was higher (greater than 20 μM). All low conversion samples contained 5 mM oxidized glutathione in a final volume of 40 mL. The pH(D) of the reaction solutions was titrated to 7.6, followed by sparging with CO_2-free nitrogen overnight. Before starting the reactions, aliquots were withdrawn

to determine the initial concentrations of 6PG by end-point assay in triplicate. Then the reactions were initiated by the addition of 2 units of 6PGDH and 100 units of glutathione reductase to recycle NADP for both high and low conversion samples.

The high conversion samples were allowed to proceed for more than 16 hours and end-point assays were used to confirm the completion of the reaction. For the low conversion samples, extents of reaction were monitored by end-point, assaying the remaining 6PG. Reactions were quenched when 50 μmole of CO_2 were produced. For both high and low conversion samples, 0.2 mL of concentrated sulfuric acid was added to quench the reactions and the generated CO_2 was isolated by vacuum distillation (*18*). Aliquots of the samples were withdrawn after the CO_2 isolation and incubated at pH 8 overnight. The next day, end-point assays were performed in triplicate to determine the exact extent of the low conversion reactions. Isotopic composition of the CO_2 was measured on a Finnigan Delta E isotope-ratio mass spectrometer in the laboratory of Dr. Michael Engel, Department of Geophysics, University of Oklahoma. All ratios were corrected for ^{17}O according to Craig (*19*).

4.2.11 Nomenclature.

Isotope effects are expressed using the nomenclature developed by Northrop (*20*) and Cook and Cleland (*21*). Deuterium, ^{13}C, and solvent deuterium kinetic isotope effects are written with a leading superscript D, 13, or D_2O, e.g. a primary deuterium

isotope effect on V/K is written $^{D}(V/K)$. Multiple isotope effects are written with a leading superscript to depict the isotope varied, and a following subscript to depict the fixed isotope, e.g. a solvent deuterium isotope effect measured with deuterated 6PG would be written $^{D2O}(V/K)_D$.

4.2.12 Data Processing.

Double reciprocal plots were used to analyze the data and all plots and replots were linear. Data were fitted using the appropriate rate equations and programs developed by Cleland (*22*). Data for substrate saturation curves obtained at a fixed concentration of the second substrate were fitted using eq. 1. Initial velocity patterns were fitted using eq. 2. Deuterium kinetic isotope effect data in H_2O and D_2O were fitted using eq. 3. In eqs. 1 and 2, v is the initial velocity, V is the maximum velocity, A and B are reactant concentrations, K_a and K_b are the Michaelis constants for NADP and 6PG, respectively, and K_{ia} is the dissociation constant for NADP. In eq. 3, F_i is the fraction of deuterium label in the substrate or solvent, and E_V and $E_{V/K}$ are the isotope effects minus 1 on V and V/K.

$$v = \frac{VA}{K_a + A} \qquad [1]$$

$$v = \frac{VAB}{K_{ia}K_b + K_aB + K_bA + AB} \qquad [2]$$

$$v = \frac{VA}{K_a\left(1 + F_i E_{V/K}\right) + A\left(1 + F_i E_V\right)} \qquad [3]$$

The pH dependence of V and V/K were fitted using eq. 4, in which y is V or V/K, C is the pH independent value of y, H is the hydrogen ion concentration, and K_1 and K_2 are the acid dissociation constants for enzyme or substrate groups important in a given protonation state for optimal binding and/or catalysis.

$$\log y = \log\left[\frac{C}{1 + H/K_1 + K_2/H}\right] \qquad [4]$$

Calculation of ^{13}C-kinetic isotope effects was performed according to eq. 5, where *f* is the fraction of completion of the reaction, R_p and R_∞ are the $^{12}C/^{13}C$ isotopic ratios for CO_2 at partial and complete conversion, respectively. Isotope ratios, given as $\delta^{13}C$, were calculated from eq. 6, where R_{smp} and R_{std} are $^{12}C/^{13}C$ isotopic ratios for sample and standard, respectively. The standard for CO_2 was calibrated from Pee Dee Belemnite with a $^{12}C/^{13}C$ of 0.0112372 (*19*).

$$^{13}(V/K) = \frac{\log(1 - f)}{\log\left(1 - f\left[R_p/R_\infty\right]\right)} \qquad [5]$$

$$\delta\left({}^{13}C\right)=\left(\frac{R_{smp}}{R_{std}}-1\right)x\,10^{3} \qquad [6]$$

4.3 Results

4.3.1 Spectral Properties of Mutant Enzymes.

Far UV CD spectra were recorded for all mutant and wild type enzymes, and all were identical after adjusting for protein concentration (data now shown). As a result, there are no major changes in the overall structure of the enzyme resulting from the mutation, and changes are restricted to the local area within the active site.

4.3.2 Kinetic Parameters of the Mutant Enzymes.

Initial velocity patterns were obtained by measuring the initial rate at pH 7.5 using variable concentrations of 6PG and NADP dependent on the mutant enzyme. Data are summarized in Table 4-2.

All three mutant enzymes exhibit a decreased V/E_t, ranging from 7- to 67-fold. No significant change was observed in K_{NADP} of the S128A and H186A mutant enzymes, while the K_{NADP} of the N187A mutant enzyme increases about 6-fold with respect to the value of the wild-type enzyme. Data suggest that changes in the 6PG binding site somehow affect the binding of NADP, i.e., there is a linkage between the two sites. In contrast, K_{6PG} increases 3- and 19-fold for the S128A and N187A

mutant enzymes, respectively, and K_{6PG} decreases about 2-fold in the H186A mutation, resulting in a decrease in $V/K_{6PG}E_t$ 3- to 1300-fold.

4.3.3 Inhibition and Dissociation Constants for NADPH.

The inhibition constants for NADPH vs NADP, obtained at saturating 6PG for the mutant enzymes, are given in Table 4-3. In addition, the K_i for NADPH as a competitive inhibitor vs NADP at K_m level of 6PG was measured. Data are summarized in Table 4-3. In all cases, K_i for NADPH of all the mutant enzymes is greater than the value estimated for the wild type enzyme.

4.3.4 Kinetic Primary Deuterium Isotope Effects.

The kinetic isotope effects on V and V/K_{6PG} were measured at saturating NADP (40 K_m) (Table 4-4). The isotope effects are smaller than the values obtained with the wild type enzyme in all cases, and within error equal to each other, consistent with the proposed rapid equilibrium random kinetic mechanism (*1*).

4.3.5 Solvent Deuterium Kinetic Isotope Effects.

The solvent deuterium kinetic isotope effects on V and V/K_{6PG} were measured at saturating NADP (40 K_m), comparing the rates in H_2O and D_2O (Table 4-4). For all three mutant enzymes, the isotope effects are smaller than those observed for the wild type protein, with the exception of $^{D2O}(V/K)$ of S128A. An inverse solvent kinetic deuterium isotope effect is obtained for the H186A and N187A mutant enzymes.

	wt	S128A	H186A	N187A
V/E_t (sec^{-1})	9.4 ± 0.4	0.49 ± 0.05	1.40 ± 0.04	0.14 ± 0.04
Fold decrease	-	19	7	67
K_{NADP} (μM)	5 ± 1	5.4 ± 0.1	2.0 ± 0.1	29.8 ± 0.5
Fold increase		-	-	6
K_{6PG} (μM)	28 ± 4	95 ± 8	12.1 ± 0.1	530 ± 1
Fold increase		3	-	19
$V/K_{6PG}E_t$ ($M^{-1}s^{-1}$)	3.4×10^5	5.2×10^3	1.2×10^5	260
Fold decrease		65	3	1.3×10^3
ΔG^o (kcal $mole^{-1}$)[b]	-6.2	-5.5	-6.7	-4.5
$\Delta\Delta G^o$ (kcal $mole^{-1}$)[b]		0.7	-	1.7

Table 4-2. Summary of the Kinetic Parameters for 6PGDH Wild Type and the S128A , H186A and N187A mutant enzymes.
[a]Values are ± S.E.
[b]Values are calculated from K_{6PG}, using $\Delta G^o = -RTlnK_{6PG}$.

	wt[d]	S128A	H186A	N187A
6PG (s)[b]	8 ± 2	19 ± 7.5	27 ± 5.7	9.3 ± 1.3
Fold increase	-	2	3	-
6PG(ns)[c]	1.8 ± 0.3	12 ± 0.7	9.5 ± 1.6	2.8 ± 0.1
Fold increase		6	5	1.6

Table 4-3. Summary of K_i for NADPH for the Wild Type and the S128A , H186A and N187A mutant enzymes.
[a]Values are ± S.E.
[b]s, saturating ($20K_m$)
[c]ns, nonsaturating (K_m)
[d]From Price and Cook, *Arch. Biochem. Biophys.* 1996

	wt	S128A	H186A	N187A
^{D}V	1.9 ± 0.1[b]	1.2 ± 0.1	1.5 ± 0.1	1.10 ± 0.04
$^{D}(V/K_{6PG})$	1.9 ± 0.1[b]	1.2 ± 0.2	1.4 ± 0.1	1.02 ± 0.02
$^{13}(V/K_{6PG})_{H}$	1.0028	1.0152	1.0088	1.0209
	(0.0007)[c]	(0.0005)	(0.0005)	(0.0011)
$^{13}(V/K_{6PG})_{D}$	1.0017	N.D.[d]	1.0083	N.D.[d]
	(0.0005)		(0.001)	
$^{D2O}V_{H}$	2.10 ± 0.05	1.5 ± 0.1	1.03 ± 0.07	1.4 ± 0.2
$^{D2O}(V/K_{6PG})_{H}$	1.9 ± 0.2	0.8 ± 0.2	0.72 ± 0.09	0.7 ± 0.3
$^{13}(V/K_{6PG})_{D2O}$	1	1.0096	1.0040	1.0096
		(0.0007)	(0.0003)	(0.0008)
pK_a (V)[f]	6.40 ± 0.04[e]	5.5 ± 0.1	6.1 ± 0.1	6.6 ± 0.1
[f]	-	9.6 ± 0.1	-	-
pK_a (V/K)[g]	6.2 ± 0.2[e]	6.3 ± 0.1	6.3 ± 0.1	6.7 ± 0.2
[g]	8.5 ± 0.1[e]	7.6 ± 0.1	8.4 ± 0.1	8.9 ± 0.1

Table 4-4. Summary of Isotope Effects and pK_a Values for the Wild Type and the S128A , H186A and N187A mutant enzymes.
[a]Values are ± S.E. [b]From Hwang, et al *Biochemistry* 1998 (*14*).
[c]Values in parenthesis are standard errors for the ^{13}C-kinetic isotope effects. [d]Not determined as a result of the deuterium isotope effect near 1. [e]From Li and Cook (*19*). [f]pKa from the V pH profile. [g]pKa from the (V/K) pH profile.

4.3.6 ^{13}C-Kinetic Isotope effects.

Data for ^{13}C-kinetic isotope effects obtained with 3-*h*-6PG and 3-*d*-6PG are shown in Table 4-4. For all of the mutant enzymes, the value of $^{13}(V/K_{6PG})_H$ minus 1 is increased at least 3-fold greater compared to the value of the wild type enzyme, indicating that the decarboxylation step has become slower for the mutant enzymes than it is in the wild type enzyme. ^{13}C-kinetic isotope effects were also measured in H_2O and D_2O to determine the multiple solvent deuterium/^{13}C isotope effects, as summarized in Table 4. Note that there is a decrease in the ^{13}C-kinetic isotope effects when measured in D_2O.

4.3.7 pH Dependence of Kinetic Parameters.

The pH dependence of the kinetic parameters was measured for all of the mutant enzyme by varying 6PG at saturating level of NADP (40 K_m). Bell shaped pH-rate profiles with limiting slopes of 1 and -1 were obtained for V/K_{6PG} and there is only one pK in the V profile, with the exception of the S128A mutant enzyme. The pK_a values are summarized in Table 4-4. The pH-rate profiles for the S128A mutant enzyme is shown in Figure 4-4.

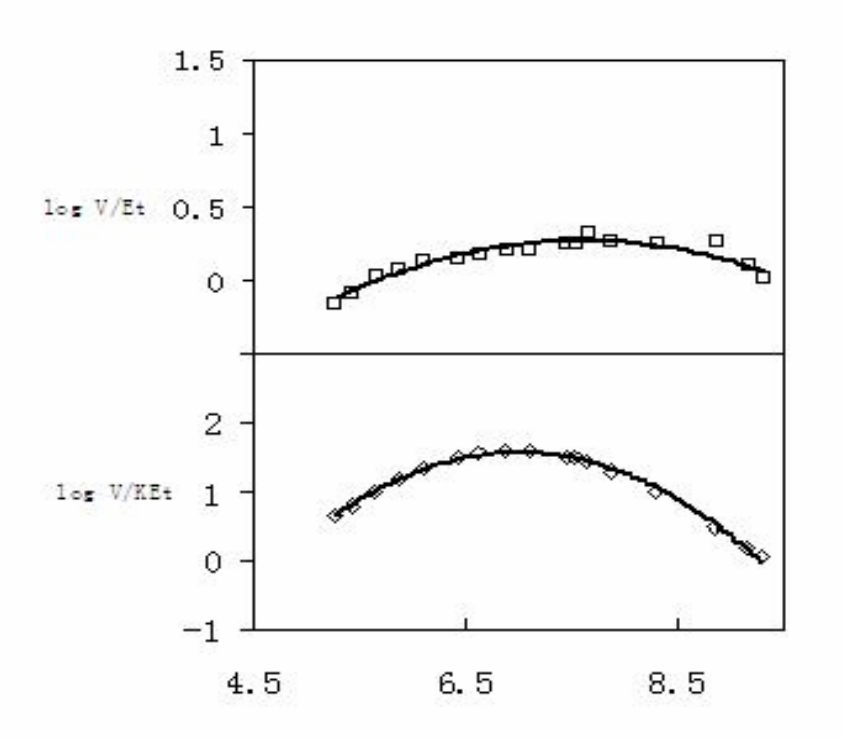

Figure 4-4. pH Dependence of Kinetic Parameters for the S128A Mutant of 6-PGDH.

4.4 Discussion

The main aim of this research was to determine the importance of residues S128, H186, and N187, which interact with both 6PG and NADPH, and their roles in providing binding energy and proper orientation of the substrates. On the basis of the crystal structure of the E:6PG and E:NADPH binary complexes, direct and indirect interactions between each of the three residues listed and the substrates are suggested. A multiple sequence alignment of 6PGDHs from a variety of species from bacteria to man indicates a complete conservation of all of the residues considered (Figure 4-3). Site-directed mutagenesis was used to change S128, H186 and N187 to alanine one at a time to eliminate the interaction between each of the residues and the substrates. Steady-state kinetic parameters and isotope effects were measured to determine the effect of the substitutions on the ability of 6PGDH to use 6PG and NADPH as a substrate.

Theory for interpretation of kinetic parameters and isotope effects in the 6PGDH reaction has been developed previously and equations are reproduced here for aid in data interpretation (*10, 14*). The oxidative decarboxylation reaction catalyzed by 6PGDH is stepwise with oxidation preceding decarboxylation as suggested by multiple deuterium/^{13}C kinetic isotope effect studies (*14*). Multiple solvent

deuterium/^{13}C kinetic isotope effect and proton inventory studies indicate the presence of an isomerization of the enzyme complex prior to hydride transfer and decarboxylation (*23*). The kinetic mechanism of 6PGDH can be written:

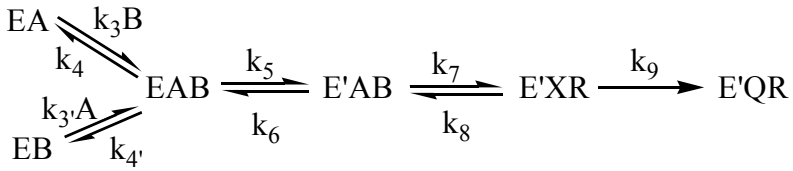

[8]

where A and B represent NADP and 6PG, respectively, and X, Q, and R represent 3-keto-6PG, ribulose 5-phosphate, and NADPH, respectively. The rate constants k_3 and k_4 are for binding and dissociation of 6PG and $k_{3'}$ and $k_{4'}$ are for binding and dissociation of NADP, k_5 and k_6 are for an isomerization of E:NADP:6PG complex, k_7 and k_8 are for forward and reverse hydride transfer, and k_9 is the rate constant for decarboxylation of the 3-keto intermediate and release of CO_2. A kinetic deuterium isotope effect is observed on the hydride transfer step, depicted by $^{D}k_7$ and $^{D}k_8$, which can be related by the equilibrium isotope effect, $^{D}K_{eq} = {}^{D}k_7 / {}^{D}k_8$, while k_9 will reflect a ^{13}C-kinetic isotope effect given by $^{13}k_9$.

Given the rapid equilibrium nature of the mechanism, central complex interconversion is rate-limiting (steps included from EAB to E'QR), and thus k_4, $k_{4'} > k_5$, while k_{11}, $k_{13} > k_7$. Finally, since the kinetic isotope effects on V and V/K are

equal to one another for the wild type and each of the mutant enzymes, $k_6 = (1 + k_6/k_5)/(1/k_5 + 1/k_9)$.

The following expressions have been developed.

$$V = \frac{\dfrac{k_7}{1+\dfrac{k_6}{k_5}}}{1+\dfrac{k_7\left(\dfrac{1}{k_5}+\dfrac{1}{k_9}\right)}{1+\dfrac{k_6}{k_5}}+\dfrac{k_8}{k_9}} \qquad [9]$$

$$\frac{V}{K_{6PG}} = \frac{\dfrac{k_3 k_5 k_7}{k_4 k_6}}{1+\dfrac{k_7}{k_6}+\dfrac{k_8}{k_9}} \qquad [10]$$

$$\frac{V}{K_{NADP}} = \frac{\dfrac{k_3, k_5 k_7}{k_4, k_6}}{1+\dfrac{k_7}{k_6}+\dfrac{k_8}{k_9}} \qquad [11]$$

$${}^{D}V = \frac{{}^{D}k_7+\dfrac{k_7\left(\dfrac{1}{k_5}+\dfrac{1}{k_9}\right)}{1+\dfrac{k_6}{k_5}}+\left({}^{D}K_{eq}\right)\left(\dfrac{k_8}{k_9}\right)}{1+\dfrac{k_7\left(\dfrac{1}{k_5}+\dfrac{1}{k_9}\right)}{1+\dfrac{k_6}{k_5}}+\dfrac{k_8}{k_9}} \qquad [12]$$

$${}^{D}\left(\frac{V}{K_{6PG}}\right) = \frac{{}^{D}k_7+\dfrac{k_7}{k_6}+\left({}^{D}K_{eq}\right)\left(\dfrac{k_8}{k_9}\right)}{1+\dfrac{k_7}{k_6}+\dfrac{k_8}{k_9}} \qquad [13]$$

$$^{13}\left(\frac{V}{K_{6PG}}\right)_H = \frac{^{13}k_9 + (k_9/k_8)(1 + k_7/k_6)}{1 + (k_9/k_8)(1 + k_7/k_6)} \quad [14]$$

$$^{13}\left(\frac{V}{K_{6PG}}\right)_D = \frac{^{13}k_9 + (^{D}k_7k_9/k_8\,^{D}K_{eq})(1 + k_7/k_6\,^{D}k_7)}{1 + (^{D}k_7k_9/k_8\,^{D}K_{eq})(1 + k_7/k_6\,^{D}k_7)} \quad [15]$$

where $^{D}k_7$ is the intrinsic deuterium isotope effect on the hydride transfer step, and $^{D}K_{eq}$ is the equilibrium isotope effect on hydride transfer (1.18 for oxidation of a secondary alcohol (*24*)).

Since K_{6PG} is the ratio of V and V/K_{6PG}, and K_{NADP} is the ratio of V and V/K_{NADP} and taking into account $k_6 = (1 + k_6/k_5)/(1/k_5 + 1/k_9)$

$$K_{6PG} = \left(\frac{k_4}{k_3}\right)\left(\frac{k_6}{k_5 + k_6}\right) = K_{d\,6PG} \quad [16]$$

$$K_{NADP} = \left(\frac{k_{4'}}{k_{3'}}\right)\left(\frac{k_6}{k_5 + k_6}\right) = K_{d\,NADP} \quad [17]$$

where k_4/k_3 is the K_d of 6PG and $k_{4'}/k_{3'}$ is the K_d of NADP for the E:NADP:6PG complex and $k_6/(k_5 + k_6)$ corrects for the distribution of the central complexes between E:NADP:6PG and E':NADP:6PG. Therefore, K_{6PG} is the equilibrium constant for dissociation of 6PG from E:NADP:6PG and E':NADP:6PG and K_{NADP} is the equilibrium constant for dissociation of NADP from E:NADP:6PG and

E':NADP:6PG. Using the above rate equations, we discuss the results for each of the mutant enzyme.

The key to interpretation of the data obtained for the mutant enzymes lies in changes in K_{6PG}, $^{D}(V/K_{6PG})$, $^{13}(V/K_{6PG})$ and $^{D2O}(V/K_{6PG})_D$. The decrease in K_{6PG} for the S128A mutant enzyme likely results from an increase in the net off-rate for 6PG from E':NADP:6PG, $k_4k_6/(k_5 + k_6)$. However, since $k_6/(k_5 + k_6)$ is present in both K_{6PG} and K_{NADP}, and no change is observed in the latter for the S128A mutant enzyme, it is k_4 that is increased. For the N187A mutant enzyme, the increase in both K_{6PG} and K_{NADP} likely results from an increase in the net off-rates for 6PG and NADP from E':NADP:6PG, $k_4k_6/(k_5 + k_6)$ ($k_4k_6/(k_5 + k_6)$ in the case of NADP), suggesting an increase in k_4 and k_6.

4.4.1 The S128A and N187A Mutant Enzymes.

Both the S128A and the N187A mutant enzymes exhibit an increased K_{6PG}. V/E_t decreases about 19- and 67-fold, resulting in a $V/K_{6PG}E_t$ 65 and 1,300 times lower than the wild type protein for the S128A and the N187A mutant enzymes, respectively. In addition, K_i for NADPH for the S128A and N187A mutant enzyme increases, suggesting that the mutant enzymes exhibit lower affinity for both 6PG and NADPH. Data are consistent with the structural data of Adams (*11*), which show that the side chains of S128 and N187 interact with 6PG in the E:6PG binary complex

and the nicotinamide ring of NADPH in the E:NADPH binary complex.

The value of $^{13}(V/K_{6PG})$ has increased from 1.0028 in the wild type enzyme to 1.0152 and 1.0209 for the S128A and N187A mutant enzymes, respectively, concomitant with a decrease in ^{D}V and $^{D}(V/K_{6PG})$ to a small finite value. Data suggest a decrease in the rate of the decarboxylation step relative to hydride transfer. The solvent deuterium isotope effect on V is finite, but smaller than the value of the wild type enzyme, while a value of 3.3 is obtained for $^{D2O}(V/K_{6PG})_H$ for the S128A mutant enzyme and an inverse $^{D2O}(V/K_{6PG})_H$ for the N187A mutant enzyme. The inverse solvent isotope effect may reflect the conformational change prior to hydride transfer. Data are consistent with the observed decrease in $^{13}(V/K_{6PG})$ when D_2O is the solvent.

V and V/K_{6PG} pH-rate profiles for the S128A mutant enzyme exhibits pK values that are closer together than those observed for the wt enzyme, Table 3. (This phenomenon was also observed for mutations in the 2'-phosphate subsite and the 6-phosphate subsite (*25, 26*).) The pH-rate profiles reflect reverse protonation states between the K183 general base and the E190 general acid (*4*), and thus the amount of active enzyme can be estimated from the antilog of the difference between the acid and base pK values. In the case of the S128A mutant enzyme, the fraction of enzyme in the right protonation state is 5%, while in the wide type enzyme the value

is 0.5%, representing a 10-fold increase. The observed V/E_t for the S128A mutant enzyme, therefore, reflects a 10-fold decreased in the actual value of V/E_t.

4.4.2 The H186A Mutant Enzyme.

H186 interacts with the nicotinamide ring in the E:NADPH binary complex with a hydrogen-bonding distance of 3.2 Å (Figure 3). In the E:6PG binary complex, the side chain of H186 does not interact with the substrate directly, but links the side chains of S128 and N187 via two hydrogen bonds as shown in Figure 2. Therefore, smaller changes in the observed kinetic parameters are not unexpected. Data suggest that H186 does not contribute to binding 6PG, but likely helps to position the substrate for catalysis.

The ^{13}C-kinetic isotope effect minus 1 obtained for the H186A mutant enzyme is increased by about 3-fold compared to the value of the wild type enzyme, while the primary deuterium isotope effect decreases to about 1.5, indicating that the relative rate for the decarboxylation step to the hydride transfer step is slower in the mutant enzyme. An inverse solvent deuterium isotope effect in the case of 6PGDH normally reflects a medium effect on the conformational change that precedes catalysis. The decrease of the ^{13}C-kinetic isotope effect when measuring in D_2O indicates that some other step(s) beside the decarboxylation step contribute to rate limitation. In this case, it may be both the conformational change and the following

hydride transfer step.

4.4.3 Roles of the Three Residues.

All three mutant enzymes exhibit decreased affinity for NADPH, but no change in the K_m of NADP, with the exception of the N187A mutant enzyme, suggesting that the mutant enzymes treat the oxidized and reduced cofactor differently and they only help to anchor the cofactor after hydride transfer accompanied by the rotation of the nicotinamide ring around the N-glycosidic bond, i.e. S128, H186 and N187 help to guide the rotation of the nicotinamide ring. The measured ^{13}C-kinetic isotope effect on all of the mutant enzyme increases compared to the value of the wild type enzyme, suggesting that the decarboxylation reaction in the mutant enzymes is not well performed as it is in the wild type enzyme, consistent with the proposed non-redox role of NADPH. The S128A and N187A mutant enzymes also exhibit higher K_m for 6PG, suggesting that these two residues also contribute to the binding of 6PG. However, the calculated binding energy that each residue contributes is less than that of the residues from the 6-phosphate binding site (*26*), indicating that S128 and N187 are not as important in providing binding energy for 6PG as residues Y191, K260,R287 and R446.

4.5 References

1. Price, N., and Cook, P. F. (1996) Kinetic and Chemical Mechanisms of the Sheep

Liver 6-Phosphogluconate Dehydrogenase. *Arch. Biochem. Biophys. 336*, 215-223.

2. Berdis, A. J., and Cook, P. F. (1993) Overall Kinetic Mechanism of 6-Phosphgluconate Dehydrogenase from *Candida utilis*. *Biochemistry 32*, 2036-2040.

3. Karsten, W. E., Chooback, L., and Cook, P. F. (1998) Glutamate 190 Is a General Acid Catalyst in the 6-Phosphogluconate Dehydrogenase-Catalyzed Reaction. *Biochemistry 37*, 15691-15697.

4. Zhang, L., Chooback, L., and Cook, P. F. (1999) Lysine 183 Is the General Base in the 6-Phosphogluconate Dehydrogenase-Catalyzed Reaction. *Biochemistry 38*, 11231-11238.

5. Rippa, M., Signorini, M., and Dallocchio, F. (1972) Differentiation Between the Structural and Redox Roles of TPNH in 6-Phosphogluconate Dehydrogenase. *Biochem. Biophys. Res. Commun.* 48, 764-768.

6. Rippa, M., Signorini, M., and Dallocchio, F. (1973) A Multiple Role for the Coenzyme in the Mechanism of Action of 6-Phosphogluconate Dehydrogenase. The Oxidative Decarboxylation of 2-Deoxy-6-Phosphogluconate. *J. Biol. Chem.* 248, 4920-4925.

7. Rippa, M., Signorini, M., and Dallocchio, F. (1973) A Role for the Pyridine of Triphosphopyridine Nucleotide in 6-Phosphogluconate Dehydrogenase. *FEBS Lett.* 36, 148-150.

8. Hanau, S., Dallocchio, F., Rippa, M. (1992) NADPH Activates a Decarboxylation Reaction Catalyzed by Lamb Liver 6-Phosphogluconate Dehydrogenase. Biochem. Biophys. Acta 1122, 273-277.

9. Rippa, M., Hanau, S., Cervellati, C., and Dallocchio, F. (2000) 6-Phosphogluconate Dehydrogenase: Structural Symmetry and Functional Asymmetry, *Protein Pept. Lett.* 7, 341-348.

10. Cervellati, C., Dallocchio, F., Bergamini, C. M., and Cook, P. F. (2005) Role of Methionine-13 in the Catalytic Mechanism of 6-Phosphogluconate Dehydrogenase from Sheep Liver. *Biochemistry 44*, 2432-2440.

11. Adams, J. M., Grant, H. E., Gover, S., Naylor, C. E., and Philips, C. (1994) Substrate Binding in 6-Phosphogluconate Dehydrogenase: Implications for NADP Specificity and the Enzyme Mechanism. *Structure 2*, 651-668.

12. Chooback, L., Price, N. E., Karsten, W. E., Nelson, J., Sundstrom, P., and Cook, P. F. (1998) Cloning, Expression, Purification, and Characterization of the 6-Phosphogluconate Dehydrogenase from Sheep Liver. *Protein Expression Purif. 13*, 251-258.

13. Bradford, M. M. (1976) A Rapid and Sensitive Method for the Quantitation of Microgram Quantities of Protein Utilizing the Principle of Protein-dye Binding. *Anal. Biochem. 72*, 248-254.

14. Hwang, C. C., Berdis, A. J., Karsten, W. E., Cleland, W. W., and Cook, P. F. (1998) Oxidative Decarboxylation of 6-Phosphgluconate by 6-Phosphogluconate Dehydrogenase Proceeds by a Stepwise Mechanism with NADP and ADADP as Oxidants. *Biochemistry 37*, 12596-12602.

15. Parkin, D. W. (1991) *Enzyme Mechanism from Isotope Effects* (Cook, P. F., Ed.), CRC Press, Inc., Boca Raton, FL, pp. 284-285.

16. O'Leary, M. H. (1980) Determination of Heavy-atom Isotope Effects on Enzyme-catalyzed Reactions. *Methods Enzymol*. *64B*, 83-104.

17. Hermes, J. D., Roeske, C. A., O'Leary, M. H., and Cleland, W. W. (1982) Use of Multiple Isotope Effects to Determine Enzyme Mechanisms and Intrinsic Isotope Effects. Malic Enzyme and Glucose 6-Phosphate Dehydrogenase. *Biochemistry 21*, 5106-5114.

18. Weiss P. M. (1991) *Enzyme Mechanism from Isotope Effects* (Cook P. F., Ed.), CRC Press, Inc., Boca Raton, FL, pp. 291-311.
19. Craig, N. (1957) Isotopic standards for carbon and oxygen and correction factors for mass-spectrometric analysis of carbon dioxide. *Geochim. Cosmochim. Acta 12*, 133-149.

20. Northrop, D. B. (1977) in *Isotope effects on Enzyme-Catalyzed Reactions* (Cleland, W. W., O'Leary, M. H. & Northrop, D. B., Eds.) p 122, University Park Press, Baltimore, MD.

21. Cook, P. F., and Cleland, W. W. (1981) Mechanistic Deductions from Isotope Effects in Multireactant Enzyme Mechanisms. *Biochemistry 20*, 1790-1796.

22. Cleland, W. W. (1979) Statistical Analysis of Enzyme Kinetic Data. *Methods Enzymol. 63*, 103-108.

23. Hwang, C. C. and Cook, P. F. (1998) Multiple Isotope Effects as a Probe of Proton and Hydride Transfer in the 6-Phosphogluconate Dehydrogenase Reaction. *Biochemistry 37*, 15698-15702.

24. Cook, P. F., Blanchard, J. S. and Cleland, W. W. (1980) Primary and Secondary Deuterium Isotope Effects on the Equilibrium Constant for Enzyme Catalyzed Reactions. *Biochemistry 19*, 4853-4858.

25. Li, L and Cook, P. F. (2006) Importance of the 2'-Phosphate of NADP in the Sheep Liver 6-Phosphogluconate Dehydrogenase Catalyzed Reaction. *Biochemistry* submitted.

26. Li, L and Cook, P. F. (2006) Importance in Catalysis of the 6-Phosphate Binding Site of 6-Phosphogluconate in Sheep Liver 6-Phosphogluconate Dehydrogenase. *J. Biol. Chem.* submitted.

Chapter 5

Overall Discussion and Conclusion

5.1 Overall Discussion and Conclusion.

6-Phosphogluconate dehydrogenase has been studied for more than fifty years. The mechanism behind the reaction is complicated and the mechanism has been refined as new theory and technology has been developed and applied to the study of 6PGDH.

The mechanism proposed in 1998 is a general acid-general base catalyzed rapid equilibrium random mechanism. The reaction is stepwise with hydride transfer from the 3-C of 6PG to the 4-position of the nicotinamide ring of NADP preceding decarboxylation of the 3-keto intermediate, as shown in Figure 1-3. There are three steps are known to contribute to rate-limitation: a conformational change prior to catalysis required to close the active site, exclude water, and bring reactants into proximity and alignment, the hydride transfer step and decarboxylation of oxaloacetate (*1-6*). Structural data have shown that the conformation of the nicotinamide ring of the cofactor is different in the E:NADP binary complex compared to the E:NADPH binary complex (*7*). Kinetic studies of mutant enzymes that have changes at M13, on which the nicotinamide ring of NADP rests, suggest

that a rotation of the nicotinamide ring around the glycosidic bond is on the catalytic pathway; the mutant enzymes have a lower affinity for the oxidized cofactor but no change in affinity for the reduced cofactor (*8*). Therefore, a modified mechanism has been proposed by Cervellati et al., in which the hydride transfer step is accompanied by the flip of the nicotinamide ring into the active site (*8*, Figure 5-1).

Similar phenomena have been observed in NAD-malic enzyme and NAD(P)-dependent aldehyde dehydrogenases (*9-13*). The hypothesis that the cofactor isomerizes after reduction in the malic enzyme is closely aligned to that of 6PGDH, with the rotational isomerization suggested to facilitate the next step, decarboxylation, by repositioning the substrate. The driving force of the rotation for both 6PGDH and malic enzyme is loss of the ionic interaction between the positively charged nicotinamide ring of the oxidized cofactor and the negatively charged pyrophosphate of the cofactor; a distance of about 5 Å is obtained fro the ionic interaction. Once rotation has occurred, the distance increases by about 2 Å. In the case of aldehyde dehydrogenases, the theory is somewhat different. After rotation, the nicotinamide ring of the cofactor flips away from the active site and make space for deacylation. However, in all cases the isomerization is thought to be essential to the catalytic mechanism.

Studies in sheep liver 6PGDH of the residues that interact with the substrate

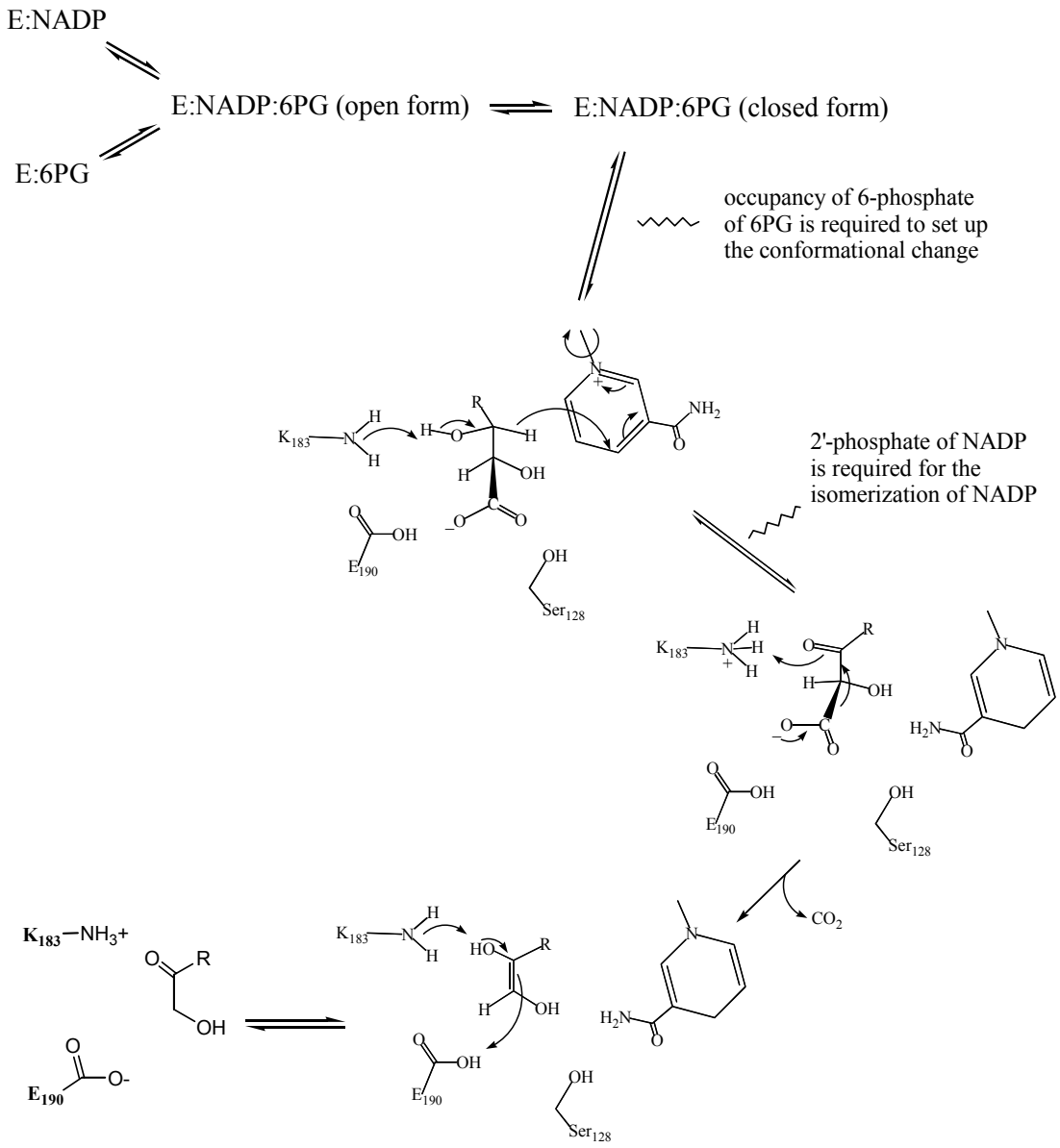

Figure 5-1. The Modified Mechanism of 6-Phosphogluconate Dehydrogenase.

and/or cofactor reveal that the 2'-phosphate of NADP is critical for making most of the interactions between the protein and the cofactor, helping position the cofactor for hydride transfer and participating in the rotational isomerization of the cofactor after reduction, probably by holding the cofactor in position so that the nicotinamide ring can flip into the right location (*14*). Destroying the interactions between the 2'-phosphate and the protein results in a slower or less efficient rotation (the nicotinamide ring does not rotate into the right position). The isomerization of the cofactor upon reduction is guided by the residues S128, H186 and N187, which interact with both 6PG and NADPH. From a dynamic point of view, the rotation of the nicotinamide ring may place it in different positions, as evidenced for the mutant enzymes when binding affinity of 2'-phosphate is lost or lacks of guidance from S128, H186 ad N187. However, only when rotation of the nicotinamide ring can completely eliminate the interactions between the 1-carboxylate of 6PG and the protein, will the decarboxylation step be catalyzed. Therefore, in the mutant enzyme (N32A, R33A, T34A, S128A, H186A and N187A), the observed rate of the decarboxylation step is decreased as shown by the large ^{13}C isotope effect.

On the other hand, the 6-phosphate of 6PG is important in anchoring the substrate for catalysis. It is also suggested that occupancy of the 6-phosphate position or proper binding of 6PG is critical for the reaction, probably inducing the

conformational change in enzyme to close the active site prior to catalysis (*15*). Altering the interactions between the 6-phosphate and the protein results in some alteration of the conformational change, but decarboxylation becomes predominantly rate-limiting, as a result of a change in the position of 6PG in the site. On the basis of the data obtained for the mutant enzymes, a linkage between the cofactor binding site and 6PG binding site is suggested (Figure 2-5), because changes in one site have effects in the other and no significant global structural change is detected in any of the mutant enzymes.

Combining all the information above together with the previously proposed mechanism, we can conclude the essentials in the reaction catalyzed by sheep liver 6PGDH. 1). Proper binding of both NADP and 6PG is required for the subsequent catalytic steps, and a conformational change is induced to close the active site, and to bring the two substrates together for catalysis. 2). With the help of K183, proton and hydride transfer is performed, and guided by residues S128, H186 and N187, a rotation of the nicotinamide ring around the N-glycosidic bond brings the carboxamide chain into the position originally occupied by the 1-carboxylate of 6PG and the interactions between the 1-carboxylate of 6PG and the enzyme is eliminated. 3). Decarboxylation is facilitated by K183 and CO_2 is released. 4). E190 assists the tautomerization step, which converts the enediol intermediate to Ru5P. 5). Binding of

NADP and 6PG and releasing of NADPH and Ru5P are random. Overall, the cofactor and 6PG binding sites are not isolated, and there is crosstalk between them.

5.2 References.

1. Rendina, A. R. Hermes, J. D. and Cleland, W. W. (1984) Use of Multiple Isotope Effects to Study the Mechanism of 6-Phosphogluconate Dehydrogenase. Biochemistry 23, 6257-6262.

2. Hwang, C-C., Berdis, A. J., Karsten, W. E., Cleland, W. W. and Cook, P. F. (1998) Oxidative Decarboxylation of 6-Phosphogluconate by 6-Phosphogluconate Dehydrogenase Proceeds by a Stepwise Mechanism with NADP and APADP as Oxidants. *Biochemistry* 37, 12596-12602.

3. Berdis, A. J. and Cook, P. F. (1993a) Overall Kinetic Mechanism of 6-Phosphogluconate Dehydrogenase from Candida utilis. *Biochemistry* 32, 2036-2040.

4. Price, N. E. and Cook, P. F. (1996) Kinetic and Chemical Mechanism of the Sheep Liver 6-Phosphogluconate Dehydrogenase. *Arch. Biochem. Biophys.* 336, 215-223.

5. Karsten, W. E., Chooback, L., and Cook, P. F. (1998) Glutamate 190 Is a General Acid Catalyst in the 6-Phosphogluconate Dehydrogenase-Catalyzed Reaction. *Biochemistry 37*, 15691-15697.

6. Zhang, L., Chooback, L., and Cook, P. F. (1999) Lysine 183 Is the General Base in the 6-Phosphogluconate Dehydrogenase-Catalyzed Reaction. *Biochemistry 38*, 11231-11238.

7. Adams, J. M., Grant, H. E., Gover, S., Naylor, C. E., and Philips, C. (1994) Substrate Binding in 6-Phosphogluconate Dehydrogenase: Implications for NADP Specificity and the Enzyme Mechanism. *Structure 2*, 651-668.

8. Cervellati, C., Dallocchio, F., Bergamini, C. M., and Cook, P. F. (2005) Role of Methionine-13 in the Catalytic Mechanism of 6-Phosphogluconate Dehydrogenase from Sheep Liver. *Biochemistry 44*, 2432-2440.

9. Hammen, P. K., Alliali-Hassani, A., Hallenga, K., Hurley, T. D. and Weiner, H. (2002) Multiple Conformations of NAD and NADH When Bound to Cytosolic and Mitochondrial Aldehyde Dehydrogenase. *Biochemistry* 41, 7156-7168.

10. Coleman, D. E., Rao, G. S. J., Goldsmith, E. J., Cook, P. F. and Harris, B. G. (2002) Crystal Structure of the Malic Enzyme from *Ascaris suum* Complexed with Nicotinamide Adenine Dinucleotide at 2.3 Å Resolution. *Biochemistry* 41, 6928-6938.

11. Perez-Miller, S. J. and Hurley, T. D. (2003) Coenzyme Isomerization Is integral to Catalysis in Aldehyde Dehydrogenase. *Biochemistry* 42, 7100-7109.

12. Rao, G. S. J., Coleman, D. E., Karsten, W. E., Cook, P. F. And Harris, B. G. (2003) Crystallographic Studies on *Ascaris suum* NAD-Malic Enzyme Bound to Reduced Cofactor and Identification of an Effector Site. *J. Biol. Chem.* 278, 38051-38058.

13. D'Ambrosio, K., Pailot, A., Talfournier, F., Didierjean, C., Benedetti, E., Aubry, A., Branlant, G. and Corbier, C (2006) The First Crystal Structure of a Thioacylenzyme Intermediate in the ALDH Family: New Coenzyme Conformation and Relevance to Catalysis. *Biochemistry* 45, 2978-2986.

14. Li, L and Cook, P. F. (2006) Importance of the 2'-Phosphate of NADP in the Sheep Liver 6-Phosphogluconate Dehydrogenase Catalyzed Reaction. *Biochemistry* submitted.

15. Li, L and Cook, P. F. (2006) Importance in Catalysis of the 6-Phosphate Binding Site of 6-Phosphogluconate in Sheep Liver 6-Phosphogluconate Dehydrogenase. *J. Biol. Chem.* submitted.

Appendix 1

Additional Projects

1. The M13 and E131 mutations.

The crystal structure of sheep liver 6-phosphogluconate dehydrogenase shows that Met13 and Glu131 interact with the nicotinamide ring of NADP, but not NADPH. Recent studies suggest that mutations at Met13 affect NADP, but not NADPH binding, consistent with rotation of the nicotinamide moiety of the coenzyme $NADP^+$ when it is reduced to NADPH during the course of the catalytic reaction. To further corroborate this hypothesis, and to explore the function of Glu131 in the mechanism of the 6PGDH reaction, site-directed mutagenesis was performed, changing Glu to Ala. The resulting mutant enzyme, E131A, exhibits a 2-fold decrease in V/E_t, while K_{NADP}, and K_{6PG} remain the same as those of the wild type enzyme (Table A-1). The primary deuterium kinetic isotope effect decreases to 1.2, while the ^{13}C-kinetic isotope effect minus 1 increases about 2-fold, indicating that the relative rate of the decarboxylation step compared to the hydride transfer step decreases in the E131A mutant enzyme (Table A-2). ^{13}C-kinetic isotope effects were also measured for three of Met13 mutant enzymes, M13V, M13Q and M13C (Table A-2). As a result, all of the mutant enzymes exhibit an increased ^{13}C-kinetic isotope effect with the exception of the M13Q mutant enzyme. A manuscript describing these data is in preparation (University of Oklahoma, USA and Università di Ferrara, Italy).

	E131A
V/E_t (sec^{-1})	4.0 ± 0.4
Fold decrease	2
K_{NADP} (μM)	5 ± 1
Fold increase	-
K_{6PG} (μM)	14 ± 3
Fold increase	-

Table A-1. Kinetic Parameters of The E131A Mutant Enzyme.

	E131A	M13V	M13Q	M13C
^{D}V	1.2 ± 0.1			
$^{D}(V/K_{6PG})$	1.1 ± 0.2			
$^{13}(V/K_{6PG})_H$	1.0046	1.0062	1.0033	1.0151
	(0.0003)[b]	(0.0004)	(0.0009)	(0.0002)
$^{13}(V/K_{6PG})_D$	-	1.0037	0.998	1.014
	-	(0.0008)	(0.001)	(0.002)

Table A-2. Summary of Isotope Effects for 6PGDH Mutant Enzymes[a]

[a]Values are ± S.E.

[b]Values in parenthesis are standard errors for the ^{13}C-kinetic isotope effects.

2. The Pre-steady State Studies on the Y191A, K260A and T262A Mutant Enzymes.

As discussed in Chapter 3, the Y191A, K260A and T262A mutant enzymes exhibit a dramatic decrease in the rate of the decarboxylation step, which becomes predominantly rate-limiting in the overall reaction, especially for the last two mutant enzymes. Therefore, pre-steady state kinetic studies have been carried out using stopped-flow spectrophotometry.

Preliminary data show a burst (accumulation of NADPH) followed by a linear steady state rate for the K260A and T262A mutant enzymes, while the Y191A mutant enzyme does not exhibit a burst (Figure A-1). Data suggest the decarboxylation step is much slower in the K260A and T262A mutant enzyme than it is in the Y191A mutant enzyme, consistent with the previously measured ^{13}C-kinetic isotope effects. Further experiments, including protein concentration dependence of the burst and isotope effect studies are needed to confirm the accumulation of NADPH results from a decreased rate of the decarboxylation step. In addition, a quantitative analysis of the data will provide information on the relative rates of steps within the catalytic pathway.

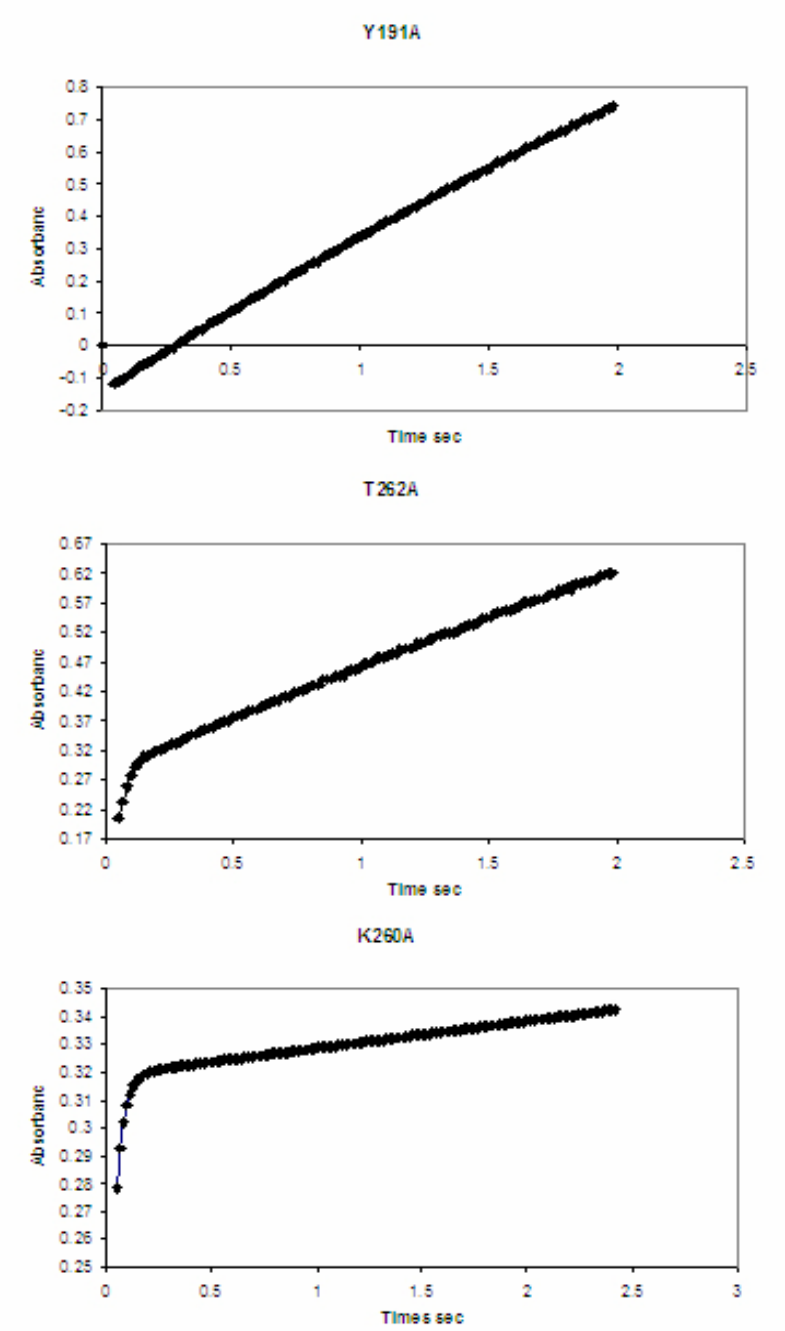

Figure A-1. The Pre-Steady State Studies of Y191A, K260A and T262A.

3. Subcloning Enzymes in the α-Aminoadipate Pathway

The α-aminoadipate pathway is a lysine biosynthetic pathway unique to fungi (*1*, Figure A-2). In addition to the enzymes that are actively being investigated in the lab, there are four enzymes we are interested in. They are homoisocitrate dehydrogenase (HICDH or Lys 10)), homoaconitase (HAT or Lys 4), alpha aminoadipate reductase (AAR), and the small subunit of AAR, phosphopantetheinyl transferase or Lys5. The genes of Lys10, Lys4, Lys2 and Lys5 from *Saccharomyces cerevisiae* genomic DNA have been amplified by using PCR (Figure A-3). Thus far, Lys 10, Lys 4, and Lys 5 have been subcloned into the pET-16b vector successfully. Dr. Ying Lin has taken over this project, has expressed and is characterizing Lys10.

References.

1. Xu, H., Andi, B., Qian, J., West, A. H. and Cook, P. F. (2006) The α-Aminoadipate Pathway for Lysine Biosynthesis in Fungi. *Cell Biochemistry and Biophysics* , In Press.

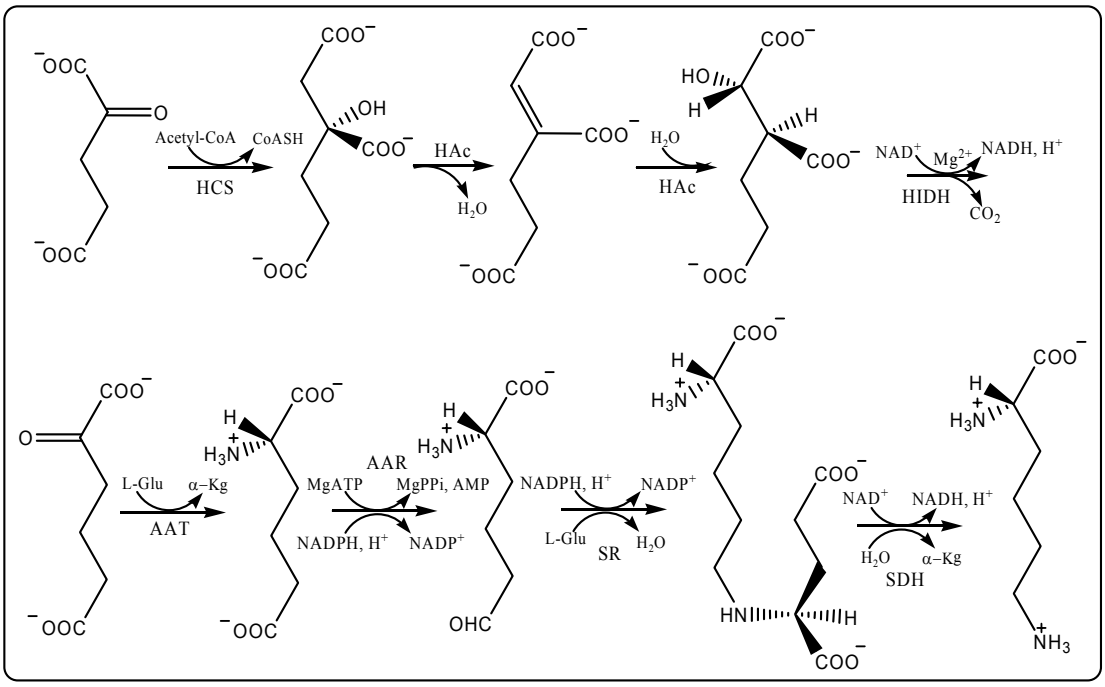

Figure A-2. The Lysine Biosynthetic Pathway in *Saccharomyces cerevisiae*. The enzymes of the lysine AAA biosynthetic pathway are as follows: (1) Homocitrate synthase (HCS, E.C. 4.1.3.21), (2) Homoaconitase (HAc, E.C. 4.2.1.36), (3) Homoisocitrate dehydrogenase (HIDH, E.C. 1.1.1.87), (4) α-aminoadipate aminotransferase (AAT, E.C. 2.6.1.39), (5) α-aminoadipate reductase (AAR, E.C. 1.2.1.31), (6) Saccharopine reductase (SR, E.C. 1.5.1.10), (7) Saccharopine dehydrogenase (SDH, E.C. 1.2.1.31).

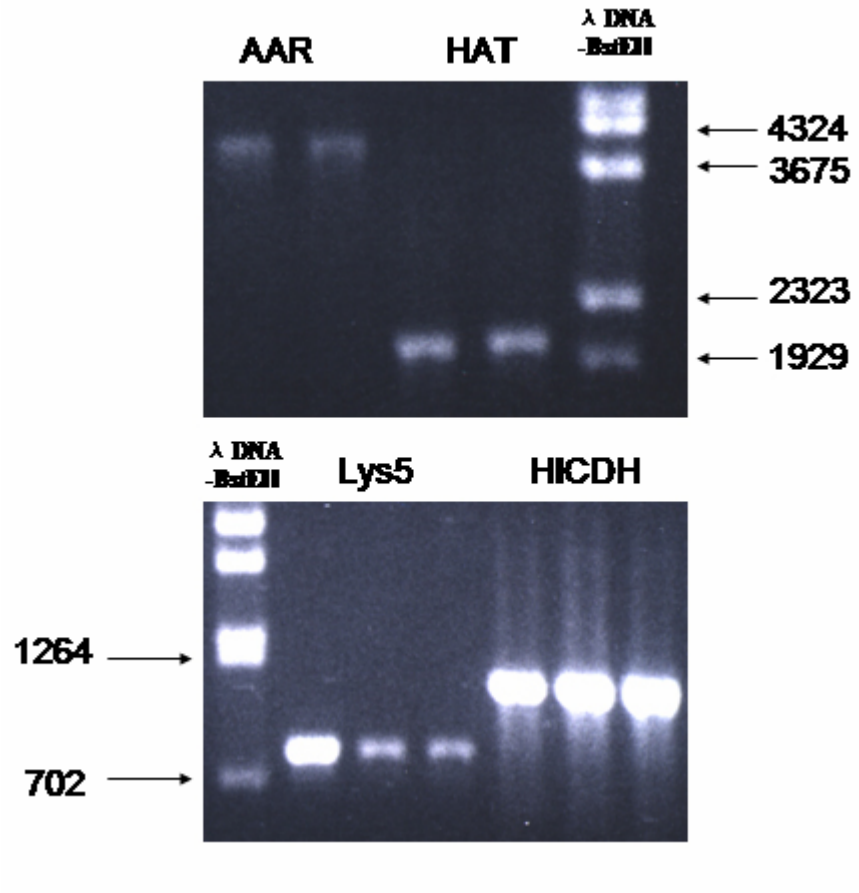

Figure A-3. PCR for the Lys5, HICDH, HAT and AAR from *Saccharomyces cerevisiae*. The sizes of the genes of Lys, HICDH, HAT and AAR are 819bp, 1116bp, 2082bp and 4199bp, respectively.

Appendix 2

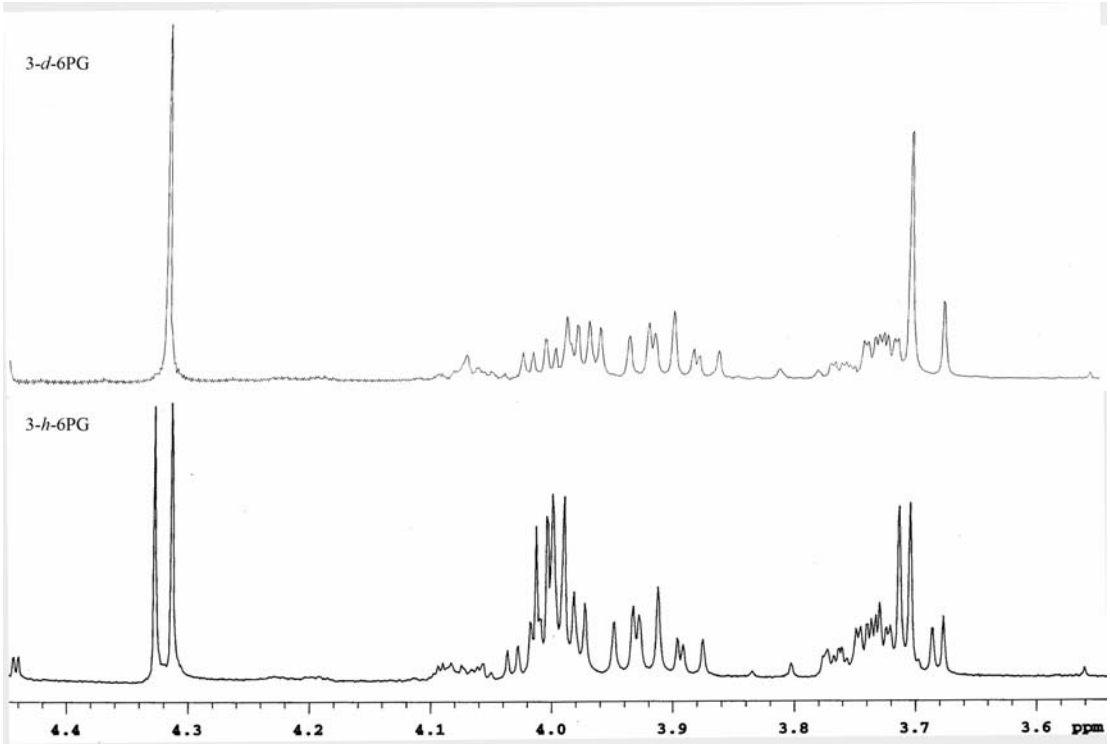

Figure A-4. NMR Spectra of 3-*h*-6PH and 3-*d*-6PG. The top panel is the NMR spectrum of 3-*d*-6PG and the bottom is the NMR spectrum of the 3-*h*-6PH.